RHEOLOGY OF CONCENTRATED SUSPENSIONS OF SPHERES

Thesis by

Joseph Harold Smith

In Partial Fulfillment of the Requirements

For the Degree of

Doctor of Philosophy

California Institute of Technology

Pasadena, California

1972

(Submitted April 24, 1972)

DEDICATION

This thesis is dedicated to

Mrs. Marcella O'Connor

who was the first to look at me and say

'Caltech' !

ACKNOWLEDGMENTS

The work reported in the pages which follow could not have gone forward without the talented and generous efforts of many people in addition to myself. Chief among those to whom I am indebted is Professor Giles R. Cokelet: without his unyielding moral support and gentle direction, this effort would have foundered in calamity. I salute the skills and patience of William R. Schuelke, Jr., John Yehle, Donald E. Haley, and Gordon R. Williamson who manufactured equipment and repeatedly rescued me from a morass of ruined and malfunctioning machinery: they are Magicians, one and all! The Chemical Engineering faculty of California Institute of Technology has been generous and patient, and I am grateful. Professor P. J. Gilinson of Massachusetts Institute of Technology was very helpful. The Chemical Engineering faculty of Montana State University has been most hospitable.

It is a pleasure to acknowledge the large value of intense discussions, both scholarly and otherwise, with Dr. Donald R. Remer, with Dr. Norman F. Weber, and especially with Dr. James H. Barbee

whose qualities of tolerance and charity mark him as a true Christian gentleman. There are others whose contributions have been less direct but no less valuable: discretion required that I not name them here. They have been beacons of lovingkindness through seasons of agony to times of joy. It is an honor to be in their debt. There are yet others. I am indebted to Sara Higgins Smith for encouraging me to get back into graduate school and out of the house. I am indebted to Theodore George Northrup, Ph.D., for my freedom. My freedom has lately become a great blessing, but a debt such as this is no honor.

This research was sponsored by the National Science Foundation through Grant GK 686. Stipends were provided by a graduate teaching assistantship, a John Stauffer Fellowship, an NSF Graduate Traineeship, and graduate research assistantships from the California Institute of Technology, and by the Veterans' Administration under public law.

I am pleased to share what credit may be due this thesis, but the responsibility for fact and expression is mine alone.

J.H.S.

Bozeman, Montana

February 29, 1972

ABSTRACT

The effects of concentration and composition upon the rheological properties of concentrated monomodal, bimodal, and trimodal suspensions of neutrally buoyant rigid spheres in Newtonian fluids were experimentally determined. Isothermal flow curves were calculated from torque measurements made with a Gilinson-Dauwalter-Merrill concentric cylinder viscometer with a stationary inner cylinder, a diameter ratio of 1.08, and a gap of 1.5 mm at as many as ten distinct shear rates between 0.06 and 100. inverse seconds. Median sphere diameters were 26, 61, 125, 183, and 221 microns. End effects were determined by a two bob technique, and smooth and artificially roughened cylinders were used to determine wall effects.

Monomodal suspensions were found to be power law fluids with strictly Newtonian flow properties at concentrations of 35 volume percent of solids or less, but exhibiting dilatancy at concentrations above 40 volume percent of solids. Relative viscosities and a value of the Mooney self-crowding factor, λ_{ii}, are reported for monomodal suspensions with concentrations between 20 and 40 volume percent of solids, and the power law parameters are reported for monomodal suspensions with concentrations between 40 and 52 volume percent of solids.

Bimodal suspensions were found to be power law fluids with strictly Newtonian flow properties in the range of total concentrations up to the onset of dilatancy at total concentrations near 60

Abstract -- Continued

volume percent of solids for compositions at which the relative viscosity was minimized. The Mooney bimodal crowding factors, λ_{ij}, were determined at nine diameter ratios between 0.12 and 0.68.

Trimodal suspensions with size ratios 0.14, 0.33, 1, at a total concentration of 45 volume percent of solids were found to be Newtonian fluids. The relative viscosities of these trimodal suspensions were found to be greater at all compositions than the minimum relative viscosity of an equally concentrated bimodal suspension of spheres with a size ratio of 0.14.

The experimental results were discussed in terms of previous investigations and of the principal theoretical results appearing in the literature. Additional work was recommended in order to define the limits of Newtonian flow and the power law parameters for bimodal and trimodal suspensions as a function of size ratio, composition, and concentration. The approximate location of the anticipated minimum in relative viscosity as a function of trimodal composition was discussed.

CONTENTS

INTRODUCTION

This is an account of research in one of the important topics in the study of the flow of fluid-solid mixtures: the rheology of suspensions. The approach taken was the first of the three described by Rivlin at the I.U.T.A.M. Symposium on the flow of fluid-solid mixtures: "...(1) find out the experimental facts, using theory only to obtain meaningful results; (2) construct physical models (a mathematical, not an engineering, exercise) and proceed from the particular to the general; (3) produce a general theory within a broad framework..." On that occasion, Rivlin was paraphrased as having "...reminded the audience of the great importance of method (1) which provides our knowledge of real materials; method (3) is often attacked as being unrelated to real materials, but that it is often method (2) which misrepresents the facts." (14)

The rheology of suspensions is one of those research areas which has both a wealth of immediate practical applications and a continuing scientific significance. The problem of measuring, controlling, and predicting the flow behavior of concentrated suspensions of solid material in a liquid vehicle has been industrially important for a long time and remains so today. The particular problem of the viscosity of concentrated suspensions of neutrally buoyant, rigid spheres in Newtonian fluids has been of theoretical interest for over sixty years. Contributions to this theory continue to appear regularly in the recent scientific literature.

The theory seems to have outstripped the evidence. The experimental evidence on monomodal suspensions has been debilitated by marked discrepancies between investigations, illustrated in Figure 1, and so has not been able to furnish a sufficiently powerful test of the many conflicting theoretical results. The experimental literature is at odds over the concentration at which suspensions become non-Newtonian, and over the range of influence of composition upon the relative viscosity of multimodal suspensions. There is a pervasive belief in a similarity between concentrated suspensions and packed beds of spheres, but that relationship has never been defined. Some potentially useful predictions of the theory, particularly in the area of viscosity minimization, have yet to be thoroughly explored.

Recent developments in rotational viscometers have made available a new instrument, the Gilinson-Dauwalter-Merrill (GDM) concentric cylinder rotational viscometer, of radically improved accuracy and precision. Use of this instrument in the determination of the flow curves of concentrated suspensions of rigid spheres offers new opportunities to make significantly more sensitive comparisons of theory and experiment. The potentially useful predictions of the theory about viscosity minimization can be carefully tested by new data of reduced experimental uncertainty and wider scope.

In the following pages, the literature on the relative viscosity of concentrated suspensions of neutrally buoyant, rigid

spheres in Newtonian fluids is summarized, with special emphasis on those investigations which included suspensions containing more than one size of spheres. The objectives of this research are set forth in the light of this summary. The materials, equipment, and methods employed in the work are described. The experimental results are stated and discussed in the framework of previous work and the objectives laid down for the present work. The conclusions are drawn to meet the objectives as far as possible, and recommendations are made for useful extensions or continuations of this research.

Nomenclature

The following symbols and conventions will be used throughout this account. Other symbols will be defined in the context in which they are employed.

μ coefficient of viscosity; the constant ratio of shear stress to shear rate in Newtonian fluids,

$$\mu = \frac{\tau}{\dot{\gamma}}$$

the slope of the flow curve for non-Newtonian fluids,

$$\mu = \frac{d\tau}{d\dot{\gamma}(\tau)}$$

poise, or g/cm sec.

μ_o the viscosity of a pure fluid or a mixture of fluids.

μ_s the viscosity of a suspension.

μ_r relative viscosity of a suspension, the ratio of the vis-

cosity of a suspension to the viscosity of the pure suspending fluid at the same conditions of shear rate, temperature:

$$\mu_r = \frac{\mu_s}{\mu_o}$$

dimensionless.

φ total volume fraction or volume percent of spheres in a suspension, dimensionless.

φ_i volume fraction of the i^{th} size, or group of spheres in a suspension containing more than one size or group of spheres.

φ_m total volume fraction of spheres of all sizes at which the relative viscosity of a suspension tends to infinity.

φ_o volume fraction of fluid in a suspension.

Ω_o angular velocity of the outer cylinder, radians per second.

τ viscous shear stress, the force per unit area exerted on a surface by a fluid in laminar flow past that surface; dynes/cm^2.

τ_1 viscous shear stress at the surface of the inner cylinder in concentric cylinder viscometer.

θ cylindrical coordinate, angle.

$\dot{\gamma}$ shear rate, the rate of change of fluid velocity with distance in the direction perpendicular to the streamlines; reciprocal seconds.

$\dot{\gamma}(\tau_1)$ shear rate at the surface of the inner cylinder in a concentric cylinder viscometer.

λ_{ij} the crowding factors of Mooney's equation for the relative viscosity of a multimodal suspension of spheres.

L height of the bob in a concentric cylinder viscometer, cm.

M torque, dyne cm.

r radius or radial space coordinate, cm, or microns (μ).

r_i, r_j radius of the i^{th}, j^{th}, size of sphere, respectively, with subscript 1 denoting the smallest sphere, microns.

s ratio of outer cylinder (cup) radius to inner cylinder (bob) radius in a concentric cylinder viscometer.

T temperature, degrees Celsius.

"Concentration" denotes the sum of the volume fractions of all sizes of spheres in a suspension of spheres; the ratio of total volume of solids to the total volume of the suspension; dimensionless, expressed either as a decimal fraction or as a percentage.

"Composition" denotes the physical make-up, on the basis of diameter, of a mixture of spheres. Composition is expressed in terms of "size distribution", the fraction of <u>solid</u> volume in a mixture contributed by each size of sphere, expressed as a percentage, and "size ratio", the ratio of radii or diameters of each size of sphere to the largest size in the mixture, expressed as a decimal fraction.

"Multimodal" is the generic term used to designate suspensions or mixtures of spheres for which a histogram of number of spheres versus diameter of sphere would show more than one distinct maximum;

"bimodal" denotes those with two predominant and clearly defined sizes;

"trimodal" denotes those with three predominant and clearly defined sizes, etc.

The "flow curve" of a material is the graph of shear stress (ordinate) versus shear rate (abscissa) under isothermal conditions; it may be on arithmetic, logarithmic, or sometimes square root coordinates. It is the basis for the rheological classification of materials.

Summary of the Literature

The more than sixty years of theoretical interest in the relative viscosity of concentrated suspensions of spheres has resulted in a luxuriant literature which Rutgers (42,43) and Thomas (51) have reviewed. More recent contributions by others and the highlights of the literature on monomodal suspensions will be summarized before going on to the more limited literature of multimodal suspensions.

The field was pioneered in 1905 by Einstein (16), who arrived at the following result for the relative viscosity of a dilute suspension of spheres in a Newtonian fluid:

$$\mu_r = \frac{1 + 1/2\varphi}{1 - 2\varphi} = 1 + 2.5\varphi$$

in which μ_r is relative viscosity and φ is the concentration (volume fraction) of spheres.

The principal assumptions in his derivation were:

the spheres were small, rigid, smooth, uniform in size, and inertialess;

there was no slip at the fluid/solid interface;

the spheres and fluid were of equal density;

the suspension was so dilute that there was no interaction between spheres, and

the suspension was isothermal.

By 1962, Rutgers (42) was able to collect no less than ninety-eight distinct theoretical equations relating relative viscosity to the concentration of solids in various sorts of suspensions. His classification of these formulas, with examples, is shown in Table 1. In his discussion, Rutgers pointed out that experimental verification had been claimed for all of the equations. For the special case of generally Newtonian suspensions of small, uniform, rigid spheres which neither aggregate nor solvate in Newtonian fluids of lower viscosity and equal density he concluded that the following five equations had validity over usefully wide ranges of concentration:

Ford (20): $$\frac{1}{\mu_r} = 1 - 2.5\varphi + 11.0\varphi^5 - 11.5\varphi^7$$

Vand (54): $\frac{1}{\mu_r} = (1 - 1.1\varphi - 0.97\varphi^2)^{2.5} = (1 - \varphi - 1.20\varphi^2)^{2.5}$

$\varphi_m = 0.59$

Simha (45): $\mu_r = 1 + 2.5\,[\lambda(\varphi,f)]\,\varphi$

Maron (34): $\mu_r = \frac{1}{(1-1.35\varphi)^2} + \frac{A(1.35\varphi)^2}{(1-1.35\varphi)^3} + \frac{B(1.35\varphi)^2}{(1-1.35\varphi)^5}$

Mooney (37): $\mu_r = \frac{2.76\varphi}{1-1.29\varphi} = \frac{2.5\varphi}{1-1.40\varphi}$

All but the Ford equation have a theoretical development, and Rutgers was unable to choose any one as being the most sound, but indicated a preference for the Vand and Mooney equations. He was of the opinion that more exact measurements of viscosities of suspensions of spheres were needed, especially at concentrations larger than twenty percent of spheres by volume.

In a companion paper, Rutgers (43) also reviewed the experimental results in the literature for monomodal suspensions of rigid spheres. On the basis of his own judgment he chose several sets of data from which he produced an "average sphere concentration curve" of relative viscosity versus volume concentration of spheres. This curve, which he termed rather arbitrary, was claimed to be valid for all shear rates for concentrations less than twenty percent, and for moderate shear rates for concentrations between twenty-five and forty-five percent, but to "merit less than reasonable confidence" for concentrations above forty-five percent. He suggested that

TABLE 1

Rutger's Classification of Relative Viscosity Equations

1. Einsteinian $\mu_r = 1 + k\varphi$

2. General progression $\mu_r = 1 + k\varphi + A\varphi^2 + B\varphi^3 + \ldots$

3. Logarithmical $\ln \mu_r = k\varphi$

4. Power $\log \mu_r = a + n \log \varphi$

5. Fluidity progression $\frac{1}{\mu_r} = 1 - k\varphi + A\varphi^2 + B\varphi^3 + \ldots$

6. (Polynomial) $\mu_r = 1 + \frac{k\varphi}{1 + A\varphi}$

7. Those with: $\frac{1}{1 - A\varphi}$ $\mu_r = \frac{1 + (k=A)\varphi}{1 - A\varphi}$

8. Logarithmical with φ terms in numerator and denominator

$$\log \mu_r = \frac{k\varphi + A\varphi^2}{1 + B\varphi}$$

9. Mixed $\mu_r = 1 + k\varphi + A\varphi^2 + B \exp(C\varphi)$

10. Various (van der Poel's numerical solution)

φ	0	0.1	0.2	0.3	0.4	0.5	0.6	0.65	0.70
μ_r	1.0	1.29	1.73	2.50	4.08	8.10	21.4	42.5	79.0

relative viscosity was independent of sphere size in good quality monomodal suspensions, except for the very small sizes less than five microns in diameter. Some critical concentrations were suggested, and the call for more accurate experimental work between twenty and fifty percent concentrations at varying shear rates was repeated. Rutger's "average sphere concentration curve" is shown in Figure 1.

The more recent review of experimental results by Thomas (51) resulted in a new summary curve of relative viscosity versus concentration of spheres as shown in Figure 1 also, and the following new equation for relative viscosity:

$$\mu_r = 1 + 2.5\varphi + 10.05\varphi^2 + 0.00273 \exp(16.6\varphi)$$

The constants in the last term are empirical and were determined by a least squares fit to the new summary curve. The other constants are from previous theoretical treatments (54,33). Thomas' handling of the published data is very interesting. By means of several extrapolations he attempted to eliminate non-Newtonian, inertial, and inhomogeniety effects so as to isolate the concentration dependence of relative viscosity. It appears from his plots that he was able to use only four of the sixteen sets of data he cited in plotting his new summary curve. Thomas attempted to fit a variety of equations to the new curve: in particular, the one given above, and a pair of theoretical equations due to Simha (45) in which he was able to evaluate an adjustable parameter, f, which had been supposed a function of concentration. Thomas got a good fit with a single value. There

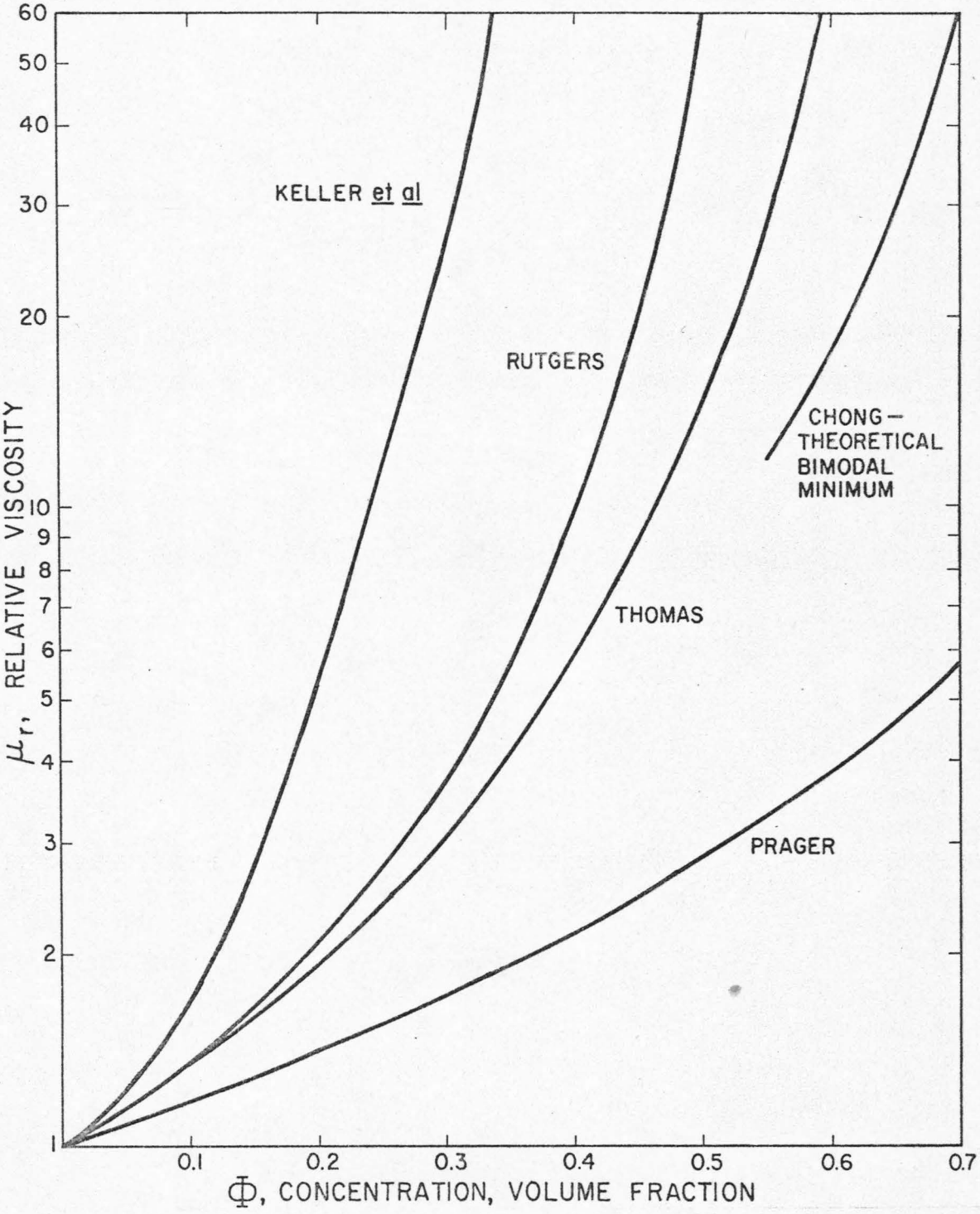

Figure 1. Relative viscosity curves.

seem to be three important features in Thomas' review:

much of the published data is not comparable (implied);

the new curve and the new equation requiring only two empirical constants; and

a new requirement for experimental data, namely that they should be taken over a sufficiently wide range of shear rate and sphere size to permit the secondary effects to be either evaluated or eliminated.

In a commentary accompanying Thomas' review, Simha and Somcynsky (46) used Thomas' new summary curve to re-examine the earlier theory by Simha, and found satisfactory agreement between the curve and the theory for a fixed value of the adjustable parameter. Here again, the existing data were suggested to be inadequate to properly test the theory, since the parameter was originally presumed to be concentration dependent.

In the more recent theoretical contributions, Chong (10) employed a solution of the equations of creeping motion and continuity to derive the following equation for relative viscosity

$$\mu_r = 1 + \frac{5}{2} \Omega_H \varphi$$

in which

$$\Omega_H = \frac{4 - \frac{16}{25}\varphi^{7/3} - \frac{84}{25}\varphi^{2/3}}{4(1 - \varphi^{5/3})^2 - 25\varphi(1 - \varphi^{2/3})^2}$$

In his discussion of this equation and the experimental evidence, Chong remarked that the hydrodynamical, fluid cage model, treatment

of the calculation of the relative viscosity of monomodal suspensions appears to be inadequate at concentrations above fifty volume percent solids.

Keller et al. (28) have derived theoretical upper and lower bounds on the relative viscosity of a suspension of identical spheres for concentrations up to that corresponding to simple cubic packing. For the case of rigid spheres, their expression simplifies to

$$\mu_r \leq 1 + \frac{5\pi}{3}\left[\frac{\lambda^3(1 - \lambda^7)}{4\lambda^{10} - 25\lambda^7 + 42\lambda^5 - 25\lambda^3 + 4}\right]$$

$$\lambda = (6\varphi/\pi)^{1/3}$$

The lower limit is a constant, $1 + \frac{\pi}{6}$, for high concentrations. At low concentrations their expressions reduce to the Einstein equation. The upper limit is plotted on Figure 1.

Frankel and Acrivos (21) derived the following equation for relative viscosity at high concentrations:

$$\mu_r = \frac{9}{8}\frac{(\varphi/\varphi_m)^{1/3}}{1 - (\varphi/\varphi_m)^{1/3}}$$

The derivation assumed high concentration of spheres, so that

$$\varphi/\varphi_m \rightarrow 1$$

and also assumed a simple cubic orientation of neighboring spheres in order to evaluate the leading constant. The leading constant is

sensitive to the geometry assumed to exist between the spheres in the suspension, but the simple cubic assumption was claimed to best fit the experimental data. This equation was shown to fit both the Rutgers and the Thomas curve in the high concentration range, provided φ_m was determined separately from each curve. Frankel and Acrivos made two especially interesting observations:

> they characterized the agreement among the various investigations of relative viscosity at high concentration as "poor", and
>
> they suggested that collisions, aggregation, and inertial effects may be of minor importance in the usual experimental arrangements.

Moulik (38) proposed the equation

$$(\mu_r)^2 = a + b\,\varphi^2$$

on empirical grounds based on observations of the change in relative viscosity of electrolyte solutions with concentration, in the concentration range beyond that in which the Einstein equation is valid.

Allen and Kline (6) employed a continuum model with a substructure to derive an expression for the relative viscosity of a suspension of rigid spheres which is of the form of a two term fluidity polynomial. The most interesting result of their theory, for present purposes, is their derivation of an internally consistent concentration limit on the validity of their theory. Allen and Kline put the limit of validity of their theory at forty volume percent or less.

Lee (30) extended Vand's equation and the Roscoe-Brinkman equation to a dependence on higher powers of concentration based on arguments concerning the hydrodynamic effects of collision multiplets and the trapping of suspending fluid by collision multiplets. His discussion of these equations in relation to the experimental data is limited to the behavior of colloidal suspensions at low to moderate concentrations where the rheological behavior resembles that of a Bingham plastic.

There is a lengthy record of theoretical and experimental effort to measure and calculate the flow behavior of suspensions of submicron and micron sized latex particles contained in the pages of Journal of Colloid and Interface Science, and elsewhere. These investigations can be characterized by a single dominating factor: the treatment of the electroviscous effect. Where electroviscous effects are neglected, incompletely suppressed, or inadequately dealt with, flow studies very nearly always report non-Newtonian flow, variation of relative viscosity with sphere diameter, and failure of the usual equations describing relative viscosity as a function of concentration. By way of contrast, Stone-Masui and Watillon (48) and Brodnyan (8) were able to report Newtonian flow, superposition for all sizes, and good agreement with the Mooney equation for low concentrations.

There was no attempt to resolve this difficulty in this account, rather the experimental conditions--namely, the sphere diameters--were chosen to avoid electroviscous effects as far as possible.

Bagnold (7), in what appears to be a unique contribution, has measured the viscosity of suspensions of 1300 micron spheres in two neutrally buoyant fluids between concentrations of 13 and 62 volume percent in a Couette viscometer of good design. He reported Newtonian flow at concentrations below 55.5 volume percent and no detectable difference between smooth or rough cylindrical surfaces. He also reported the presence of a normal stress on the inner cylindrical surface and related it to the solids concentration. He correlated his results for relative viscosity at concentrations below 55.5 volume percent with the equation

$$\tau = (1 + \lambda)(1 + \tfrac{1}{2}\lambda)\,\mu\,\dot{\gamma}$$

in which

$$\lambda = \frac{1}{(\varphi_m/\varphi) - 1} \quad , \quad \varphi_m = 0.74$$

In a more familiar form this is a second order polynomial in $\frac{\varphi/\varphi_m}{1 - \varphi/\varphi_m}$.

Clarke (11) reported measurements of the viscosity of water suspensions of glass and poly(methylmethacrylate) spheres of 53-76 micron diameter at concentrations up to 50 volume percent solids. The viscosity of these suspensions were reported as Newtonian for concentrations up to 50 volume percent, with viscosity a function of particle density. Evidence of a minimum in viscosity with size distribution in a bimodal suspension was found. Evidence of a wall-suspension slip was claimed, and artificially roughened cylindrical

surfaces were employed in the rotational instrument used in order to prevent such an effect. Unfortunately, the rotational instrument used in these measurements did not appear to have produced a viscometric flow, nor were the measurements interpreted in rheological terms.

Lewis and Nielsen (31) reported experimental measurements of the relative viscosity of suspensions of dispersed and aggregated spheres of 7, 34, 51, and 95 micron diameter at concentrations from 5 to 50 volume percent solids in a Couette apparatus. They report Newtonian flow up to about 45 volume percent and a good fit to the Mooney equation in that range of concentrations. Their value of 1.35 for the self-crowding factor corresponds to a maximum monomodal concentration of 0.74. Their measurements showed no electroviscous effects at the small diameters, possibly because of the high viscosity of their suspending medium, and no influence of sphere diameter upon relative viscosity. Their measurements of the relative viscosity of suspensions of permanent aggregates of single-size spheres also showed Newtonian flow at concentrations up to 35 volume percent.

Gay et al. (24) reported pipe flow measurements on suspensions of 34.5 and 64 micron glass spheres suspended in glycerine at concentrations of 51 and 55 volume percent, respectively. They found pronounced non-Newtonian flow, a yield stress, and a complex three-part flow curve in the shear rate range between 0.5 and 5.0 inverse seconds.

Seshadri and Sutera (47) reported the relative fluidities of suspensions of 43, 460, and 920 micron spheres of styrene divinyl benzene and Dylene 8 in neutrally buoyant fluids, at concentrations between five and forty volume percent solids. The flow curves and fluidity functions as a function of concentration are not displayed. The relative fluidity of the suspensions does not appear to be a function of sphere size or shear rate.

Chong et al. (10) determined the relative viscosity of monomodal suspensions of glass spheres suspended in polyisobutylene in concentrations from forty-five to sixty volume percent solids at shear rates between zero and six inverse seconds in an orifice-jet viscometer of his own design. Pseudoplastic flow was observed, but the extrapolated viscosity at zero shear rate was determined. Relative viscosity at zero shear rate was found to be independent of sphere diameter and temperature. The maximum concentration for monomodal suspensions was found to be 0.605, and anomalous flow curves were observed at concentrations near or exceeding this concentration with volumetric dilatancy presumed to be the cause. Chong was able to correlate his own and very much other relative viscosity and relative modulus data with the following equation:

$$\frac{\mu_s}{\mu_o} = \frac{E_s}{E_o} = \left[1 + 0.75\left(\frac{\varphi/\varphi_m}{1 - \varphi/\varphi_m}\right)\right]^2$$

in which $\varphi_m = 0.605$.

The literature specifically concerned with multimodal suspensions of spheres has not been so well reviewed. In the following summary, the principal theoretical and experimental results for the effects of size distribution of spheres upon the relative viscosity of multimodal suspensions are cited. The theoretical predictions of the lower bound on relative viscosity are also given.

The theoretical results for the combined effects of the composition of the mixture of spheres in a multimodal suspension upon relative viscosity are of two general types: Mooney's equation and equations involving only φ_m. The term "composition" will be used to denote the make-up of a mixture of spheres on the basis of diameter as described by size distribution (percent of solid volume contributed by each size of sphere), and size ratio (ratio of radii or diameters of each size of sphere to the largest size in the mixture). By contrast, "concentration" will always be used to denote the total volume fraction of spheres of all sizes in a suspension.

Mooney (37) gave two forms of his equation:

$$\ln \mu_r = 2.5 \sum_{i=1}^{n} \frac{\varphi_i}{\sum_{j=1}^{n} \lambda_{ji}\varphi_j}$$

for multimodal suspensions of n sizes of spheres, and

$$\ln \mu_r = 2.5 \int_0^{\varphi} \frac{d\varphi_i}{1 - \int_0^{\varphi} \lambda_{ji} d\varphi_j}$$

for suspensions with a continuous distribution of sphere sizes. φ_i is the volume fraction of the i^{th} size of sphere, and λ_{ij} is an interaction or crowding factor. Mooney did not evaluate the interaction factors in detail, but deduced their general behavior as a function of radius ratio as shown in Figure 2. λ_{ii} is the constant in the denominator in the monomodal form of Mooney's equation discussed previously. Mooney left the determination of the interaction, or crowding, factors to experiment. He called for experimental data from measurements on mono-, bi-, and multimodal suspensions over a range of closely controlled composition and concentration.

Farris (19) employed the synthetic fluid concept to derive on phenomenological grounds an equation of the Roscoe-Brinkman type for the relative viscosity of multimodal suspensions of spheres whose size ratios are always less than 0.1 so that they may be considered non-interacting. The minimum relative viscosity for multimodal suspensions of any composition at a given concentration, and the optimum compositions of bimodal, trimodal, and tetramodal suspensions of non-interacting spheres were calculated for concentrations between sixty-four and ninety volume percent solids. The effect upon relative viscosity of the conversion of a concentrated monomodal suspension to a bimodal suspension by the successive additions of larger, or smaller, non-interacting spheres was calculated. For bimodal suspensions of spheres in which the size ratio is larger than 0.1, a crowding factor resembling Mooney's small-sphere crowding factor was introduced, and the need for experimental data with

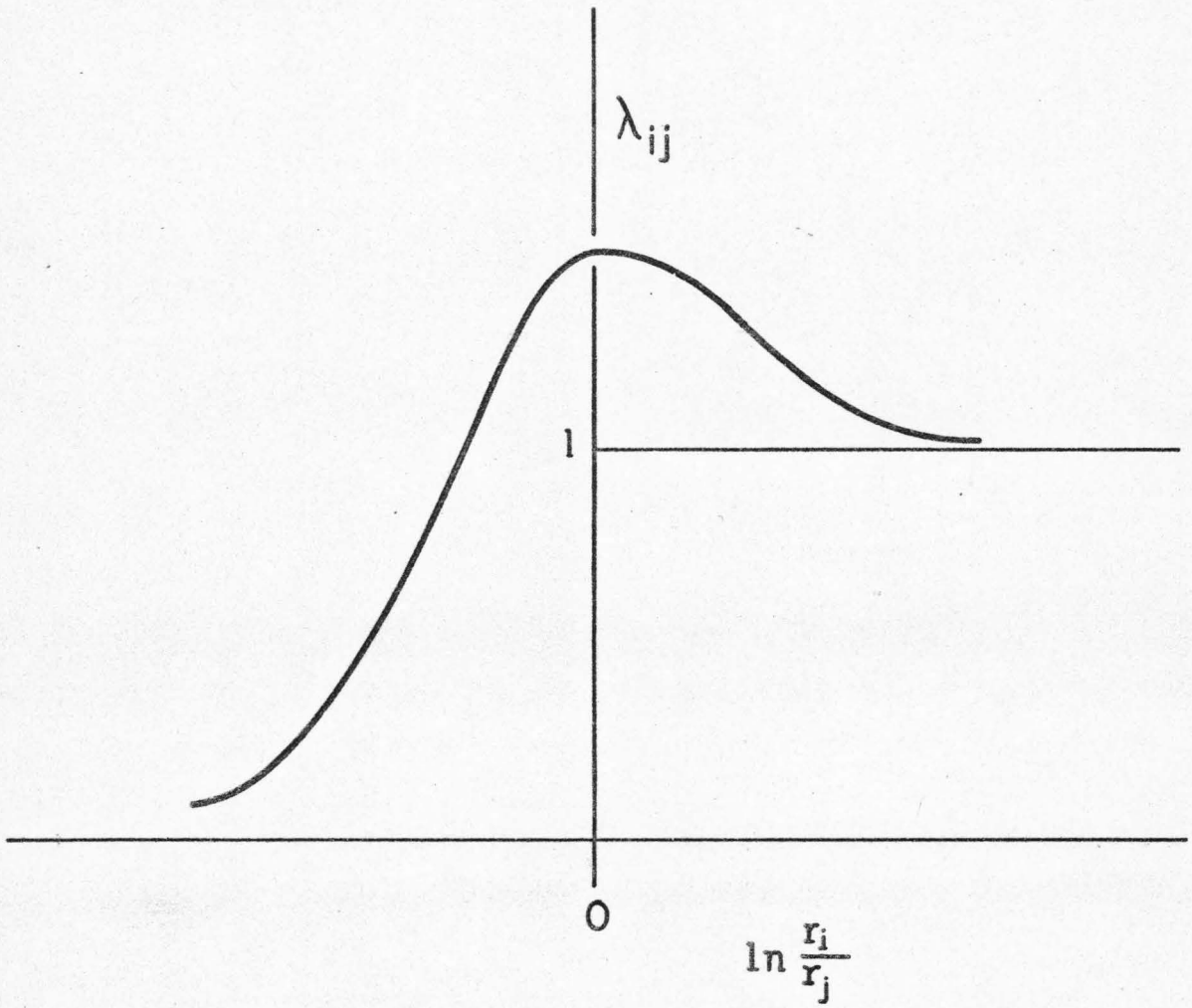

Figure 2. Properties of the Mooney bimodal crowding factor, λ_{ij}.

which to evaluate it was expressed.

It is important to note that Farris writes of the viscosity of monomodal suspensions of concentrations of sixty volume percent and of multimodal suspensions of concentrations of ninety volume percent. There may be some question as to whether or not these concentrations are rheologically attainable.

The second type of theoretical result is the class of relative viscosity equations which incorporate the φ_m parameter. φ_m is the total volume fraction of spheres of all sizes taken together at which the relative viscosity of a suspension tends to infinity. Some examples of these equations are:

Eilers (15) $$\mu_r = \left[1 + \frac{2.5\varphi}{2(1-\varphi/\varphi_m)}\right]^2$$

Roscoe (41) $$\mu_r = \left[1 - \frac{\varphi}{\varphi_m}\right]^{-2.5}$$

Frankel and Acrivos (21) $$\mu_r = \frac{9}{8} \frac{(\varphi/\varphi_m)^{1/3}}{1 - (\varphi/\varphi_m)^{1/3}} \quad .$$

The appropriate value for φ_m has been discussed most widely in the context of monomodal suspensions of equal sized spheres, using the packing behavior of equal sized spheres as a model. However, there exists a considerable body of information on the packing behavior of mixtures of different sizes of spheres which has been reviewed by Haughey and Beveridge (26). Several previous investigators

(8,10,49,55) have suggested that the dependence of maximum density upon composition in multimodal packed beds of spheres may offer a means of applying the φ_m form of relative viscosity equations to multimodal suspensions.

A recurring feature of the theoretical treatment of multimodal suspensions is the concept of a synthetic fluid. The largest spheres in a multimodal suspension are viewed as being immersed in a synthetic fluid composed of the liquid plus all the smaller sizes of spheres. The relative viscosity of the suspension is calculated on the basis of a monomodal suspension of the large spheres in a fluid of increased viscosity. The relative viscosity of the synthetic fluid is calculated on the basis of a monomodal suspension of the second largest spheres in a synthetic fluid composed of the liquid and all smaller sizes of spheres, and so on. The relative viscosity of the multimodal suspension is ultimately expressed as the product of monomodal relative viscosity factors, one factor for each size of sphere:

$$\mu_r = (\varphi_1, \varphi_2, \ldots \varphi_i, \ldots \varphi_n) = \mu_r(\varphi_1) \sum_{i=2}^{n} \mu_r(\varphi_i')$$

In the relative viscosity factor for the i^{th} size of sphere, the volume fraction φ_i' is to be adjusted as though the larger sizes of spheres were not present, e.g.:

$$\varphi_i' = \frac{\varphi_i}{1 - \sum_{1}^{i-1} \varphi_i}$$

in which the i^{th} size of sphere is presumed to be smaller than the $i+1^{st}$.

It should be mentioned here that λ_{ii} or the constant in the denominator of the monomodal form of the Mooney equation is often considered to be $(\varphi_m)^{-1}$.

In most of the treatments of φ_m to date, φ_m has been determined by fitting the relative viscosity equation to the experimental data using φ_m as an adjustable parameter. The value of φ_m so determined has been interpreted as indicating the type of sphere packing obtained in the suspension for which relative viscosity is infinite.

The experimental literature for multimodal suspensions has been summarized in two parts: Table 2 is a summary of the concentrations, sizes, size ratios and size distributions of the multimodal suspensions reported in the literature. (It can be made to fold out for convenient reference.) A brief statement of the findings of the previous investigators, and other comments, is given below. The order is approximately chronological.

Ward and Whitmore (55) used a rising sphere viscometer to measure the viscosity of suspensions of methyl methacrylate polymer spheres in an aqueous solution of lead nitrate and glycerol. Their results were stated in terms of relative viscosity as a function of concentration and size ratio. They plotted relative viscosity versus size ratio, with concentration as a parameter. By extrapolating these curves to a size ratio of unity, they obtained the relative viscosity of perfectly monomodal suspensions as a function of con-

centration. They concluded that relative viscosity was independent of shear rate, sphere size, and liquid viscosity for concentrations up to 30%. They found that relative viscosity at a fixed concentration decreased as the size ratio of the smallest to the largest sphere decreased from unity. The limiting value of relative viscosity was reached at size ratios of about 0.3 for all concentrations up to 30%. They note the possibility of electrostatic effects upon the viscosity of dielectric spheres in a non-polar liquid, but attribute the effect to forces other than the electrical double layer "zeta potential."

Eveson, Ward, and Whitmore (18) used a concentric cylinder viscometer to measure the properties of bimodal suspensions of methyl methacrylate spheres in an aqueous solution of lead nitrate and glycerol. Non-Newtonian behavior was reported for concentrations greater than 5%. The properties of the liquid were claimed to be unimportant so long as chemical reactions, flocculation, or electrostatic effects were absent. Systematic variation of relative viscosity with size distribution, with a minimum, was found at concentrations greater than 10%. This was concluded not to be due to the effect of packing among the spheres since closest packing in beds of spheres was claimed to occur at compositions of about 1% small spheres. The minimums in relative viscosity versus size distribution were observed at suspension compositions of slightly less than 50% small spheres. Surface area was not considered to be an important variable. The suspensions were suggested to behave as suspensions

of the larger spheres in a (synthetic) fluid consisting of a suspension of small spheres.

The source of their information about the packing of spheres is not cited; it would seem to be in error.

Maron and Madow (34) used capillary tube and concentric cylinder viscometers to make measurements on bimodal suspensions of rubber latices. The bimodal suspensions were found to be non-Newtonian above concentrations of 25%. Relative viscosity as a function of size distribution was found to have a minimum for size distributions of 50% to 90% small spheres at concentrations higher than about 30%. The experimental results were fitted with an equation of the Mooney type, with φ_m to be determined. φ_m was found to be a function of size distribution, and to compare very well with the values of maximum volume fraction of solids in packed beds of spheres as predicted by the theories of Furnas (23) and Frazer (22). The results were considered to be in excellent agreement with Frazer. The results were claimed to show that multimodality can contribute materially to the tightness of packing of spheres in a suspension, and hence multimodal suspensions should exhibit flow at higher concentrations than monomodal suspensions.

Williams (56) used a concentric cylinder viscometer to make measurements upon bimodal suspensions of glass spheres in solutions of glycerol and water. The suspensions were Newtonian for concentrations up to 50%. The plots of relative viscosity versus size distribution did not display definite minima. He offered the

generalization that size distribution of rigid spheres in a multimodal suspension markedly affected the viscosity at concentrations higher than 30%. He observed that the data then available on the effect of size distribution were insufficient to allow conclusive empirical relationships to be derived.

As a part of his discussion, Williams gave a compact description of the preparation, fractionation, and particle size analysis of small glass spheres.

Sweeny and Geckler (50) used a concentric cylinder viscometer to measure the properties of four bimodal suspensions of glass spheres in an aqueous solution of zinc bromide and glycerol over a range of shear rates. The size ratios of the spheres were chosen in accordance with the theory by Hudson (27) on the packing of spheres. Viscosity of the bimodal suspensions was found to be reduced from the viscosity of monomodal suspensions of the same concentration. The authors concluded that the data presented gave quantitative evidence of the effect of bimodal size distribution in reducing the viscosity of concentrated suspensions and qualitative proof of the interpretation of the crowding factors of the Mooney equation.

Ting and Luebbers (52) used a Brookfield viscometer to measure the viscosity of binary and trimodal mixtures of glass beads in mixtures of carbon tetrachloride and s-tetrabromoethane, castor oil and s-tetrabromoethane, and possibly corn syrup. Measurements were made at only a single shear rate for each suspension. These

authors do not present their results in terms of relative viscosity and size distribution or concentration, but give instead a correlation equation in a rearrangement of the following equation:

$$\mu_r = (1 - \varphi/\varphi_m)^{-1}$$

They note that φ_m of a multimodal mixture can be greater than in a monomodal mixture, but recommend the use of φ_m from monomodal mixtures in their correlation, compensating with an empirical coefficient. It was pointed out that the size distribution of particles does affect the viscosity of suspensions and that the effect is related to the packing of the spheres in the suspension.

Metzner and Whitlock (35) used both rotational and capillary viscometers to measure the flow properties of monomodal and one trimodal suspension of glass beads in a sucrose solution. Their principal purpose was to investigate rheological dilatancy, and since dilatancy was not observed in any of the suspensions of glass beads, they didn't report the results of the measurements. Presumably the trimodal suspensions were Newtonian.

Eveson (17) reported results based on measurements taken with a concentric cylinder viscometer on several bimodal and one trimodal suspension of methyl methacrylate spheres in an aqueous solution of lead nitrate and glycerol. He found Newtonian behavior at all concentrations up to 22.5%. An effect of size distribution on relative viscosity was found only at concentrations over 20%. He compared the

experimental relative viscosities to those calculated from a synthetic fluid formulation using experimental monomodal relative viscosities, and found good agreement up to a different concentration for each composition. The single trimodal suspension showed generally lower relative viscosity than for monomodal suspensions of equal concentration. The methacrylate spheres were noted to absorb water from the suspending solution. Eveson recommended further work on trimodal suspensions.

Sweeny (49) determined relative viscosity as a function of size distribution in bimodal suspensions of glass beads in an aqueous solution of zinc bromide and glycerol. The size ratios were chosen on the basis of the sphere packing theory of Hudson (27). The results show that minima in relative viscosity as a function of size distribution occur at 25% to 50% small spheres in agreement with the theories of bulk density in packed beds of spheres (22,23). The interaction factors, λ_{12} and λ_{21}, appearing in the bimodal form of the Mooney equation are evaluated at the chosen size ratios. The behavior of the interaction factors as a function of size ratio was in general agreement with Mooney's theoretical deductions, but were generally smaller in magnitude and appeared to be concentration dependent. The close resemblance between the bulk density and relative viscosity relations was pointed out and further work was suggested to relate the Mooney theory to the packed bed theory.

These results are somewhat marred by a time dependency of the properties of the suspensions which may have been caused by

hygroscopic behavior of the suspending solution, and by a shear rate dependency.

Chong (10) measured the properties of bimodal suspensions of glass spheres in poly-isobutylene with an orifice-jet viscometer. The size ratios were chosen on the basis of Hudson's (27) theory of sphere packing. The suspensions were found to be Newtonian at low shear rates, but pseudoplastic at shear rates greater than 0.2 inverse seconds. He concluded that relative viscosity in bimodal suspensions decreased with decreasing size ratio, with relative viscosity approaching a limiting value at a size ratio of 0.10. He offered the generalization that the decrease in relative viscosity of bimodal suspensions occurs in the direction of increasing bulk density. The zero shear relative viscosity was correlated with φ_m and concentration with the equation mentioned earlier.

Brodnyan (8) determined the relative viscosities of monomodal and bimodal suspensions of submicron poly(n-butyl methacrylate) latices in an aqueous salt solution from measurements in both capillary tube and rotational viscometers. The Mooney equation, in a form involving φ_m, was fitted to each set of relative viscosity-concentration results with the constants to be determined. The values of φ_m for the monomodal suspensions were 0.65, 0.645, and 0.645. φ_m for the bimodal suspensions was 0.82 and 0.70. He pointed out that the values of φ_m for the monomodal suspensions are not significantly different from the value of 0.636 observed for packed beds of equal-sized spheres. He further noted that the increase in

φ_m observed for the bimodal suspensions was also noted in packed beds of mixed sizes of spheres. He found reasonable agreement between the experimental values of φ_m for the suspensions and the results of Yerazunis, et al. (57) for the packing of macroscopic spheres.

Parkinson et al. (39) reported measurements of the viscosities of dilute mono-, bi-, tri-, and tetra-modal suspensions of micron and submicron polymer latices in which a minimum in relative viscosity with composition occurred near twenty-five volume percent small sphere in the bimodal suspensions but no minimum occurred in the higher order multimodal suspensions. Regrettably, these results were marked by the usual difficulties associated with electroviscous effects.

Sacks et al. (44) reported similar results in the pumping characteristics of coal char slurries in which a bimodal suspension of coal char reduced the pressure drop at constant average velocity compared to monomodal or to polydisperse slurries.

The question of the lower bound on relative viscosity has been considered by Chong (10), by Prager (40), and by Keller et al. (28). Chong claimed to have used the synthetic fluid formulation to calculate the lower limit on the relative viscosity of bimodal suspensions in which the size ratio approached zero. His values are shown on Figure 1. Prager derived the following equation for the minimum possible relative viscosity for any suspension whatever:

(This page intentionally left blank)

TABLE 2

Previous Investigations of Multimodal Suspensions

Investigator	Type	Sphere Diameter, μ
Ward and Whitmore	continuous	152-177
		147-208
		72-208
		38
Eveson, Ward, and Whitmore	bimodal	38, 182
Maron and Madow	bimodal	980 A, 1920 A
Williams	bimodal	4, 12
Sweeny and Geckler	bimodal	164, 261.6
	bimodal	97, 261.6
	bimodal	35.9, 261.6
	bimodal	12.6, 261.6
Ting and Luebbers	bimodal	not stated
	trimodal	not stated
	trimodal	not stated
Metzner and Whitlock	trimodal	28, 57, 100
Eveson	bimodal	46.5, 377
	bimodal	46.5, 199
	trimodal	46.5, 199, 377
Sweeny	bimodal	164-262
	bimodal	97-262
	bimodal	36-262
	bimodal	12.6-262
Chong	bimodal	112.5-236
	bimodal	73.8-236
	bimodal	33.0-236
Brodnyan	bimodal	0.028-0.074
	bimodal	0.028-0.23

(Note to reader: Attach to righthand edge of preceding page.)

TABLE 2 -- Continued

Previous Investigations of Multimodal Suspensions

Composition	
Size Ratio	Size Distribution % Small Spheres
0.854 to 1.0	flat-topped continuous
0.708 to 1.0	flat-topped continuous
0.365 to 1.0	flat-topped continuous
0.556 to 1.0	normal distribution
0.208	5, 10, 33.3, 50, 66.6, 90
0.51	0, 9.4, 23.9, 48.6, 73.9, 89.4, 100
0.33	0, 10, 30, 50
0.627	25
0.371	25
0.137	25
0.048	25
0.59 to 0.85	from 9.1 to 91
0.84/0.42-0.84	28.5, 57.2, 14.3
0.84/0.42-0.84	33.3, 44.4, 22.2
0.28, 0.57, 1	33.3, 33.3, 33.3,
0.1234	0, 50, 75, 100
0.234	0, 25, 50, 75, 100
0.1234, 0.528, 1	33.3, 33.3, 33.3
0.627	25, 50, 75, 100
0.371	25, 50, 75, 100
0.137	25, 50, 75, 100
0.048	25, 50, 75, 100
0.477	25
0.333	25
0.048	25
0.378	50
0.122	50

(Note to reader: Attach to righthand margin of preceding page.)

TABLE 2 -- Continued

Previous Investigations of Multimodal Suspensions

	Concentration Volume % of Spheres
	5, 10, 15, 20, 25, 30
	5, 10, 15, 20, 25, 30
	5, 10, 15, 20, 25, 30
	5, 10, 15, 20, 25, 30
	2-1/2, 5, 7-1/2, 10, 12-1/2, 15, 17-1/2, 20
	23-1/2, 35-1/2, 47-1/2, 56-1/2
	40, 50
	55
	55
	55
	55
	0 to 45
	0 to 45
	0 to 45
	46.0, 58.6, 64.4
	from 2-1/2 to 22-1/2 at 2-1/2 intervals
	same
	same
	40, 55
	40, 55
	40, 55
	40, 55
	54 to 74
	54 to 74
	54 to 74
	5 to 40
	5 to 40

(Note to reader: Clip and attach to righthand margin of preceding page.)

$$\frac{1}{\mu_r} = \varphi_o \left[1 - \frac{3}{5}(1-\varphi_o)\right]$$

where φ_o is the volume fraction of the liquid in the suspension. His curve is also shown on Figure 1. The results of Keller *et al.* have already been mentioned.

Three salient points concerning the rheological behavior of suspensions of spheres seem to be at issue in this literature. First is the question of rheological characterization: under what conditions are concentrated suspensions Newtonian or non-Newtonian? Second, what role does composition play; in determining the relative viscosity, for example? Third, what is the nature of the undefined connection between the behavior of concentrated suspensions and packed beds which has been affirmed so often? A further point of emphasis is the lack of agreement between and among investigators, both theoretical and experimental.

The theoretical equations for relative viscosity imply Newtonian behavior at all concentrations, irrespective of composition; none have explicit dependence on shear rate, and only the Mooney equation is explicitly dependent upon composition. In contrast, experimental observations of the onset of non-Newtonian behavior have been reported at concentrations as low as 10%, and as high as 55.5%. Indeed, for multimodal suspensions, simple concentration may not be an appropriate index to the rheological behavior of concentrated suspensions.

Effects of composition upon the relative viscosity of bimodal suspensions have been reported as beginning at concentrations ranging between 10% and 30%. In this matter in particular, simple total concentration is unlikely to be an adequate index to rheological behavior. The effect of absolute sphere size as distinct from size ratio in multimodal suspensions is largely unexplored. Previous investigators have laid uneven emphasis upon the several composition variables.

There is general agreement that the properties of concentrated suspensions are in some way related to the properties of packed beds, based on the bimodal results. The trimodal data are not sufficient to support more than a corresponding suspicion. The hypothesized relationship has not been explored or defined in detail.

The lack of agreement between experimental results from similar systems, and the general incommensurability of separate results, compounds the fundamental uncertainties with confusion. Several authors, especially the reviewers, have suggested or implied a need for more and better experimental data. Rutgers made an explicit call for it. Thomas, although terming the data "extensive", after much manipulation was able to use only four of the sixteen sets of data he cited. Simha and Somcynsky echoed the epithet "extensive", but called attention to the discrepancies between investigators. Frankel and Acrivos described the data as "limited." Chong and Sweeny both recommended the determination of relative viscosities of multimodal suspensions at several compositions and concen-

trations and at several shear rates; for use in checking the (many) φ_m correlations on the one hand, and for use in determining the Mooney crowding factors on the other. The same data would be useful to explore the connection between the behavior of concentrated suspensions and packed beds surmised by so many previous investigators.

The current status of the rheology of concentrated suspensions of neutrally buoyant rigid spheres in Newtonian fluids may be fairly summarized as being in need of improved experimental data aimed at these three goals:

better rheological characterization of concentrated suspensions;

exploration of the effects of composition on the properties of concentrated multimodal suspensions; and

definition of the relationship between the behavior of concentrated suspensions and packed beds of spheres.

Objective of This Research

The objective of this research was to experimentally determine the effects of concentration and composition upon the rheological properties of concentrated multimodal suspensions of neutrally buoyant rigid spheres in Newtonian fluids. The isothermal flow curves, shear stress versus shear rate at each concentration and composition, were determined from torque measurements made with a Gilinson-Dauwalter-Merrill concentric cylinder viscometer at up to ten shear rates between 0.06 and 100 inverse seconds. The rheo-

logical character of these flow curves, and the differential and relative viscosities calculated from them, were related to the characteristics of the suspensions. The following characteristics of monomodal suspensions were controlled: volume concentration of spheres, sphere diameter, temperature, and shear rate. The following characteristics of multimodal suspensions were controlled: total volume concentration of spheres, relative volume concentration of each size of sphere (size distribution), sphere diameters, ratios of sphere diameters (size ratio), temperature, and shear rate.

The total volume concentrations of principal interest were those above twenty percent up to the maximum practical concentration. Sphere diameters were from twenty-six to two hundred twenty-one microns. Mono- and multimodal suspensions were prepared from size fractions of spheres separated with standard testing screens and the effect of the width of the size distributions upon the flow curves estimated.

A particular goal of this research was to determine those parameters describing the suspension composition at which relative viscosity is minimized for a given concentration and shear rate. The experimental data are examined in the light of those theoretical equations which predict minima in relative viscosity as a function of sphere size distribution; Mooney's equation in particular.

The following new scientific information is contributed by this research:

experimental data showing the effect of sphere size, size ratio, size distribution, and concentration upon the rheological properties of bimodal and trimodal suspensions of spheres;

an evaluation of the crowding factors appearing in Mooney's equation for relative viscosity, as applied to these multimodal suspensions; and

an evaluation of the effect of using screened fractions of particles instead of very narrow size fractions to make bimodal and trimodal suspensions.

II

MATERIALS, EQUIPMENT, AND METHODS

The physical components of the suspensions studied are identified and described, as are the standardizing oils. The GDM viscometer and its auxiliary equipment are described, and the important physical constants of the cup and bob sets are listed. The manipulative procedures employed in the experiment are described and the calculations involved in reducing the experimental observations to flow curves and viscosities are outlined.

Materials

The rigid spheres used were SUPERBRITE ® Class B Glass Beads (Controlled Sizes) manufactured by the Minnesota Mining and Manufacturing Company, Reflective Products Division. The general properties of these beads are described in the manufacturer's Technical Data Sheets (36). The initial size separation of the glass beads was made by use of the usual testing sieves (5), followed by a simple elutriation with water in which the center fraction of the beads was retained for use. An additional separation by specific gravity was found to be necessary and was performed by sedimentation at two temperatures (30, 45C) in the experimental fluids, the center fraction being retained for use, with an approximate range of one percent in specific gravity.

Size determinations were done by direct measurement of sphere diameters on optical photomicrographs. The size distributions of the five sizes of spheres employed are shown in Table 3 and in Figures 3 and 4.

The apparent specific gravity of the glass beads was measured at 37 degrees C in a Le Chatelier specific gravity bottle as described in ASTM C188-44 (2), but using the calculations described in ASTM C128-67 (1), paragraph 7, with all volumes determined at 37 degrees C. The values of apparent specific gravity so determined are shown by sphere diameter in Table 4. These are average values, of course, and do not indicate the remaining distribution of specific gravity about the measured value.

The Newtonian liquids used to suspend the glass spheres were:

1,1,2,2-tetrabromoethane, M.W. 345.7, density 2.96 g/ml, and viscosity (25 C) 9.6 cp.

1-bromododecane, M.W. 249.24, density 1.05 g/ml, and viscosity (25 C) 3.3 cp.

These fluids were chosen for density, insolubility in water, and low vapor pressure. They are miscible in all proportions. The detailed mixture properties of these fluids have been published elsewhere (12). Practical grade tetrabromoethane was substituted in the latter stages of the work.

TABLE 3

Size Distributions of Spheres

Diameter Microns	%	Cum. %	%	Cum. %	%	Cum. %	%	Cum. %	%	Cum. %
	"26 microns"									
0	0.	0.								
10	1.3	1.3								
20	41.1	42.4								
30	23.6	66.0	"61 microns"							
40	34.	100.	.4	.4						
50			.6	1.0						
60			61.4	62.4						
70			30.5	92.9						
80			7.1	100.						
90					"125 microns"					
100					1.2	1.2				
110					10.1	11.3				
120					21.1	32.4				
130					46.1	78.5				
140					17.6	96.1	"183 microns"			
150					3.9	100.	.6	.6		
160							3.4	4.0		
170							8.7	12.7		
180							23.5	36.2	"221 microns"	
190							38.9	75.	2.2	2.2
200							16.1	91.2	7.8	10.
210							3.9	95.1	20.2	30.2
220							4.9	100.	18.1	48.3
230									14.8	63.1
240									13.4	76.5
250									16.4	92.9
260									7.1	100.

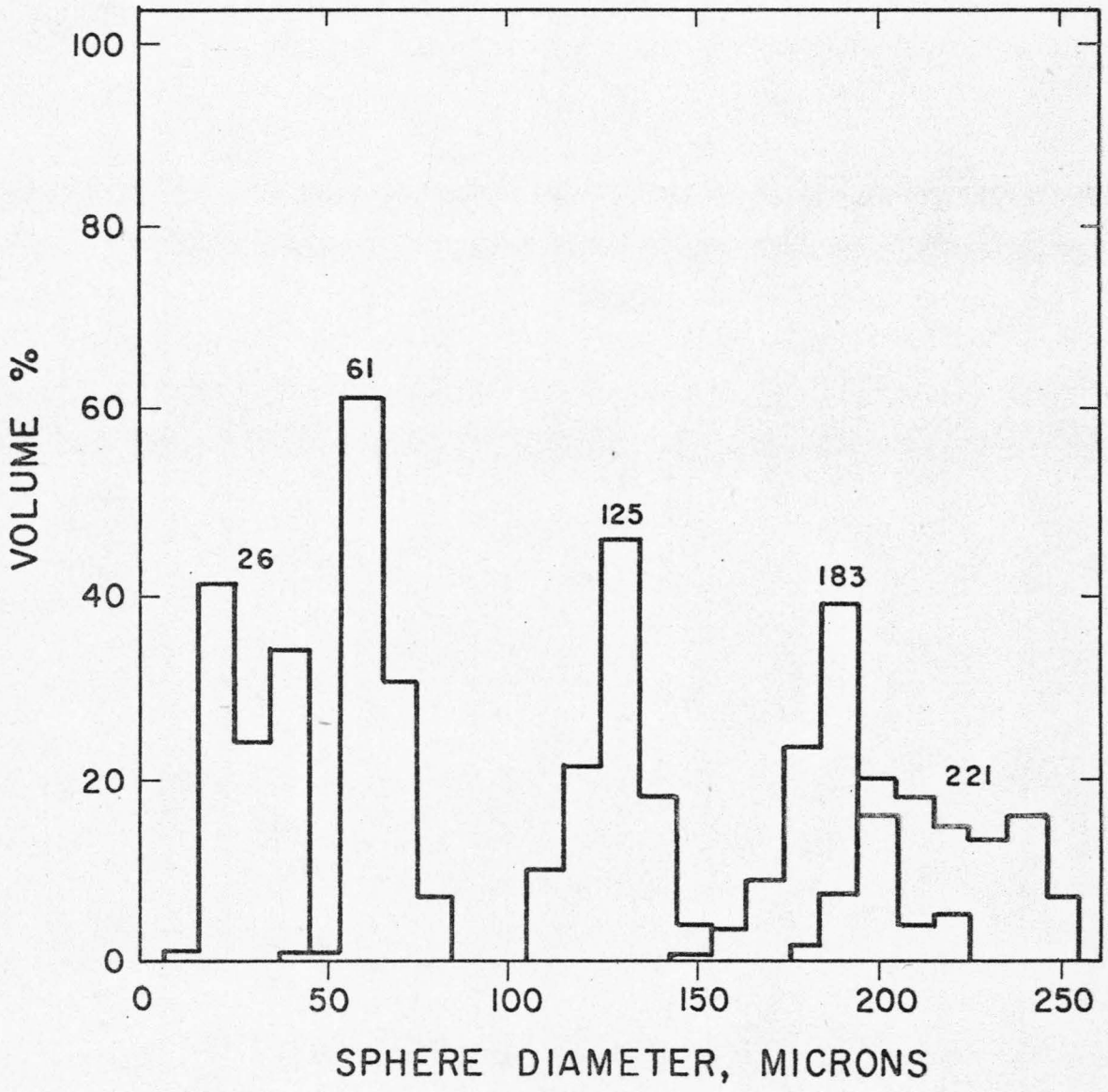

Figure 3. Differential size distributions of spheres.

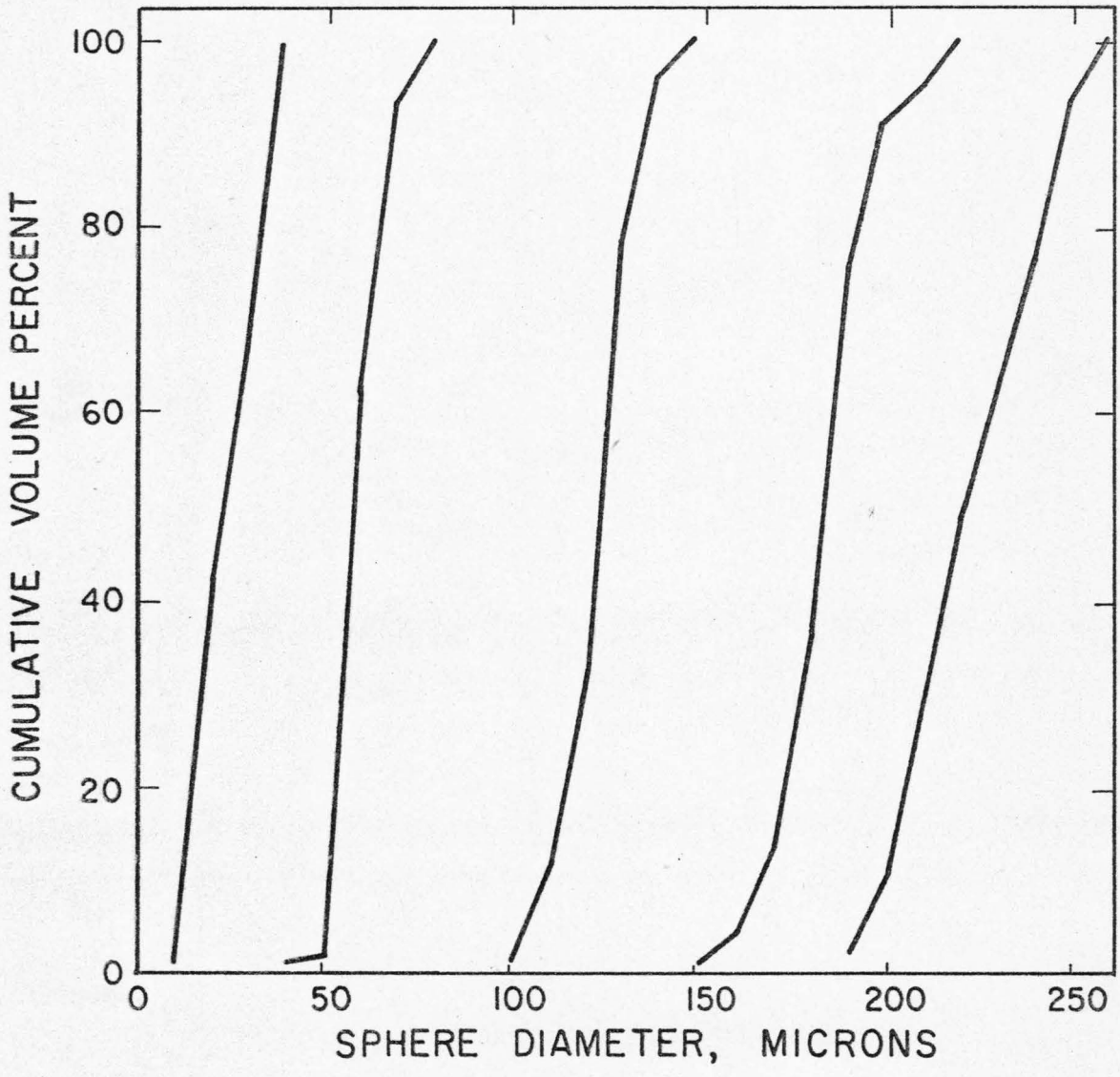

Figure 4. Cumulative size distributions of spheres.

TABLE 4

Apparent Specific Gravity of Spheres

Sphere diameter, microns	26	61	125	183	221
Measured Apparent Specific Gravity	2.474	2.478	2.498	2.483	2.504
	2.432	2.456		2.492	2.499
				2.488	
				2.498	

Cannon Instrument Company standard oils:

S-6-57-2h

S-60-65-1a

S-60-68-1c

S-3-70101

S-60-70105

were used for standardization of the viscometer. The properties of, and the experimental measurements made on, the several oils are tabulated in Appendix A. The pint samples were sampled without replacement in 30 milliliter aliquots, and the remaining oil was stored for later use.

Equipment

The viscometer used is the Gilinson-Dauwalter-Merrill (GDM) rotational, concentric cylinder viscometer which uses an A.C. torque-to-balance loop and an air bearing (25). The outer cylinder is a cylindrical cup rotated by a locally designed machine incorporating interchangeable cups, a five gallon reservoir as a thermostat, and a variable speed, reversible drive train. The inner cylinder, or bob, is a short right circular cylinder with a conical bottom supported from above by a rigid shaft and a coaxial air bearing. The air bearing is supplied with dry, filtered, pressure regulated air from the building's utility lines. The air is dried by passing it through an absorbent bed in series with a Model 15L Grove Loader. The air bearing was built with an integral Millipore air filter. Appropriate gauges and valves are installed.

The output signal from the viscometer is a 0 to $\pm$0.05 volt D.C. voltage directly proportional to the total torque exerted on the bob by the sheared suspension, with the polarity indicating direction of the torque. This signal is available in three forms: as a meter indication, as a filtered $\pm$ .05 v. D.C. voltage, or as an unfiltered 0 to $\pm$ 0.05 v. D.C. voltage. The filtered 0 to $\pm$ 0.05 v. signal is presently used to drive a Bausch & Lomb, 10 mv, VOM 5, single pen, strip chart recorder.

The general arrangement of the equipment is shown in Figure 5.

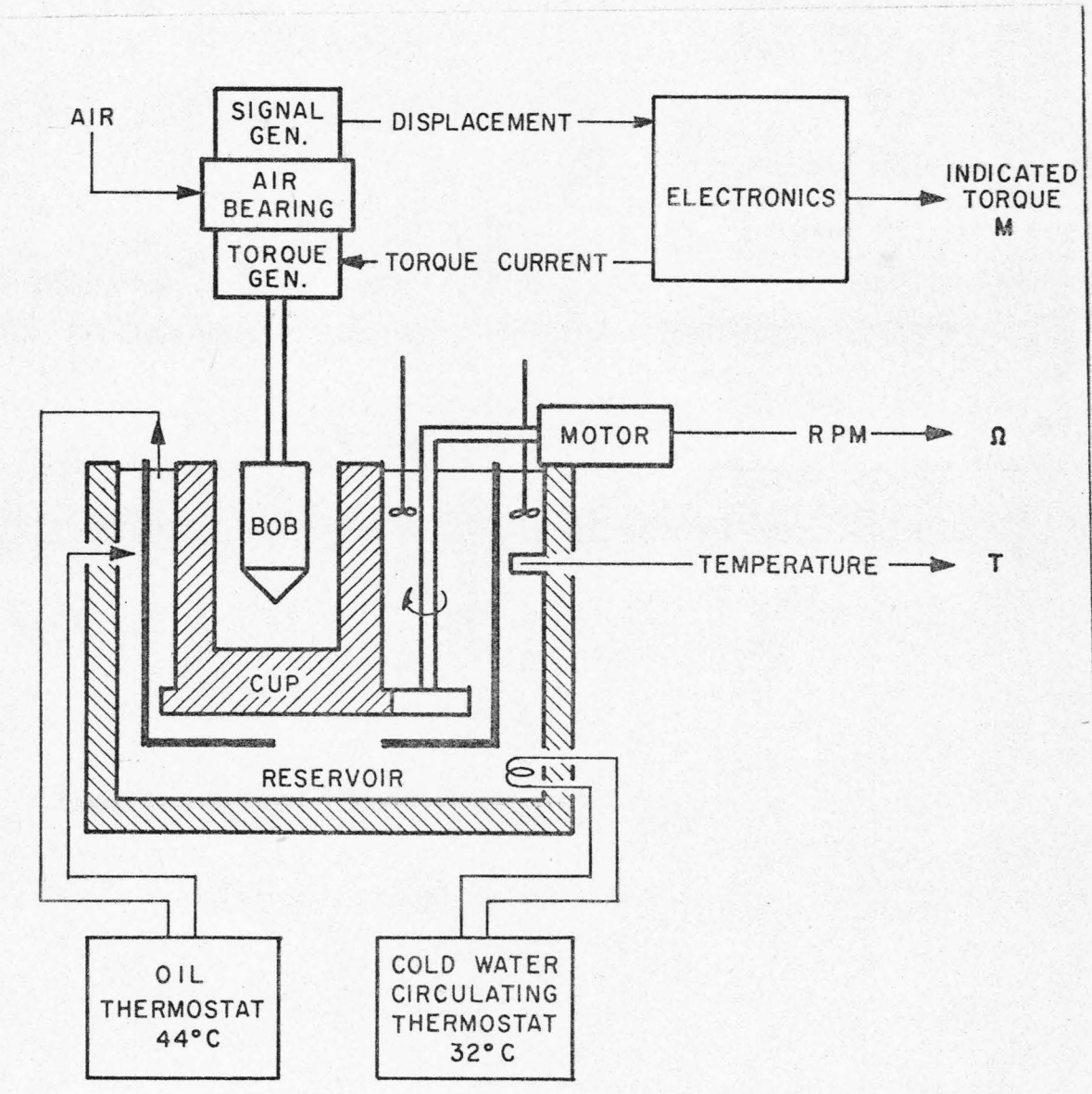

Figure 5. General arrangement of equipment (schematic).

In simple terms, the instrument works as follows. The cup is turned in either a clockwise or counter-clockwise direction at one of ten available speeds between 0.04 and 46. rpm by the 1300 rpm electric motor and gear box, and between .05 and 63.9 rpm by the 1800 rpm electric motor and gear box, the direction of rotation being electrically reversible. The cup and gear drive are arranged so that the cup is immersed in the oil reservoir. The sample suspension is contained in the annular radial gap and in the end gap between the rotating cup and the stationary bob and in the overhead gap with a free surface. The suspension in the radial gap is set into (laminar) circular flow, and transmits a torque from the outer to the inner of the opposed cylindrical surfaces. The total torque due to viscous shear stresses acting on the wetted surfaces of the bob is sensed, counterbalanced, measured, and indicated by the electronics of the GDM viscometer.

The stationary bob, or inner cylinder, is supported by an air bearing which floats on a film of air. The bearing supports the bob vertically and fixes the position of the rotational axis of the bob, but the bob is very nearly unrestrained in rotation. Mounted coaxially on the air bearing to which the bob is connected by a rigid shaft are also:

a signal generator, which detects rotational motion of the bearing (and bob), and

a torque generator, which exerts the counter-balancing torque on the bearing.

As the bob begins to rotate from its null position, due to the torque rising from the viscous shear stresses on its wetted surfaces, the signal generator develops an A.C. output whose voltage is proportional to angular displacement and whose phase shift from a reference voltage indicates the direction of motion. This signal is processed by a feedback amplifier which in turn excites the torque generator with an A.C. current of the correct phase and voltage to produce a counterbalancing torque which is proportional to the angular displacement from the null position. The bearing rotates until the net torque on the bob is zero. At most, the bearing moves through 0.002 degrees of arc (25). The sheared suspension supplies the damping. The current to the torque generator is measured by the output circuits and converted to a direct readout of torque in dyne centimeters by means of a manually switched electrical scaling circuit through which 0.05 v. D.C. can be made to indicate torques of 1000, 100, 10, 1.0 and 0.1 dyne-cm, full scale, in either clockwise or counterclockwise direction. An additional precision transformer permits the full scale indication to represent any desired submultiple of the full scale values given above: for example, 333.33 dyne-cm, or 0.75 dyne-cm.

The outstanding characteristics of the GDM viscometer are its sensitivity, range, and accuracy. The rotational friction of the air bearing is claimed to be less than 0.0001 dyne-cm, permitting the machine to measure torques from 0.0001 to 1.000 dyne-cm in

either direction of rotation. The accuracy of torque sensing is claimed to be within one-tenth percent, or $\pm$ 1 digit, whichever is larger.

The data actually taken from the instrument are:

magnitude and direction of the counterbalancing torque exerted on the bob;

speed and direction of cup rotation; and

temperature of the oil reservoir.

This information is combined with the physical dimensions of the cup and bob combination being used, to calculate the shear stress on the cylindrical surface of the bob and the shear rate in the suspension at the cylindrical surface of the bob for each of several cup speeds. The resulting plot of shear stress versus shear rate is the desired flow curve for the suspension under test.

Cup rotation rates were determined directly, by counting the number of cup revolutions in a given time period resulting from a fixed motor speed. Two motors were used during the experiment: the first was a D.C. shunt wound motor, equipped with a feedback motor speed controller which was monitored with a stroboscope, and the second was a synchronous hysteresis motor which turned at exactly half the line voltage frequency. The cup rotation rates are tabulated in Appendix A. The physical dimensions and the diameter ratios for the cups and bobs used are shown in Figure 6.

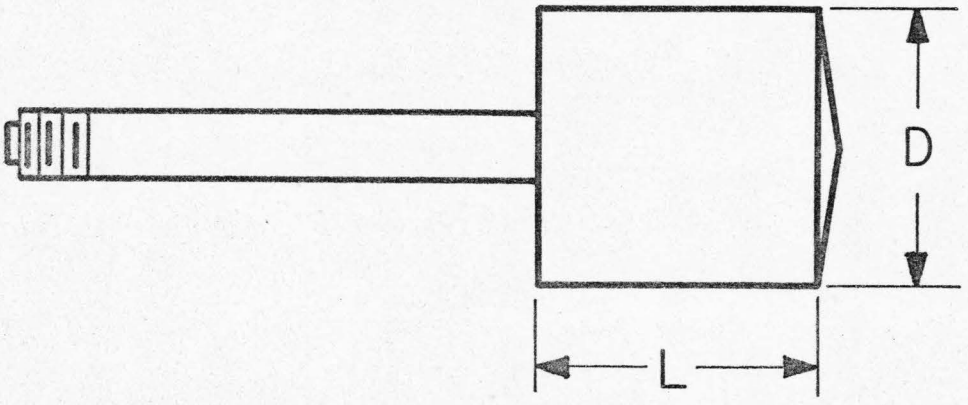

Bob Nr.	D cm	L cm	s Smooth Cup	Grooved Cup*
1	3.830	3.647	1.078	#
2	3.830	2.5387	1.078	#
2M	3.8303	2.0396	1.0782	#
3*	3.8303	3.6464	1.0782	1.0780
4*	3.8293	2.5382	#	1.0783
5	3.8298	3.6467	1.0784	#
6	3.8301	2.5380	1.0783	#

*Grooved cylindrical surfaces

#Not used.

Cup Diameter
Smooth cup 4.1300 cm
Grooved cup 4.1290 cm

$$s = \frac{1}{K} \quad \frac{\text{Cup diameter}}{\text{Bob diameter}}$$

Figure 6. Physical constants of the cups and bobs.

Precision grade, mercury-in-glass thermometers were used to measure the temperature of the thermostat. The utility thermometers have a -2 to 51 C range, with one-tenth degree subdivisions, and were standardized with an ASTM 64 C short range, precision grade, mercury-in-glass thermometer (4,5). The latter is furnished with a manufacturer's certificate of accuracy incorporating the necessary corrections to its readings. The thermometer standardizations are tabulated in Appendix A. The difference between cup temperature and oil temperature was 0.15 C at 37 C.

Temperature regulation of the viscometer reservoir was achieved with a P.M. Tamson Model TZ3 Circulating Thermostat, 0 to 50 C range, which circulated a polyalkylene glycol (53) (UCON LB-65) lubricant at a regulated temperature, 44 C, and a fixed flow rate to the insulated, stirred reservoir of five gallons capacity in which the test section was immersed. Cooling was provided by a coil immersed in the hot oil, through which chilled (2 C) water was circulated. The flow rate of the chilled water was regulated by means of a variable speed pump. The opposing rates of heat addition in the flowing oil, and of heat removal in the flowing water, were balanced by trial and error at rates high enough to absorb the variation in heat loss to the laboratory air and still maintain the measured temperature of the reservoir within 0.05 C as measured by the mercury-in-glass thermometer.

Methods

Experimental technique. Suspensions were prepared individually, by weighing out samples of hot, dry spheres (to 0.01 g) on a Mettler top loading balance, and combining them in the viscometer cup with premixed suspending fluid measured by volume (to 0.1 ml) from a 50 milliliter burette. The samples were mixed with a spatula and inserted into the viscometer thermostat for one half hour equilibration time. A sample set of suspension recipes is shown in Table 5.

A constant total volume of 30 ml was used to permit evaluation and correction of end effects. Based on subjective estimates, the likely error in weighing out glass beads should be less than 0.1 g, and the error in measuring and delivering suspending fluid should be less than 0.1 ml. These errors combine to produce errors of $\pm$ 0.002 in the volume fraction of solids in the suspensions. That is, the concentration of a 20 volume percent suspension is estimated to lie between 19.8 and 20.2 volume percent solids, and the concentration of a 50 percent suspension is estimated to lie between 49.8 and 50.2 volume percent solids.

The suspending fluid was prepared in 300-400 ml batches for each set of measurements; i.e., for each sphere size in the monomodal suspensions and for each combination of sizes in the bimodal suspensions. The fluid density was adjusted so that an estimated 80-90% of a sample of the spheres to be used would eventually sink in an undisturbed suspension thermostatted at 37 C.

TABLE 5

Bimodal Suspension Recipes for 61 Micron, 183 Micron Spheres

Basis: 30 ml total volume of suspension

$\rho_{61} = 2.456$

$\rho_{183} = 2.498$

Variable Composition, 40% Total Concentration

Composition	Liquid	61 Micron Spheres		183 Micron Spheres	
100/0	18 ml	12 ml	29.47 g	0. ml	0. g
70/30	18	8.4	20.63	3.6	8.99
60/40	18	7.2	17.68	4.8	11.99
30/70	18	3.6	8.84	8.4	20.98
0/100	18	0.	0.	12.	29.98

Variable Total Concentration, 40/60 Composition

Composition	Liquid	61 Micron Spheres		183 Micron Spheres	
20%	24	2.4 ml	5.89 g	3.6 ml	8.99 g
30	21	3.6	8.84	5.4	13.49
40	18	4.8	11.79	7.2	17.99
50	15	6.0	14.74	9.0	22.48

After being measured, the components of the suspension were reclaimed: the fluid was filtered off and saved for re-use, and the spheres were washed in acetone, air-dried, sieved, and saved for re-use.

Viscometer cups containing either mixed suspensions or pure fluids were allowed to equilibrate for one half hour with the bob inserted, and the cup turning. The suspensions were all re-mixed before each measurement was taken. That is, the suspensions were subjected to the following sequence:

initial mixing, following combination of components;

equilibration;

remixing;

observation of torque, 1000/1 gear box setting,

clockwise rotation;

remixing;

observation of torque, 100/1 gear box setting,

clockwise rotation;

and so on . . .

The range of cup speeds was covered in three overlapping stages, usually in the following order of gear box settings:

1000/1;

100/1;

10/1;

1/1;

500/1;

50/1;

5/1;

200/1;

20/1;

2/1.

This decade by decade order simplified the coordination of viscometer range switching with the gear box settings, and in addition, prevented the confounding of the effects of unwanted secular changes in the experimental conditions with the measured flow properties of the fluid under observation. For example, steady changes in the suspension temperature due to viscous heating or thermostat drift, or steady changes in suspension concentration caused by fluid loss due to rapid evaporation (acetone contamination of fluid) or a leaky cup, or rapid settling or floating of the spheres due to a bad density match, would produce a saw-tooth flow curve rather than a smooth flow curve with a gradual but peculiar curvature.

Torques were observed in both clockwise and counterclockwise directions of cup rotations, and the torque values averaged to yield a single value of torque at each cup speed which had been corrected for any shift in the null reading of the viscometer.

The interpretation of the strip chart record produced by the viscometer, which constitutes the primary data output from the instrument, is illustrated in Figure 7.

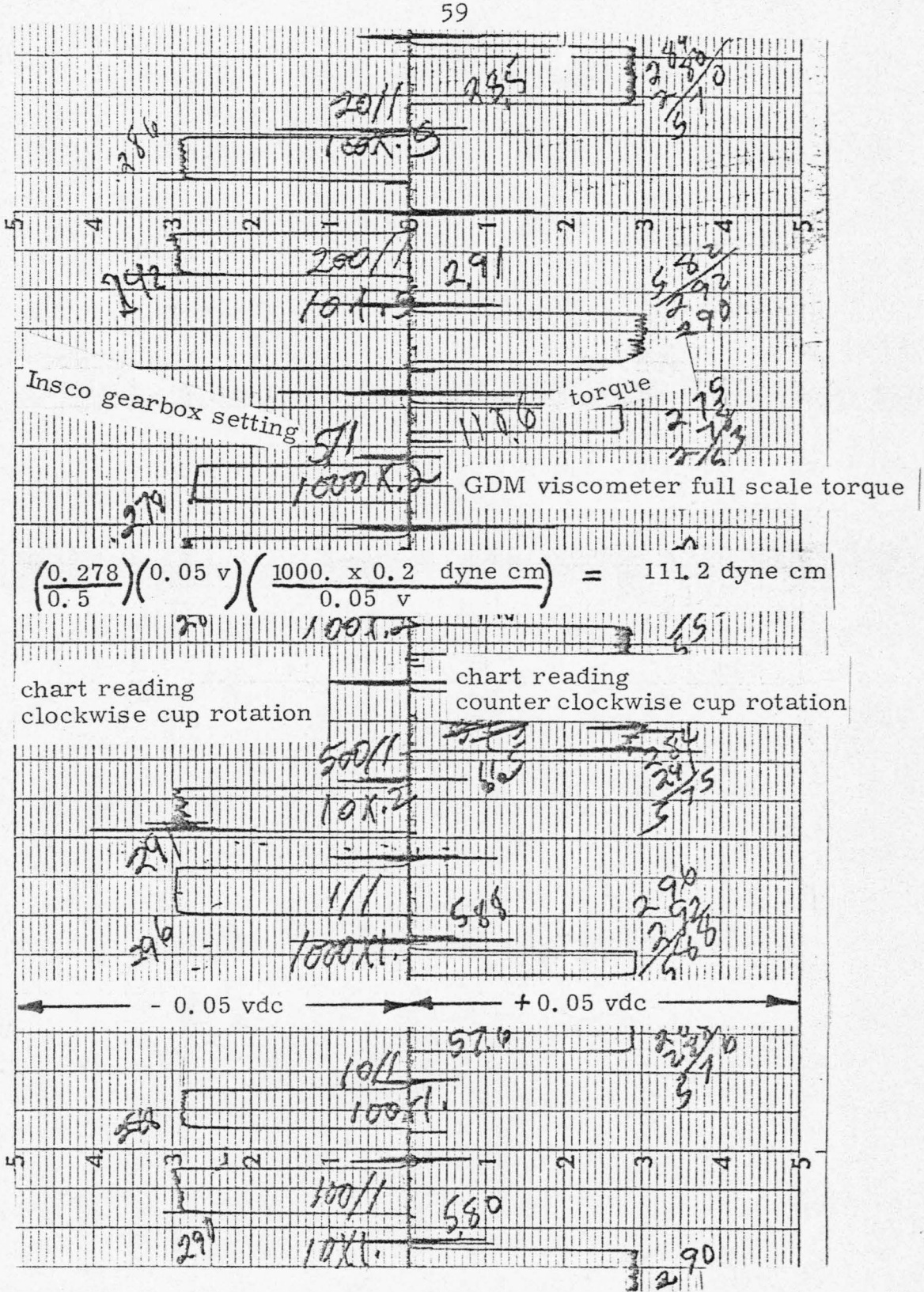

Figure 7. Interpretation of the GDM viscometer's strip chart record.

As the reported torque value at each gear box setting was calculated from the strip chart record, it was entered in the research notebook, and also plotted on a log-log chart of Torque, dyne-cm, versus cup speed, Angular Rate, radians/second, and evaluated. Measurements whose points did not seem to fall on the curve through the rest of the points (the tentative flow curve) were repeated until either a definite, regular sequence of points was obtained, or until the whole set was abandoned and the sample suspension scrapped. Multiple observations of torque values were reported as their average; when a single inconsistent observation was followed by subsequent observations clustered about the tentative flow curve, the inconsistent observation was deleted from the average. The resulting set of (average) torque values at fixed cup speeds was termed "raw data" and is tabulated, with identifying compositions and concentrations, in Appendix A.

Reduction of the raw data to flow curves and viscosities. The typical set of raw data consists of ten pairs of torque values in dyne-cm associated with a cup speed expressed in radians/second, in the form (Ω_o, M). For suspensions of high concentration, the sets of raw data are truncated, those pairs of (Ω_o, M) for which the torque value would have been greater than 1000 dyne-cm being missing. The independent variable, Ω_o, the rate of rotation of the outer cylindrical surface, must be reduced to the corresponding rate of shear $(\dot{\gamma})$ in the fluid at the surface of the inner cylindrical

surface. The total couple exerted by the fluid on the entire wetted surface of the bob must be reduced to the corresponding shear stress ($\tau_{r\theta}$ rendered simply, τ) exerted by the fluid upon the inner cylindrical surface.

The observed torque value, M, is reduced to shear stress τ, by the expression:

$$\tau = \frac{F\ M}{2\pi\ R^2\ L^*}$$

in which R is the radius of the inner cylindrical surface, cm;

F is a calibration factor, dimensionless; and

L* is a fictitious bob length, cm.

The use of L* in place of the actual physical length of the cylindrical surface of the bob is a convenient, empirical device by which to account for the additional torque contributed to the observed torque value, M, by the top and bottom edges, the flat top surface, the conical bottom surface, and by the wetted length of the small diameter shaft of the bob. A derivation of L* from the results of measurements taken with two bobs identical in all respects save length is given in the discussion of the results of the measurements made upon the standard oils. The results in terms of the length of the longer of the two bobs is

$$L^* = L\left[1 + \frac{C-K}{C(K-1)}\right]$$

in which L is the physical length of the cylindrical surface of the bob, cm;

C is the ratio of the length of the long bob to the short bob, dimensionless;

K is the constant ratio of torque values observed with the long bob to those observed with the short bob for the same fluid and cup speed.

Krieger's method (29) for calculating shear rate in the concentric cylinder viscometer was employed, in which the shear rate at the inner cylinder is given by

$$\dot{\gamma} = \frac{2N\,\Omega_o}{1 - S^{-2N}} \left[1 + \frac{N'}{N^2}\, f(t) \right]$$

with s = ratio of outer cylinder diameter to inner cylinder diameter,

$$N = \frac{d\Omega_o}{d \log \tau}$$

$$\frac{N'}{N^2} = -\left(-\frac{N'}{N^2}\right) = -\frac{d(1/N)}{d \log \tau}$$

$$t = 2N \ln (s)$$

$$f(t) = \frac{t\,[e^t(t-2) + t + 2]}{2(e^t-1)^2} = \frac{t}{12}\left(1 - \frac{t}{2} + \frac{t^2}{15} + \ldots\right)$$

In the description of the equipment, s, the ratio of cylindrical diameters was given as approximately 1.08. Section III will show

that N is very nearly constant at a value of 1 and that N' is very nearly zero. Substitution of these values results in:

$$t = 0.15$$

$$f(t) = 0.002$$

$$\dot{\gamma} = 1.4\,\Omega_o$$

The true flow curve of the fluid or suspension under observation is constructed from the calculated $(\dot{\gamma}, \tau)$ pairs. The differential viscosity of the fluid sample is then represented by the slope of the flow curve.

The several differentiations required in these calculations, such as that by which differential viscosity is determined from the shear stress, shear rate curve, were performed by fitting the numerical data with a low degree polynomial with a least squared error computer subroutine, analytically differentiating that polynomial, and then numerically evaluating the derivative polynomial at the appropriate values of the independent variable. For example, the differential viscosity of a Newtonian fluid would be determined by fitting the shear stress-shear rate data with a first degree polynomial

$$\tau = A_1 + A_2\,(\dot{\gamma})$$

from which

$$\mu = \frac{d\tau}{d\dot{\gamma}} = A_2$$

The data for a strongly non-Newtonian fluid would be fitted with a third degree polynomial

$$\tau = A_1 + A_2 (\dot{\gamma}) + A_3 (\dot{\gamma})^2 + A_4 (\dot{\gamma})^3$$

so that the differential viscosity

$$\mu = \frac{d\tau}{d\dot{\gamma}} = A_2 + A_3 (\dot{\gamma}) + 3A_4 (\dot{\gamma})^2$$

could show a smooth, non-linear variation with shear rate if appropriate.

The methods used to obtain relative viscosities from the differential viscosities, and the methods used to determine values for the Mooney interaction parameters from the relative viscosities, are explained in contect with the experimental results in Part III --Results and Discussion of Results.

III

RESULTS AND DISCUSSION OF RESULTS

The results of experimental measurements upon standard oils are tabulated in terms of viscosities and power law indices, and the end effects correction and calibration factor for the GDM viscometer system are determined. The results of experimental measurements upon monomodal and bimodal suspensions of spheres ranging from 26 to 221 microns in diameter are tabulated in terms of relative viscosities and power law indices, and are discussed in terms of the principal theoretical and empirical results appearing in the literature. The results of experimental measurements upon a system of trimodal suspensions are tabulated in terms of relative viscosities and power law indices, and the location of the three-component minimum-viscosity composition is discussed.

Standard Oils

The standard oils used to calibrate the GDM viscometer system for these measurements were Cannon Instrument Company oils in the S-3, S-6, S-60 series, with the bulk of the observations being performed on the S-60 oils. The oil viscosity was interpolated at 0.1 C intervals by means of a second degree polynomial fitted to the certified viscosity-temperature properties as represented on a log (viscosity) versus reciprocal absolute temperature plot. The raw

data, consisting of torques observed at specified cup speeds, are tabulated in Appendix A: these observed torques must be corrected for end effects and for machine calibration.

End effects in the concentric cylinder viscometer. The torque experienced by the stationary inner cylinder, or bob, in a concentric cylinder viscometer in which the outer cylinder, or cup, is rotated, is the sum of the action of the sheared fluid upon the remaining wetted surfaces of the bob. These extraneous torques arising from all sources other than the large diameter cylindrical surface of the bob are commonly lumped together and termed "end effects". For a bob with a cylindrical surface of diameter, D, and length, L, the observed torque, M, at a specified rate of shear in the experimental fluid may be represented by

$$M = (\pi \frac{D^2}{2} L)\, \tau + \epsilon$$

where τ is the shear stress exerted upon the cylindrical surface by the sheared fluid, and ϵ is the end effects term.

For convenience in the analysis of experimental data, we seek a correction to the bob length, ΔL, such that

$$M = (\pi \frac{D^2}{2} L)\, \tau + \epsilon = \pi \frac{D^2}{2} (L + \Delta L)\, \tau$$

If the same fluid is observed in a viscometer with two inner cylinders identical in all respects save the length of the cylindrical surface, especially in regard to diameter, bottom clear-

ance, immersion depth, and end geometry, then we might suppose the end effects to be equal for corresponding measurements.

Denoting the longer of the two bobs by a subscript 1, and the shorter with a subscript 2, then for corresponding conditions

$$M_1 = (\pi \frac{D^2}{2} L_1)\, \tau + \epsilon = \frac{\pi D^2}{2} (L_1 + \Delta L)\, \tau \ ,$$

$$M_2 = (\pi \frac{D^2}{2} L_2)\, \tau + \epsilon = \frac{\pi D^2}{2} (L_2 + \Delta L)\, \tau \ ,$$

$$\frac{M_1}{M_2} = \frac{L_1 + \Delta L}{L_2 + \Delta L} = K$$

K should be, at most, a function of the shear rate. For the experimental data reported here, K is a constant, independent of shear rate. We may solve for ΔL in terms of the torque ratio and the ratio of bob lengths, L_1/L_2 :

$$\Delta L = \frac{K L_2 - L_1}{1 - K} = L_2 \left(\frac{K - L_1/L_2}{1 - K}\right) .$$

Let $L_1/L_2 = C$,

so that $$\Delta L = L_2 \left(\frac{C - K}{K - 1}\right) = L_1 \left[\frac{C - K}{C(K-1)}\right] .$$

In the reduction of observed torques to shear rates, the measured bob lengths should be replaced by a fictitious bob length, L* :

$$L^* = L + \Delta L$$

or

$$L_1^* = L_1 \left[1 + \frac{C - K}{C(K-1)} \right]$$

$$L_2^* = L_2 \left[1 + \frac{C - K}{K - 1} \right]$$

in order to correct for end effects.

For bobs 5 and 6 in the smooth walled cup, including the small correction for the smaller diameter of bob 6, the raw data yield

$$M_5/M_6 = K = 1.39$$

which leads to

$$\Delta L = 0.305 \text{ cm.}$$

For bobs 3 and 4 in the grooved wall cup, the raw data yield

$$M_3/M_4 = K = 1.38$$

which leads to

$$\Delta L = 0.378 \text{ cm.}$$

For bobs 3 and 4 in the smooth walled cup

$$M_3/M_4 = K = 1.39$$

which leads to

$$\Delta L = 0.303 \text{ cm.}$$

The fictitious bob lengths, L*, found in this manner are shown in Table 6.

TABLE 6

Fictitious Bob Lengths

Bob Nr.	Cup	
	Smooth	Grooved
3	3.950 cm.	4.024 cm.
4	2.841	2.916
5	3.952	not used
6	2.843	not used

Calibration factor. The machine calibration factor was determined by forming the ratio of the standard viscosity of the oil and the experimental viscosity of the oil as calculated from the experimental measurements. This factor is applied to the observed torque as a correction to the calibration of the torque scaling circuits of the GDM viscometer. The results of 47 measurements of standard oils is tabulated in Table 7. The calibration factor is determined to be 1.17 with 95% confidence limits of $\pm$ 0.009.

TABLE 7

Experimental Results for Standard Oils

Bob	Temperature, °C	Calculated Viscosity, poise	Power Law Index	Actual Viscosity, poise	Calibration Factor
	S - 3 - 70101				
5S	37.0	.0217	1.00	.0250	1.152
3G	37.0	.0208	.998	.0250	1.202
	S - 6 - 57 - 2h				
3G	37.0	.0464	.967	.0538	1.159
3G	37.0	.0447	.977	.0538	1.204
4G	37.0	.0458	1.00	.0538	1.175
3G	37.0	.0444		.0538	1.212
5S	37.0	.0458	.993	.0538	1.175
	S - 60 - 65 - 1a				
4G	37.2	.499	.995	.574	1.150
3G	37.2	.506	.998	.574	1.134
3S	37.0	.485	.997	.580	1.196
	S - 60 - 68 - 1c				
3G	37.1	.502	.996	.601	1.197
4G	37.2	.504	1.00	.598	1.187
5S	37.1	.529	.997	.601	1.136
6S	37.1	.526	.997	.601	1.143
5S	36.1	.557	.998	.633	1.136
6S	36.1	.550	.996	.633	1.151
5S	35.1	.563	.998	.668	1.187
6S	35.1	.573	.997	.668	1.166
5S	34.1	.610	.999	.705	1.156
6S	34.1	.595	.997	.705	1.185
5S	33.1	.628	.996	.744	1.185
6S	33.1	.637	.997	.744	1.168
5S	37.9	.507	.995	.577	1.138
6S	37.9	.498	.995	.577	1.159
5S	39.1	.474	.997	.543	1.146
6S	39.1	.464	.994	.543	1.170

(cont.)

TABLE 7 -- Continued

Experimental Results for Standard Oils

Bob	Temperature, °C	Calculated Viscosity, poise	Power Law Index	Actual Viscosity, poise	Calibration Factor
5S	37.9	.508	.999	.577	1.136
6S	37.9	.498	.999	.577	1.159
3G	37.9	.484	.999	.577	1.192
4G	37.9	.494	1.00	.577	1.168
3G	37.7	.480	.998	.583	1.215
3G	37.1	.491	.998	.601	1.224
4G	37.1	.525	.999	.601	1.145
6S	37.6	.509	.997	.586	1.151
5S	37.6	.496	.999	.586	1.181
5S	37.0	.515	1.00	.604	1.173
3G	37.0	.498	1.00	.604	1.213
5S	37.0	.500	1.00	.604	1.208
	S - 60 - 70105				
5S	37.0	.446	.999	.532	1.193
3G	37.0	.439	.999	.532	1.212
3S	37.0	.436	1.00	.532	1.220
3S	37.0	.461	.999	.532	1.154
4S	37.0	.456	.998	.532	1.167
3S	37.0	.461	1.00	.532	1.154
4S	37.0	.456	.998	.532	1.167
3S	37.0	.480	.999	.532	1.108
4S	37.0	.487	.999	.532	1.092
				Average	1.170

Monomodal Suspensions

The results of the experimental measurements of the properties of monomodal suspension provide a qualification of the experimental apparatus and technique and a background against which subsequent results for multimodal suspensions may be highlighted and interpreted.

The results of the monomodal measurements should bear directly on the first of the three salient points at issue in the literature: under what conditions are concentrated suspensions Newtonian or non-Newtonian. The results should also add information of value to the literature of concentrated monomodal suspensions especially since these measurements were designed with the Thomas conditions in mind.

Definition of relative viscosity. The relative viscosity of a suspension is universally defined as

$$\mu_r = \frac{\mu \text{ suspension}}{\mu \text{ suspending fluid}}$$

This simple definition is unambiguous only for the differential viscosities of a Newtonian suspension and a Newtonian suspending fluid. Non-Newtonian flow in either suspension or suspending fluid would require further specification in terms of additional rheological parameters. Whenever used in the discussion of the results of this research, the term 'relative viscosity' refers only to Newtonian flow. The limits of validity of this term is one of the back-

ground questions to which the monomodal results are applied.

Results. The collected results of all measurements taken on monomodal suspensions, including those taken as a part of the bimodal investigation, are tabulated in Table 8. These results state the power law model flow index and the relative viscosity of monomodal suspensions of spheres of specified median diameter, of specified volume percent concentration in a Newtonian fluid whose specific gravity closely matches that of the spheres.

These results are used to assess the reproductibility of the experimental method, to assess the magnitude of wall effects, to qualify the experimental method by comparison with the results of previous experimental work, and to provide an answer to the question of under what conditions are monomodal suspensions Newtonian.

The limits of Newtonian flow. The values of average power law index are plotted in Figure 8 as a function of concentration for all the measurements shown in Table 8 (except the last three values in the 26-micron group which will be discussed under Electroviscous Effects). The average values of power law index as a function of concentration are tabulated in Table 9 where the 95% confidence limits on the averages are shown also.

On the basis of the experimental results reported here, there is less than 1/2% probability that monomodal suspensions of spheres will have Newtonian flow curves at concentration of 50 volume percent solids or higher. On the other hand, a power law index

TABLE 8

Experimental Results for Monomodal Suspensions

Bob, Cup	Total Concentration Volume %	Power Law Index	Relative Viscosity
	26 micron spheres		
3G	20.	1.00	1.98
3G	30.	1.01	3.36
3G	40.	1.01	7.88
3G	47.5	1.03	20.4
3G	50.	1.16	(37.3)
4G	20.	.994	2.16
4G	30.	.987	3.71
4G	40.13	1.02	9.07
4G	47.5	1.02	29.5
4G	50.	1.09	(46.5)
5S	20.	.995	1.96
5S	30.	.995	3.25
5S	40.	.995	8.03
5S	47.5	1.07	(22.9)
5S	50.	1.12	(36.3)
6S	20.	1.00	1.87
6S	30.	.997	3.11
6S	40.	1.01	7.06
6S	47.5	1.07	(19.6)
6S	50.	1.08	(32.9)
3S	40.	.391	(9.06)
5S	40.	.951	(9.95)
3S	40.	.823	(9.06)
	61 micron spheres		
3G	20.	.997	1.95
3G	35.	.994	5.59
3G	42.5	1.04	(13.9)
3G	50.	1.11	(56.)
4G	20.	1.00	1.98
4G	35.	1.02	5.19
4G	42.5	1.06	(12.3)
4G	50.	1.28	(72.2)

TABLE 8 -- Continued

Experimental Results for Monomodal Suspensions

Bob, Cup	Total Concentration Volume %	Power Law Index	Relative Viscosity
	61 micron spheres continued		
5S	20.	1.00	2.01
5S	35.	1.01	4.92
5S	42.5	1.03	11.3
5S	50.	1.13	(37.3)
6G	20.	1.00	1.92
6G	35.	.998	4.84
6G	42.5	1.03	10.9
6G	50.	1.10	(38.1)
3S	40.	.994	7.51
3S	40.	1.02	9.56
3S	40.	1.02	6.99
	125 micron spheres		
3G	20.	1.01	2.01
3G	30.	1.01	3.62
3G	40.	1.04	(8.44)
3G	45.	1.02	15.6
3G	45.	1.05	(22.0)
3G	52.36	1.30	(171.0)
4G	20.	1.00	2.08
4G	30.	1.01	3.58
4G	40.	1.06	(10.1)
4G	45.	1.04	(15.9)
4G	52.36	1.33	(138.0)
4G	20.	.998	1.94
4G	20.	.986	1.93
4G	30.	.997	3.28
4G	30.	.980	3.21
4G	40.	1.00	7.96
4G	40.	1.01	8.00
4G	52.36	1.12	(82.4)
5S	20.	1.01	1.97
5S	30.	1.02	3.51

TABLE 8 -- Continued

Experimental Results of Monomodal Suspensions

Bob, Cup	Total Concentration Volume %	Power Law Index	Relative Viscosity
	125 micron spheres continued		
5S	40.	1.06	(8.89)
5S	45.	1.09	(19.8)
5S	52.36	1.27	(78.1)
6S	20.	1.01	1.98
6S	30.	1.02	3.35
6S	40.	1.05	(8.15)
6S	45.	1.09	(15.6)
6S	52.36	1.24	(59.2)
3S	40.	1.00	7.31
3S	40.	.995	7.92
3S	30.	1.00	3.17
3S	40.	.982	7.23
	183 micron spheres		
5S	15.	.977	1.37
5S	20.	.996	1.67
5S	30.	.993	2.93
5S	40.	1.01	6.05
5S	50.	.94	(17.)
5S	55.	1.09	(44.7)
5S	5.	.985	1.05
5S	10.	.995	1.18
5S	25.	1.00	2.17
5S	35.	1.01	4.08
5S	40.	1.02	6.15
5S	45.	.954	(9.34)
5S	30.	1.01	2.74
5S	30.	.991	2.71
5S	30.	.968	2.57
5S	30.	.967	3.03
5S	30.	.975	2.86
5S	30.	.964	(2.79)
5S	30.	.968	2.70
5S	30.	.989	2.85
5S	30.	.939	(2.56)

TABLE 8 -- Continued

Experimental Results of Monomodal Suspensions

Bob, Cup	Total Concentration Volume %	Power Law Index	Relative Viscosity
	183 micron spheres continued		
4G	35.	.966	3.68
4G	35.	.978	3.92
4G	45.	.925	(7.69)
3G	35.	1.03	--
3G	45.	1.03	--
3G	5.	.995	1.13
3G	10.	.994	1.27
3G	15.	.996	1.51
3G	20.	.997	1.85
3G	25.	.997	2.39
3G	30.	1.00	3.03
3G	35.	1.02	5.07
3G	40.	.995	7.98
3G	45.	1.00	12.3
3G	50.	1.05	(37.8)
4G	5.	1.01	1.05
4G	10.	.993	1.27
4G	15.	1.00	1.51
4G	20.	.998	1.85
4G	25.	1.01	2.41
4G	30.	1.01	3.36
4G	35.	1.00	5.17
4G	40.	1.00	7.16
4G	45.	1.02	11.6
4G	50.	1.10	(32.2)
5S	10.	.998	1.29
5S	20.	.994	1.94
5S	30.	.993	3.38
5S	40.	1.02	8.26
5S	50.	1.10	(29.3)
6S	10.	1.00	1.29
6S	20.	1.00	1.89
6S	30.	.999	3.35
6S	40.	1.03	8.65
6S	50.	1.12	(30.6)

TABLE 8 -- Continued

Experimental Results of Monomodal Suspensions

Bob, Cup	Total Concentration Volume %	Power Law Index	Relative Viscosity
	183 micron spheres continued		
5S	40.	1.01	7.00
3S	40.	.995	6.94
3S	30.	.999	3.14
	221 micron spheres		
3G	20.	.981	1.89
3G	40.	1.00	9.74
3G	45.	1.04	(19.9)
3G	50.	1.11	(52.8)
4G	20.	1.01	1.94
4G	40.	1.01	8.42
4G	45.	1.03	16.0
4G	50.	1.09	(45.1)
5S	20.	1.01	2.02
5S	40.	1.02	8.51
5S	45.	1.01	13.8
5S	50.	1.10	(32.7)
6S	20.	1.01	1.90
6S	40.	1.02	7.96
6S	45.	1.02	13.9
6S	50.	1.10	(31.9)
3S	40.	.979	6.86
3S	40.	1.00	7.75
3S	40.	.99	7.35

(...) denotes results for non-Newtonian suspensions.

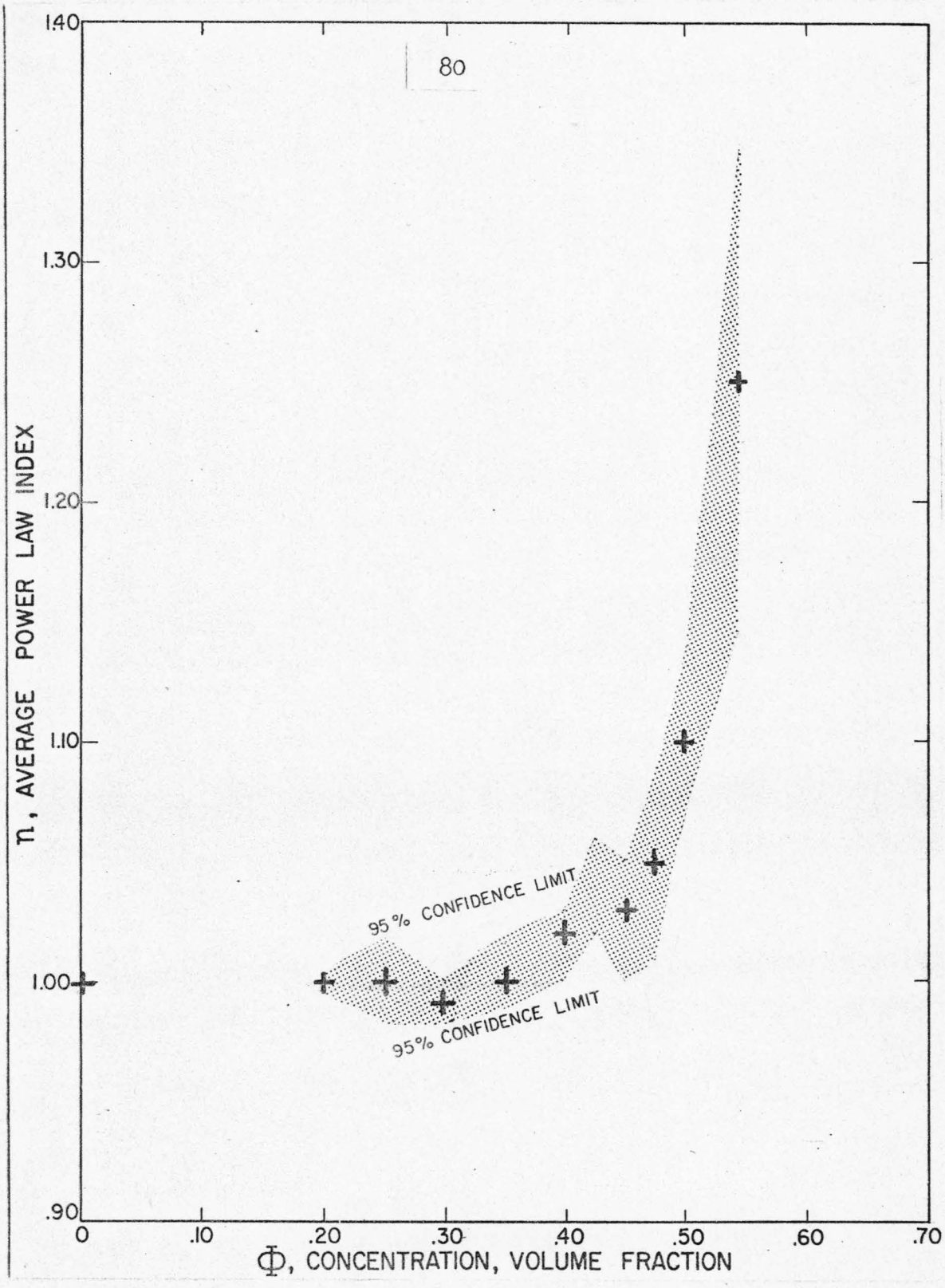

Figure 8. Power law index as a function of concentration in monomodal suspensions.

TABLE 9

Average Power Law Index as a Function of Concentration in Monomodal Suspensions

Concentration	Average Power Law Index	Number of Suspensions	95% Confidence Limits
0	.999	27	.996, 1.00
5	.997	3	
10	.997	5	
15	.991	3	
20	1.00	23	.996, 1.00
25	1.00	3	.985, 1.02
30	.991	24	.982, .999
35	1.00	10	.988, 1.02
40	1.02	20	1.00, 1.03
42.5	1.04	4	1.02, 1.06
45	1.03	14	1.00, 1.05
47.5	1.05	4	1.01, 1.09
50	1.10	17	1.07, 1.14
52.36	1.25	5	1.15, 1.35
55	1.09	1	-- --

of unity is included within the 95% confidence limits on the mean experimental power law index at concentrations of 45 volume percent and lower. This experimental result supplies quantitative corroboration of the theoretical predictions by Chong (10) and by Allen and Kline (6) of the limiting concentrations to which hydrodynamic and continuum models of suspensions are valid. There was no experimental indication of a yield stress for any of these suspensions (except the last three entries in the 26-micron group). The raw data plots are linear on log-log coordinates to a very high approximation.

On the basis of this variation of power law flow index with concentration, suspensions whose power law flow indices lie within the range 0.97-1.03 will be considered Newtonian fluids for the purpose of calculating viscosity and relative viscosity. Suspensions whose power law indices lie outside that range will be considered non-Newtonian fluids.

Reproducibility. As a test of the reproducibility of the experimental technique, a nine-fold replicate observation of the viscosity of 30 volume percent suspensions of 183 micron spheres was carried out. Nine separate suspensions were individually prepared from the same recipe, suspending fluid, and spheres and measured in the 5S cup and bob set; two results were eliminated because their power law flow indices were less than 0.965. The suspending fluid and spheres were sampled without replacement. The

coefficient of variation for the power law index was 2.1%, and the coefficient of variation of the relative viscosity was 5.3%.

Two other 30 volume percent suspensions of 183 micron spheres were prepared and measured in the 5S set at other times for a total of 11 measurements at this size and concentration. Of these 11 measurements, two resulted in power law indices outside the range 0.97-1.03 and were deleted. For these nine collected measurements, the average relative viscosity was 2.86 with a coefficient of variation of 8.3% and 95% confidence limits of 2.68, 3.04.

Wall effects. The existence of a wall effect was investigated by comparing relative viscosities from smooth walled and rough walled cups and bobs in two ways. First, the ratios of relative viscosities in rough walled cups and bobs to relative viscosities in smooth walled cups and bobs were formed, and compared to unity by means of the 't' test for significance of the difference between means. The test was applied to the data arranged in the following classifications: all data as a group, individual sphere diameters, and by bob length. None of the differences were statistically different from zero, indicating that if there is a wall effect, it is not large enough to reliably distinguish from the experimental variation in these data. It is important to recognize that this conclusion does not eliminate the possibility of a wall effect. Second, the relative viscosity was plotted versus sphere diameter for each of the two wall conditions and the "zero diameter"

relative viscosity determined by extrapolation, with the results shown in Table 10. The differences between the two wall conditions are systematic and, for 30 volume percent, slightly larger than the single-sided width of the 95% confidence limit on the mean. These extrapolated differences are large enough to possibly be of real significance, in contrast to the results of the direct examination of the experimental data. The existence of a wall effect is uncertain but the indicated magnitude seems to be ten percent or less of the smooth wall viscosity. In the absence of a reliable demonstration of a wall effect, the distinction between rough walled and smooth walled results will be dropped in the remainder of the discussion of the results.

Electroviscous effects. Electroviscous effects were apparent in a few of the 26 and 61 micron sphere suspensions. The last three entries under 26 microns in Table 8 are the major cases.

There were several obvious symptoms. The first was the unusual gel-like nature of the test suspensions used to check the suspending fluid specific gravity. In the usual check, a test suspension thermostatted at 37 C would separate noticeably in an afternoon, with some of the spheres sinking and some floating with no noticeable agglomeration. The 26 and 61 micron bimodal test suspension didn't settle at all, and was visibly flocculated. The second symptom was the complete disruption of the anticipated schedule of torque range switching during the experiment due to the ab-

TABLE 10

Extrapolated Zero Diameter Relative Viscosities

As a Function of Wall Condition

Concentration Volume Percent	Relative Viscosity		Difference Percent
	Smooth Wall	Grooved Wall	
20	1.95	2.07	6.2
30	3.37	3.62	7.4
35	5.28	5.85	10.8
40	7.39	8.17	10.5

normally large torques observed at slow cup speeds. The third developed concurrently with the second in the form of a glaringly unusual raw data flow curve. The raw data flow curves for the troublesome suspensions were strongly curved, concave upward on log-log coordinates, tending toward a constant torque at low cup speed (a yield stress) and tending very gradually toward a Newtonian line at high cup speeds. The curvature of the raw data flow curves was much more pronounced for the 26 micron spheres than for the 61 micron spheres.

The circumstance under which these effects appeared was a change in the nature of the suspending fluid mixture. The suspending fluid mixture used for all the monomodal suspensions preceding those measured in the bimodal investigation had also been used in the specific gravity separations and had been in contact with the glass spheres and the tramp metal accompanying the spheres for many hours. This old fluid had been discolored to a rosy golden color with various contaminants including, presumably, metal ions and free bromine. This old fluid was all inadvertently contaminated beyond reclamation with acetone by an unwise change in the clean-up procedure, so a fresh batch of fluid was prepared from virgin material. The new suspending fluid mixture was very clean, and nearly colorless, but suspensions of 26 and 61 micron spheres prepared from it were very non-Newtonian.

The non-Newtonian character of the suspensions of 61 micron spheres was easily suppressed by the addition of a relatively

small fraction of old fluid to the new, but the non-Newtonian characteristics of suspensions of the 26 micron spheres in the new fluid mixture could not be suppressed in this way. Hence, the very low power law flow indices in the last three entries under 26 microns in Table 8.

Summary curves. Following the recommendations by Thomas (51), the relative viscosity as a function of sphere diameter at each concentration was extrapolated to zero sphere diameter in order to remove diameter dependence. Shear rate dependence was eliminated by excluding the relative viscosities of suspensions whose calculated power law index lay outside the range 0.97-1.03. The extrapolation was accomplished by fitting a least squared error polynomial of degree one to the relative viscosity, as a function of sphere diameter. The intercept of each polynomial was taken as the zero diameter relative viscosity at that concentration. Strictly speaking, four such values could be obtained, as shown in Table 11. These points are shown in Figure 9, representing the relative viscosity of monomodal suspensions between 20 and 40 percent by volume solids, with the sphere diameter and shear rate dependence removed. The point at 35 volume percent tends to stray due to the smaller data set used in the extrapolation.

The relative fluidity function, $\frac{1}{\mu_r}$, is shown in Figure 10. Figure 11 shows the plot of $(\ln \mu_r)^{-1}$ as a function of $(\varphi)^{-1}$, and Figure 12 shows the plot of $\varphi/(\ln \mu_r)$ versus φ; the monomodal Mooney equation is a straight line on both these latter two figures.

TABLE 11

Extrapolated Zero Diameter, Relative Viscosity of

Newtonian Monomodal Suspensions

Concentration Volume %	Relative Viscosity	Number of Sphere Sizes	Number of Measure-ments
20	2.00	5	22
30	3.40	3	15
35	5.42	2	8
40	7.92	5	26

Smoothed Experimental Results

20	1.97
25	2.54
30	3.44
35	5.04
40	8.18
45	15.5

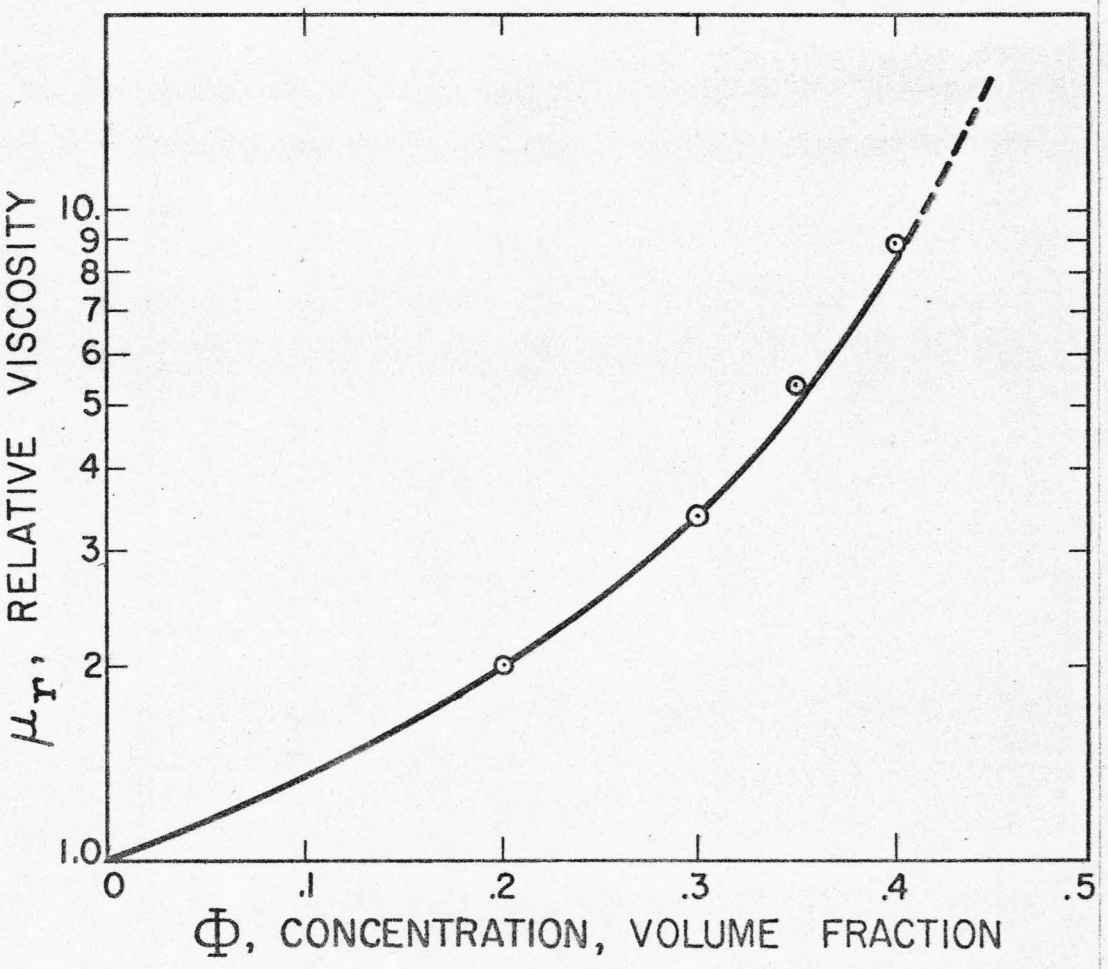

Figure 9. Extrapolated, zero diameter, relative viscosity of Newtonian monomodal suspensions as a function of concentration.

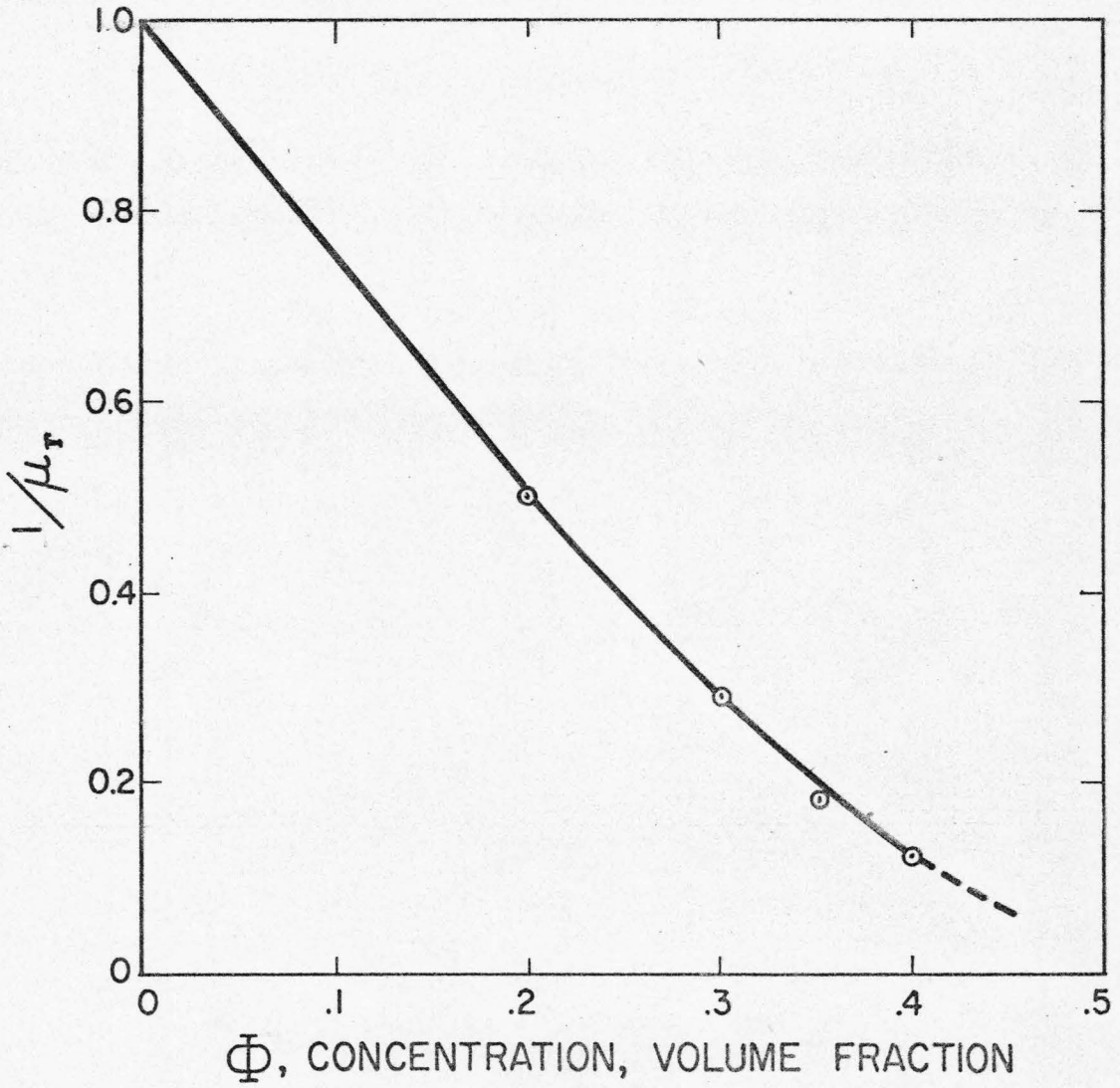

Figure 10. Relative fluidity of Newtonian monomodal suspensions as a function of concentration.

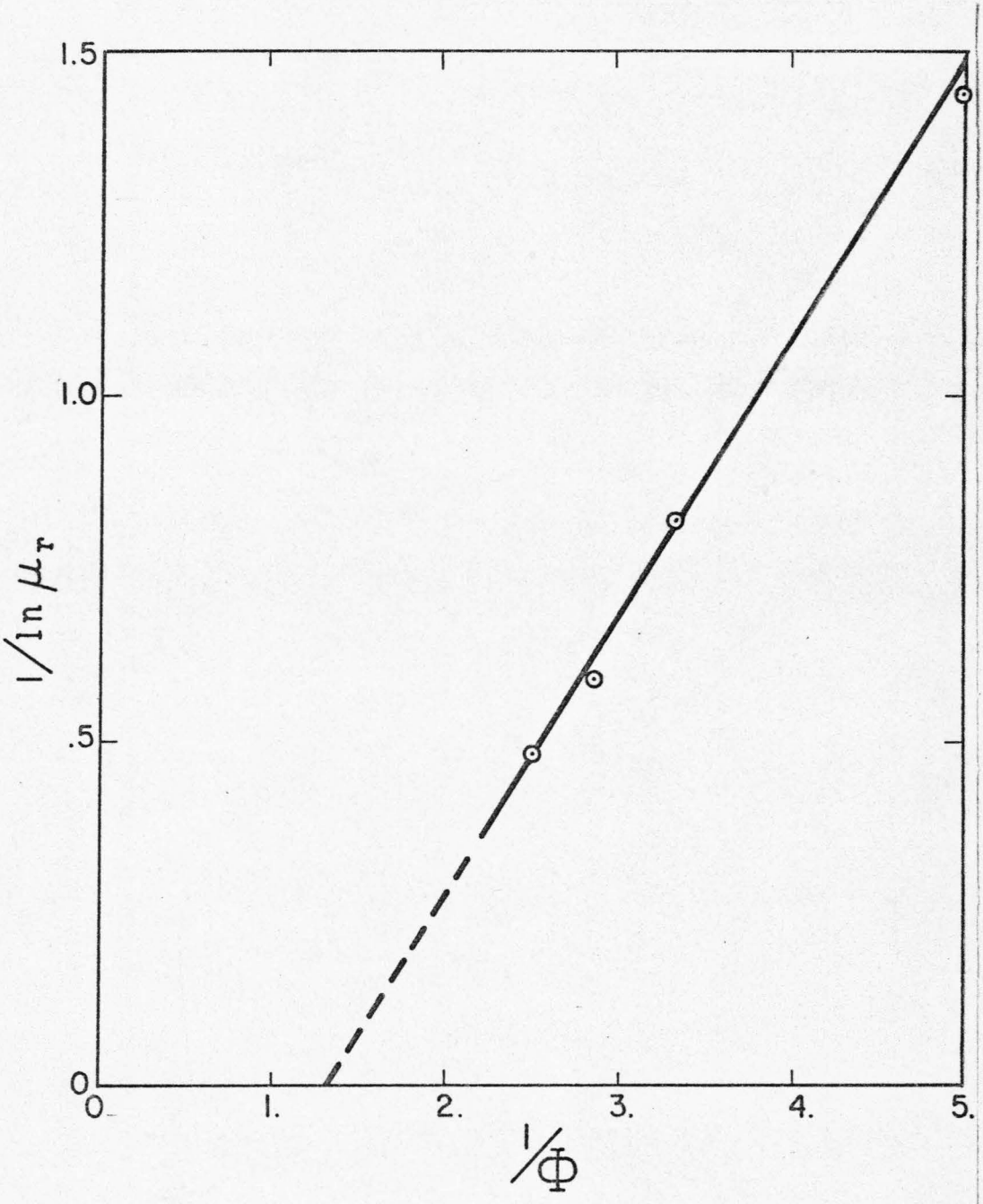

Figure 11. $(\ln \mu_r)^{-1}$ versus $(\varphi)^{-1}$ for Newtonian monomodal suspensions.

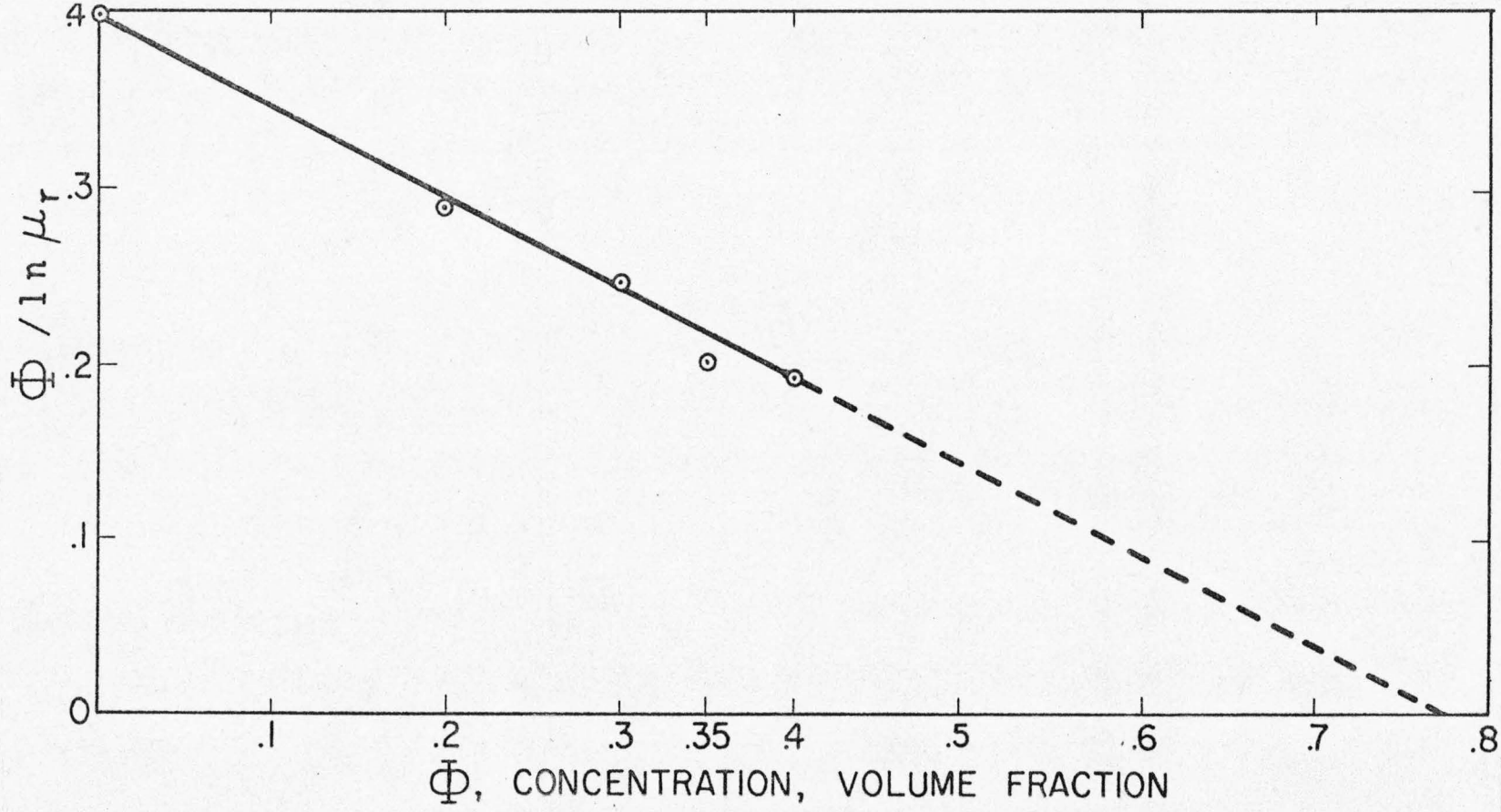

Figure 12. $\varphi/\ln \mu_r$ versus φ for Newtonian monomodal suspensions.

If the Newtonian results for each size of sphere are smoothed and interpolated with the monomodal Mooney equation, it is possible to use all the Newtonian experimental results to extrapolate to the zero diameter relative viscosity at closely spaced intervals in concentration. The $\varphi/\ln \mu_r$ versus φ plot was used for smoothing and interpolating and the results are tabulated in Table 11 and shown as the solid lines in Figures 9, 10, 11, and 12.

The theoretical maximum concentration is determined to be 0.764 and the self-crowding factor is found to be 1.308. This smoothed curve incorporating all the Newtonian results will be compared to the literature results.

Comparison of experimental results with the literature. The smoothed curve of experimental results is compared to the published experimental data and to the recent theoretical results, and some of the standard theoretical forms. The φ_m parameter is estimated and discussed and some empirical coefficients are stated for the most appropriate theoretical equations.

The comparison of the present results to the reviews of the previous experimental literature by Rutgers (43) and Thomas (51) is shown in Figure 13, where the present results are seen to lie between the previous recommended curves. This location is interpreted as an indication of favorable agreement with the results of the earlier work. Figure 14 displays the excellent agreement of the present results with those of Lewis and Nielsen, whose results

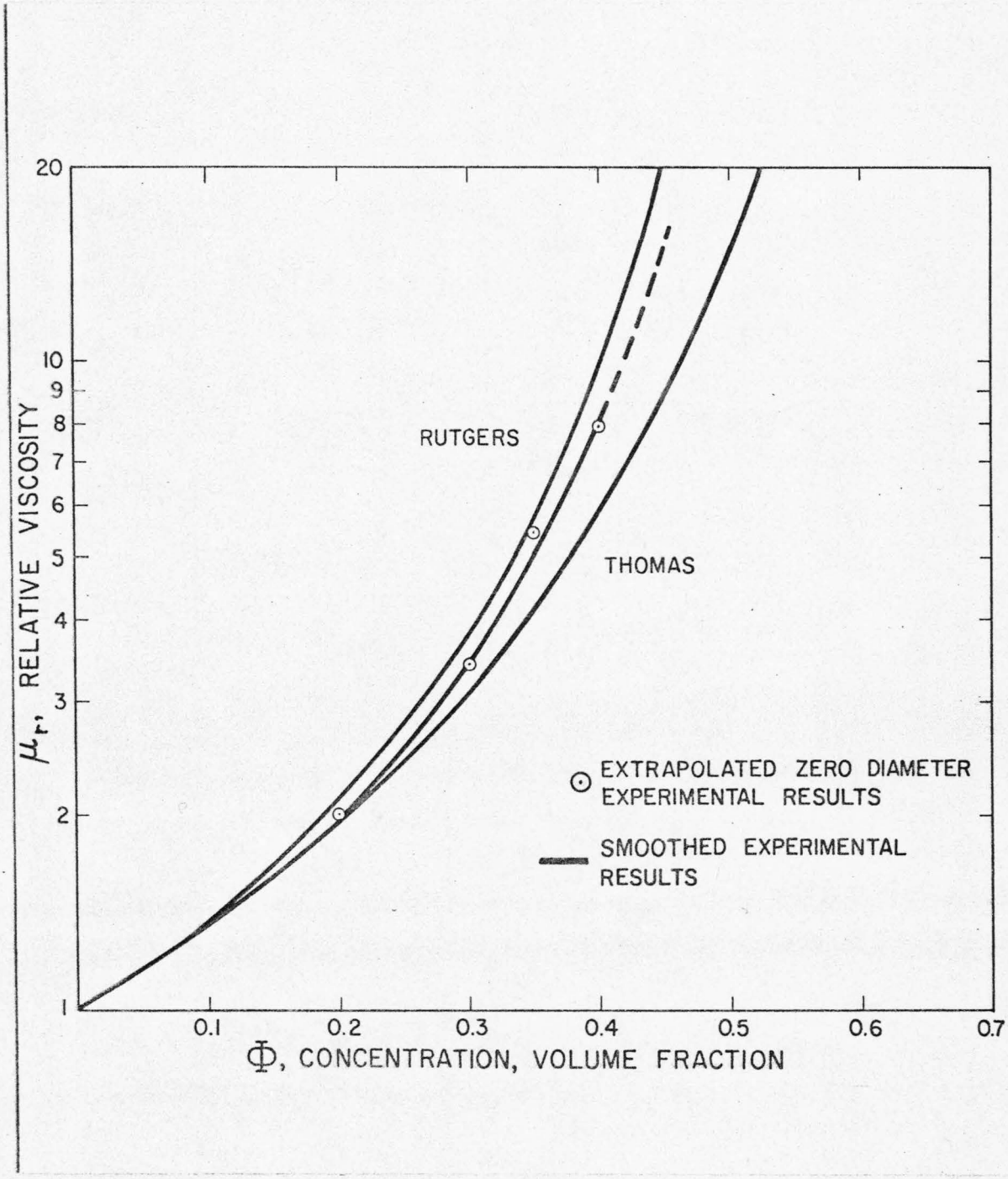

Figure 13. Comparison of experimental relative viscosity curves.

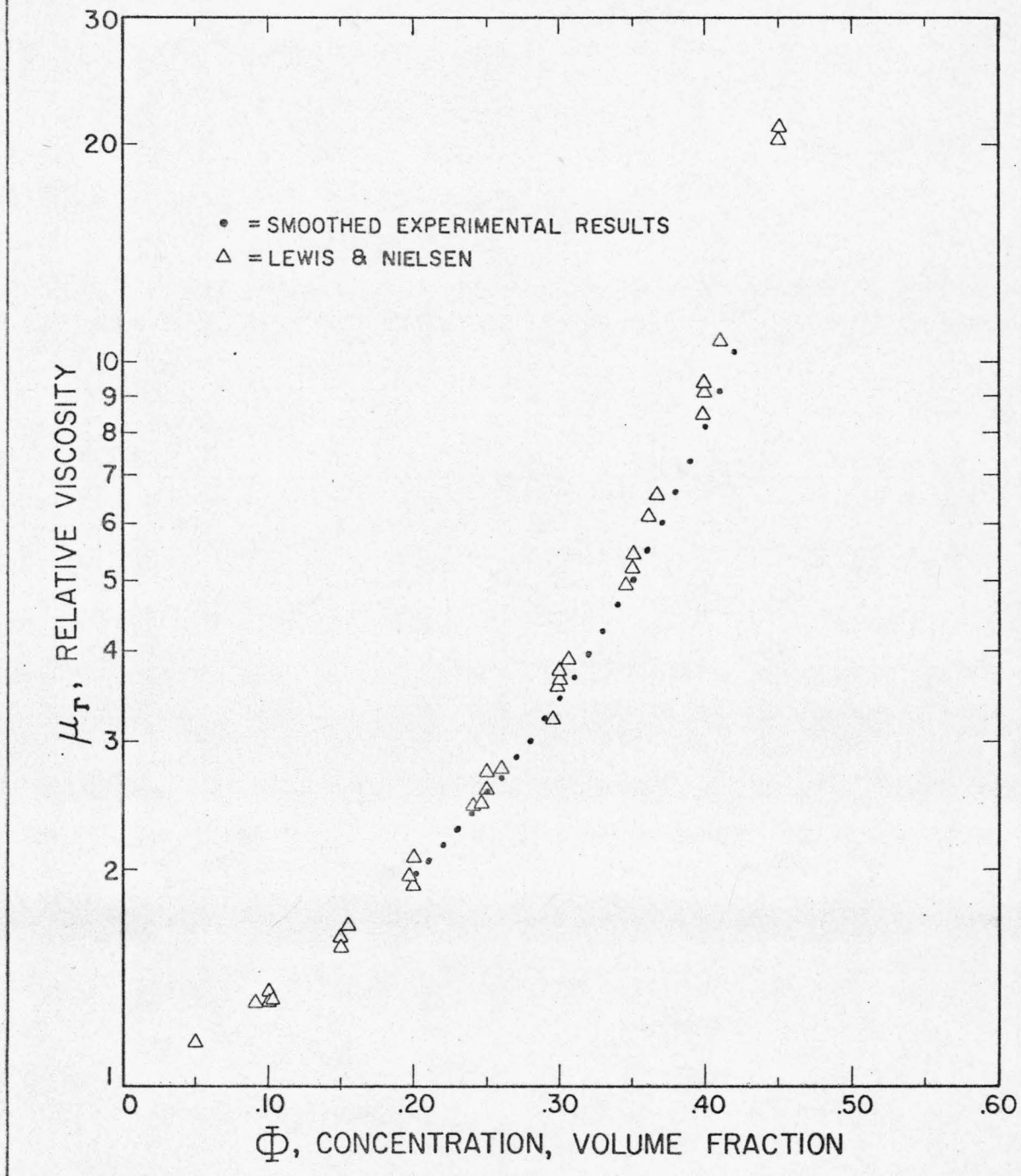

Figure 14. Comparison of smoothed experimental results with those of Lewis and Nielsen.

also showed non-Newtonian flow at concentrations above 45 volume percent. Figure 15 shows the good agreement of the present results with those of Seshadri and Sutera (47) in terms of the relative fluidity function, $1/\mu_r$. Bagnold's (7) results were not published in a form convenient for direct comparison but the present results are in general agreement in the matters of the limits of Newtonian flow and wall effects. The results of Clarke (11), Gay et al. (24), and Chong (10) are, in general, not comparable in a rheological sense, mainly due to disqualifying discrepancies in instruments, experimental conditions, or rheological interpretation of experimental data.

The good agreement with the reviewers' recommended curves, and with comparable published experimental results is interpreted as qualifying the experimental equipment and method for the experimental study of the rheology of suspensions of rigid, neutrally buoyant spheres in Newtonian liquids.

The principal theoretical result to which the present experimental results are compared is the monomodal form of Mooney's equation. The two constants in Mooney's (37) equation for the relative viscosity of monomodal suspensions were evaluated from the four points of the unsmoothed experimental results following the method of Sweeny and Geckler (50), in which Mooney's equation

$$\ln \mu_r = \frac{a \varphi}{1-\lambda_{11}\varphi}$$

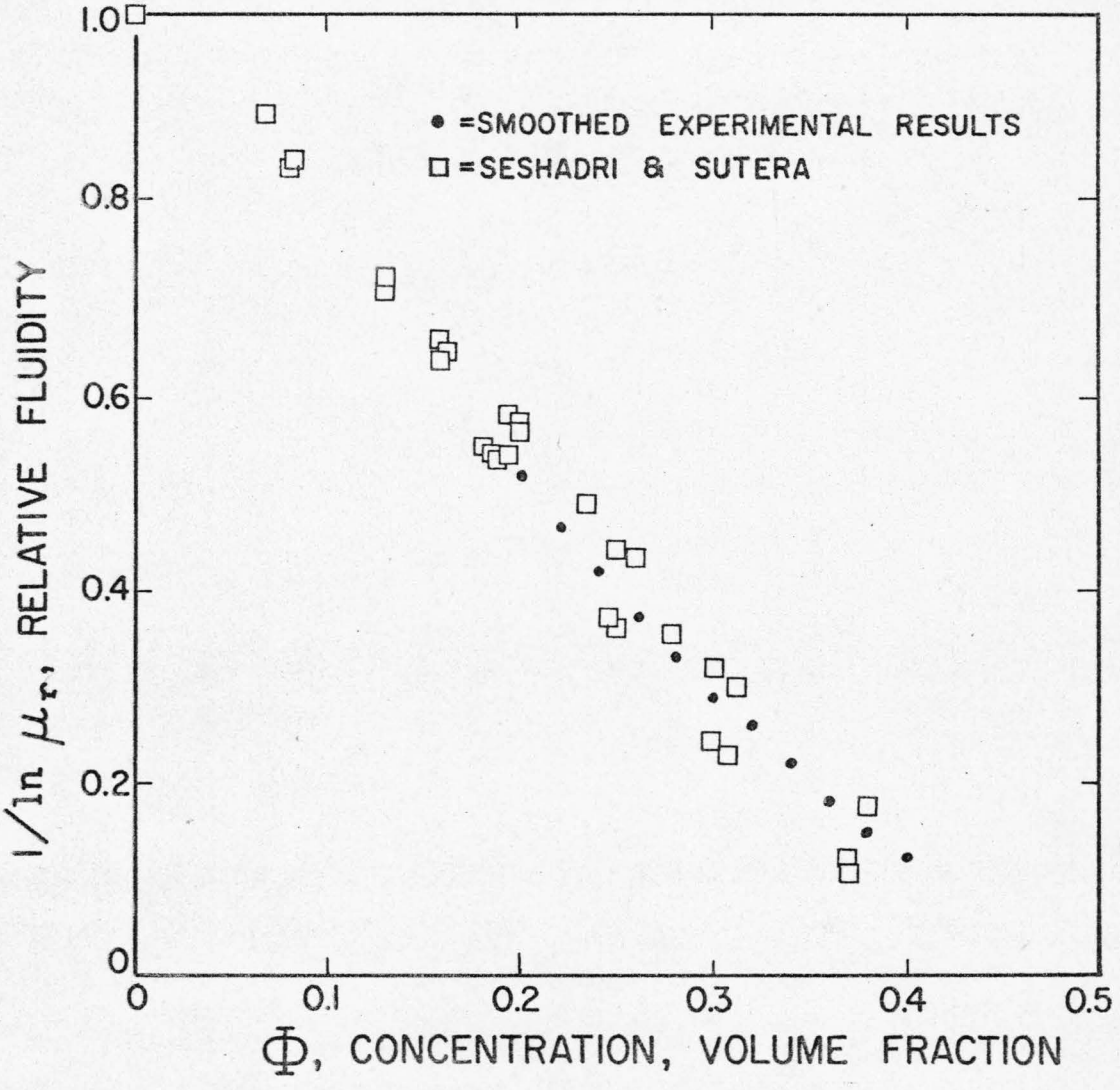

Figure 15. Comparison of smoothed experimental results with those of Seshadri and Sutera.

is rearranged to

$$\frac{1}{\ln \mu_r} = -\frac{\lambda_{11}}{a} + \frac{1}{a}\left(\frac{1}{\varphi}\right)$$

in which $-\frac{\lambda_{11}}{a}$ is the intercept, and $\frac{1}{a}$ is the slope of a straight line through the $\left(\frac{1}{\varphi}, \frac{1}{\ln \mu_r}\right)$ points. A least squared error polynomial of degree one was fitted to the $\left(\frac{1}{\varphi}, \frac{1}{\ln \mu_r}\right)$ data, with the result:

$$\frac{1}{\ln \mu_r} = -0.493794 + 0.387856 \left(\frac{1}{\varphi}\right)$$

Mooney's equation is then found to be:

$$\mu_r = \exp\left(\frac{2.58\,\varphi}{1.273\,\varphi}\right)$$

The theoretical maximum concentration, φ_m, is represented by the zero of the fitted polynomial from which

$$\varphi_m = 0.785 .$$

These values for slope and intercept of the rearranged monomodal Mooney equation compare very favorably with the values tabulated by Sweeny and Geckler (50) for their own and previous work. The present results enjoy additional advantages by virtue of having dependence upon sphere size and shear rate removed. A related procedure was applied to get smoothed experimental results, in which a least squared error straight line was fitted to all the extrapolated experimental results on $\left(\varphi, \frac{\varphi}{\ln \mu_r}\right)$ coordinates with the line constrained

to pass through (0,.4), in order to determine the hydrodynamic, or self crowding, factor, λ_{11}, for subsequent use with the bimodal results. This procedure resulted in the following form of the monomodal Mooney equation:

$$\mu_r = \exp\left(\frac{2.5\,\varphi}{1 - 1.308\,\varphi}\right) .$$

The corresponding value of φ_m is 0.764.

The comparison of the present smoothed experimental results to the recent theoretical contributions is shown in Figure 16. The modified Vand equation proposed by Lee (30) does not fit these experimental results very well but the modified Roscoe Brinkman equation proposed by Lee (30) is close in magnitude and very good in terms of shape, suggesting that perhaps the constants are off a little. The modified Einstein equation proposed by Chong (10) does not match the shape of the smoothed experimental curve very well but the modified Eiler's equation, ($\varphi_m = 0.605$) put forward by Chong (10) matches the shape very well, again suggesting a modification of some of the constants. The Bagnold equation is essentially equivalent to Chong's modified Eiler's equation so the poor showing of the Bagnold equation can be attributed to the choice of $\varphi_m = 0.74$, suggesting that both the Chong and Bagnold equations could be fitted to the present smoothed experimental results with a better choice of φ_m. The equation proposed by Frankel and Acrivos (21), with $\varphi_m = 0.764$, is closer to the present smoothed experimental results at low concentrations than at high concentration, contrary to the

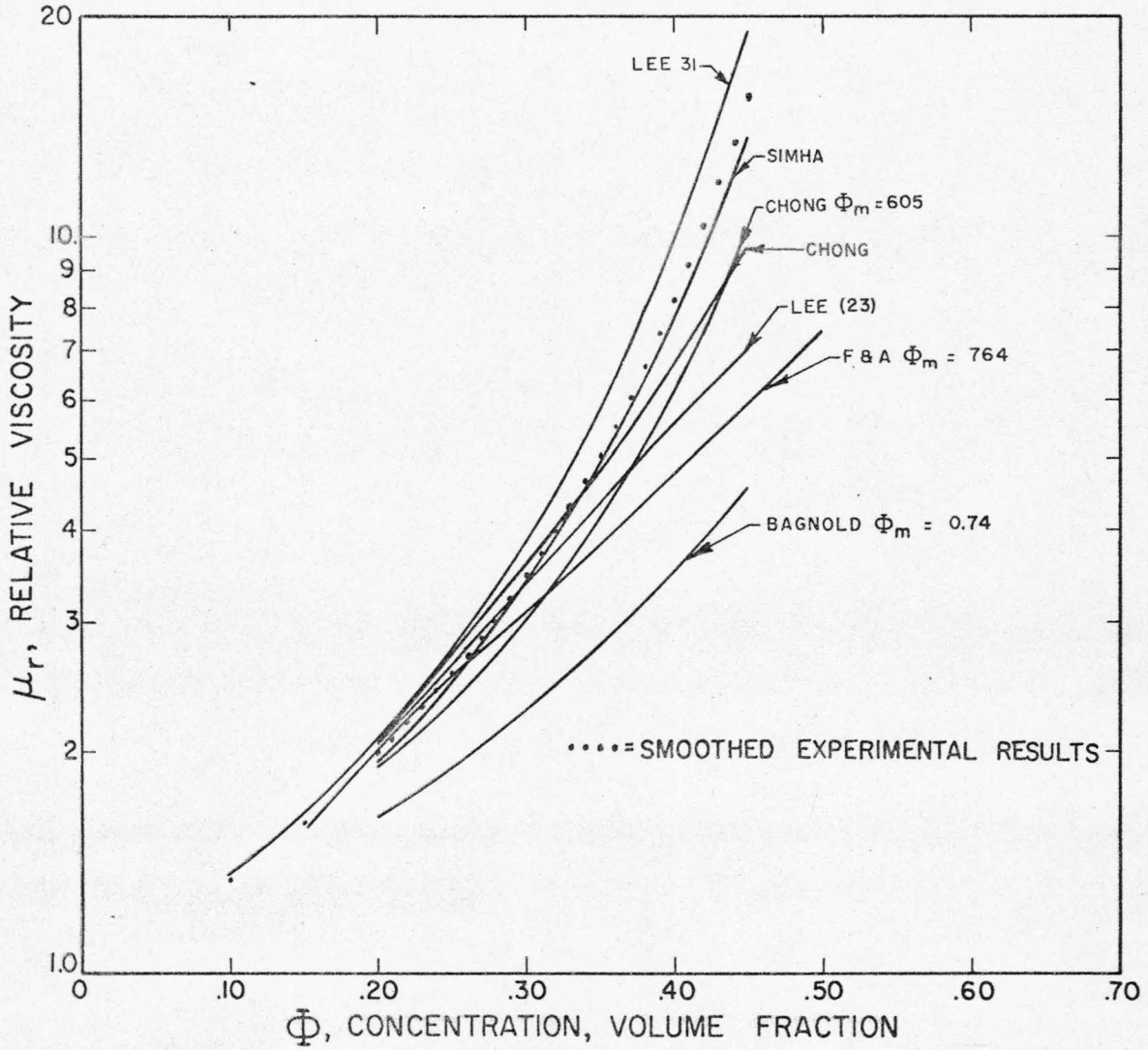

Figure 16. Comparison of smoothed experimental results to recent theoretical contributions.

restrictions of the equation's development, suggesting that a different choice of φ_m is required. The equation proposed by Moulik (38) was tested by plotting $(\mu_r)^2$ versus φ^2 to reveal a highly non-linear relationship, which eliminates his equation from further consideration for suspensions of spheres, although it may still be useful for solutions.

Figure 17 shows a comparison of the present smoothed experimental results and the Ford (20) and Vand (54) equations for relative fluidity, $\frac{1}{\mu_r}$. The Ford (20) equation has its first zero at a concentration between 51 and 52 volume percent which seems too low, resulting in fluidity values smaller than the experimental results over the range of measurements. The Vand equations also give fluidities smaller than the experimental values but the shape of the Vand curves match the smoothed experimental data better than the Ford curve does. The overall good agreement suggests that the smoothed experimental curve could be fitted with either of the forms of the Ford or Vand equations.

The equations by Frankel and Acrivos (21), Chong (10), and Bagnold (7) may all be used to estimate a value for φ_m appropriate to the smoothed experimental results. When the Frankel and Acrivos equation is recast in terms of $\varphi_r \equiv \varphi/\varphi_m$ and the Chong and Bagnold equations are recast in terms of $\varphi^* \equiv (\varphi/\varphi_m)/(1 - \varphi/\varphi_m)$ the following procedure will apply to both forms: compute μ_r as a function of φ_r and as a function of φ^* and plot; from the plots read the values

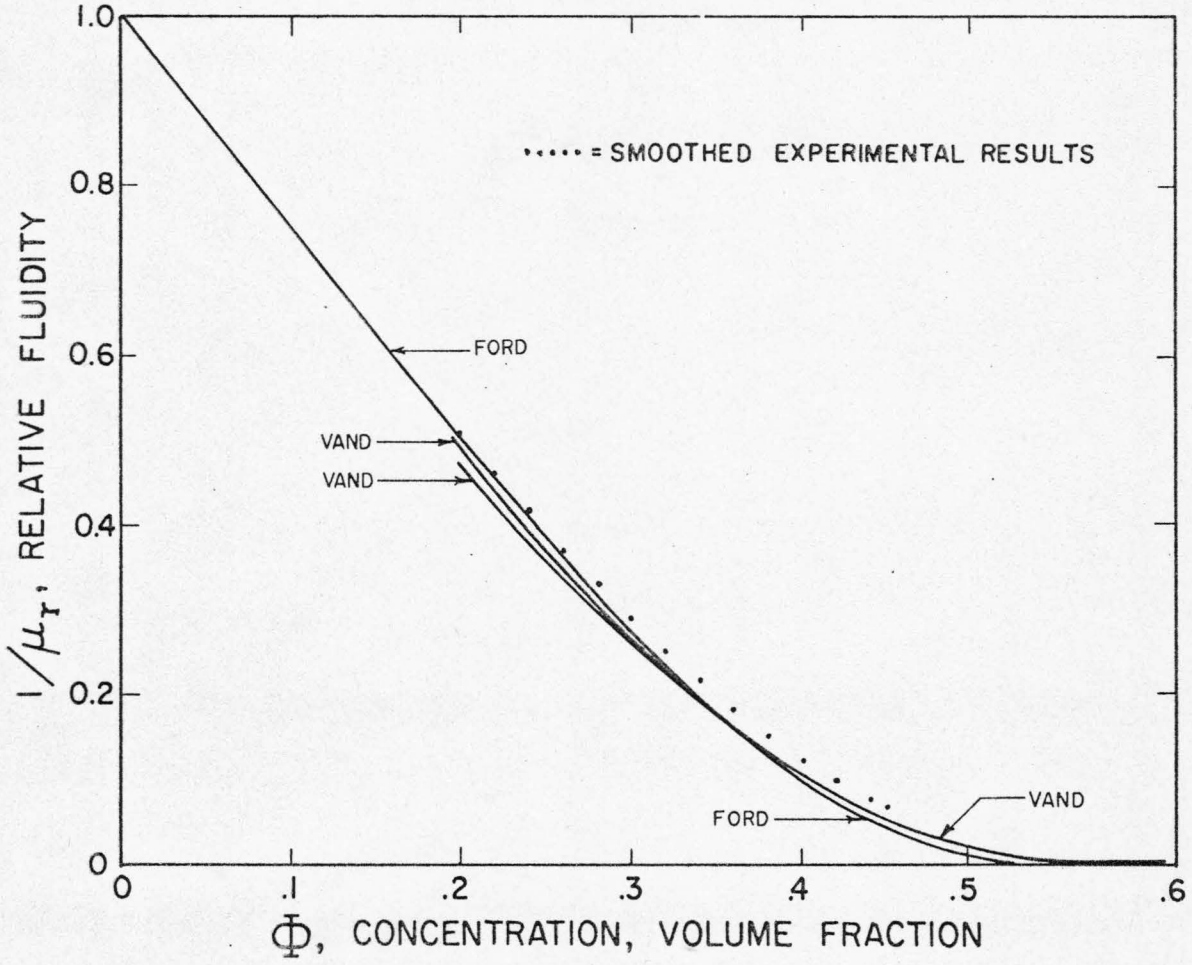

Figure 17. Comparison of smoothed experimental results to the Ford and Vand equations.

of φ_r and φ^* corresponding to experimental values of μ_r ; compute φ_m from the experimental values of φ and the graphical values of φ_r and φ^* ; plot φ_m as a function of φ and determine the limiting value at the upper values of φ . The result is $\varphi_m = 0.55$ for <u>both</u> the Frankel and Acrivos (21) equation and the Chong (10) and Bagnold (7) equations, bringing to mind the volume fraction of the simple cubic packing of spheres 0.5236. There are two quick possible explanations why the experimental result is greater than the simple cubic packing volume fraction: the first is the slight dispersion in sphere diameter and the second is the inclusion of relative viscosities for suspensions whose power law indices were greater than one. Both these influences would tend to increase φ_m over the single-size, simple cubic packing value.

The smoothed experimental results and a least squared error polynomial fit computer program were used to determine the coefficients in the following equations:

Mooney equation: $\mu_r = \exp [2.5 \varphi/(1-1.31 \varphi)]$

Fluidity polynomial: $\frac{1}{\mu_r} = a_o + a_1 \varphi + a_2 \varphi^2 + \ldots ,$

coefficients are shown in Table 12.

Relative Viscosity polynomial: $\mu_r = a_o + a_1 \varphi + a_2 \varphi^2 + \ldots ,$

coefficients are shown in Table 12.

TABLE 12

Least Square Fitted Polynomial Coefficients

a_o	a_1	a_2	a_3	a_4	a_5	a_6	a_7
Fluidity Polynomial							
.977	-2.18						
1.00	-2.82	1.55					
1.00	-2.46	- .775	+3.58				
1.00	-2.50	- .266	1.72	2.10			
1.00	-2.51	- .00327	.0375	6.42	-3.86		
1.00	-2.50	- .260	2.51	-4.25	17.3	-15.7	
1.00	-2.49	- .586	6.81	-31.3	105.	-157.	89.8
Relative Viscosity Polynomial							
- .409	21.6	108.					
1.51	-22.9	-195.	466.				
1.03	-11.7	239.	-1.12×10^3	1.79×10^3			
.994	10.5	-19.3	1.63×10^3	-5.29×10^3	6.32×10^3		
1.00	-1.66	148.	-1.65×10^3	8.86×10^3	-2.17×10^4	2.08×10^4	
1.00	4.63	-84.	1.41×10^3	1.04×10^4	4.08×10^4	-8.01×10^4	6.41×10^4

Lee's Modified Roscoe-Brinkman equation:

$$\mu_r = \left(\frac{1}{1 - \varphi}\right)^{(2.5 + 1.16\varphi + 7.33\,\varphi^2)} .$$

Chong-Bagnold polynomial in φ^* :

$$\mu_r = 1 + 1.70\,\varphi^* + 0.337\,(\varphi^*)^2 .$$

Vand's equation:

$$\frac{1}{\mu_r} = (1 - .991\,\varphi - 1.07\,\varphi^2)^{2.5} .$$

Simha's (45) "f" parameter was evaluated, following the procedure indicated by Simha and Somcynsky (46), with the result: f = 1.79. The resulting values of relative viscosity are shown on Figure 16 where the agreement of Simha's equation with the smoothed experimental results is seen to be very good. "f" varies with concentration and, in fact, has a maximum near 30 volume percent in the present results and near 40 volume percent in Simha and Somcynsky's determination. Simha and Somcynsky chose the maximum value for their comparison with the summary curve by Thomas, but the good agreement between the present smoothed experimental results and the Simha equation would be further improved by the use of the high concentration limiting value, f = 1.74, in place of the maximum value. By way of contrast, Simha's (45) expression for relative viscosity in the limit of high concentration is a very poor fit to the present results, since the calculated expression approaches

the experimental results from below with a large value of the slope.

An alternate representation of the experimental data. Monomodal suspensions are power law fluids, with a shear stress-shear rate relationship given by

$$\tau = m \left|\dot{\gamma}\right|^{n-1} \dot{\gamma}$$

in which n is the power law index, and

m is the consistency coefficient.

At concentrations below approximately 35 volume percent solids, $n = 1.0$ and m is the same as μ, the viscosity, so that monomodal suspensions are well characterized by a Newtonian relative viscosity, μ_r. Above 35 volume percent, $n > 1.0$, and monomodal suspensions require more than one parameter to characterize their flow properties. An alternative to the relative viscosity is shown in Figure 18 where the "relative consistency, m/μ_o", is shown as a function of concentration. This function, together with the power law index shown in Figure 8, provides an accurate power law representation of the experimental flow properties of concentrated monomodal suspensions beyond the range of validity of the relative viscosity. At low concentrations, the relative viscosity curve and the relative consistency curve coincide.

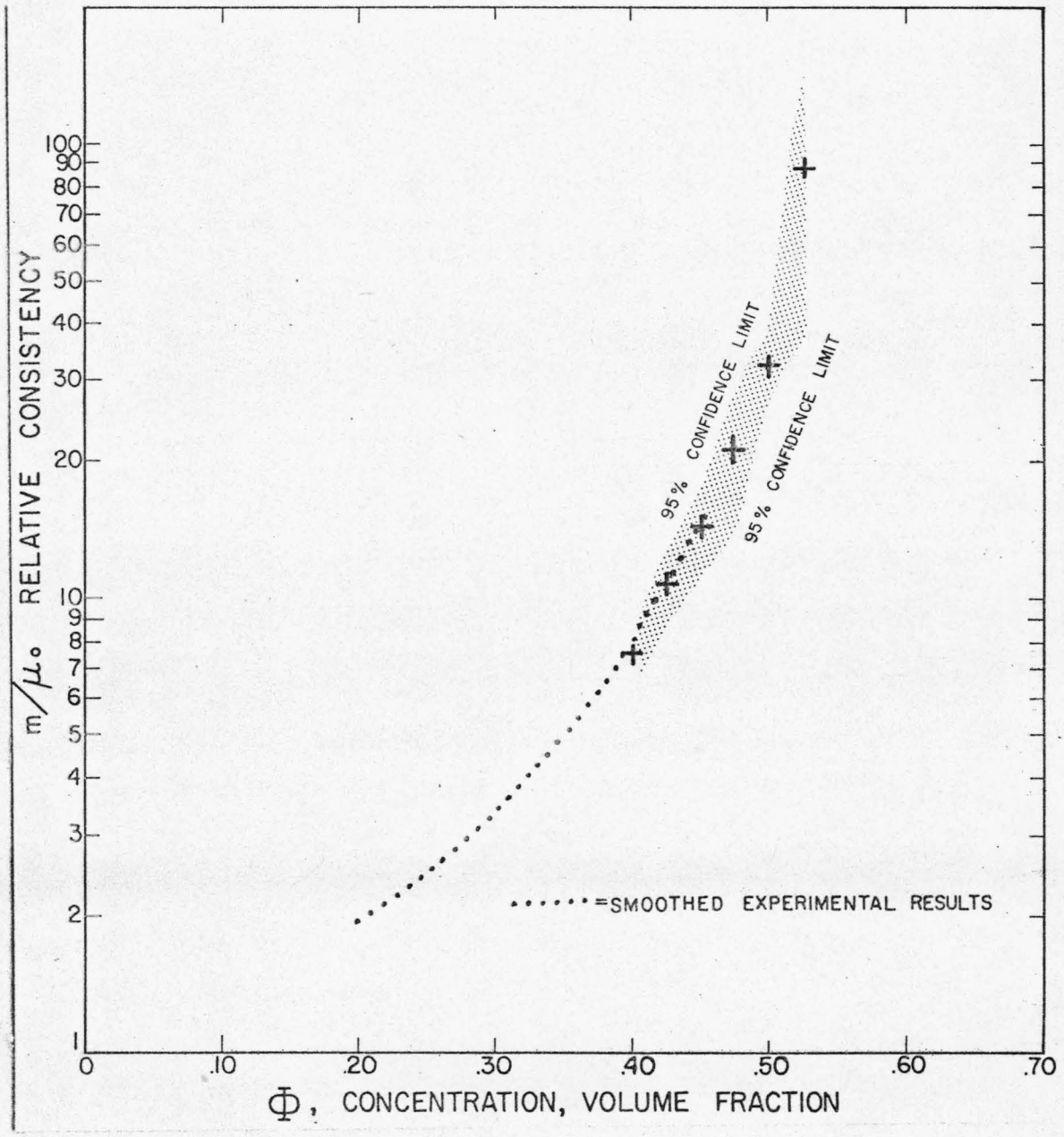

Figure 18. Average relative consistency for monomodal suspensions as a function of concentration.

(This page intentionally blank)

Bimodal Suspensions

Results. The results of the bimodal measurements are tabulated in Table 13. The unhappy effect of the combination of the 26 micron spheres and the new suspending fluid is especially noticeable in the 26/61, 26/125, and 26/221 series of measurements in which all the suspensions having an appreciable volume fraction of 26 micron spheres exhibit abnormally low power law flow indices. This effect does not appear in the extensive 26/183 series because the old fluid was used for those measurements, and the measurements were made before the old fluid was ruined. The power law index for the 40 volume percent bimodal suspensions is generally smaller than that for a monomodal suspension of the same concentration.

The viscosities of those suspensions for which electroviscous effects were apparent were calculated by means of a least square error fit of the experimental shear stress, shear rate data to the Casson equation (9):

$$(\tau)^{1/2} = K(\dot{\gamma})^{1/2} + (\tau_y)^{1/2}$$

from which K^2 represents the limiting differential viscosity of the Casson fluid. The experimental data were satisfactorily linear on the square root coordinates. The relative viscosities of such suspensions were calculated as $\mu_r^* = K^2/\mu_o$. These values are marked with an asterisk in Table 13. This definition of relative viscosity is a departure from previous practice but is adopted here as a consistent and accurate representation of the experimental data.

TABLE 13

Experimental Results for Bimodal Suspensions

Concentration Volume %	Composition % Small/% Large	Power Law Index	Relative Viscosity, μ_r, or μ_r^*
	26, 61 micron spheres	r_i/r_j = .43	
40	30/70	.944	6.23*
40	40/60	.920	5.93*
40	50/50	.853	6.19*
	26, 125 micron spheres	r_i/r_j = .21	
40	30/70	.939	5.12*
40	40/60	.929	5.25*
40	50/50	.927	5.35*
20	30/70	1.01	1.90
30	30/70	.970	2.76
50	30/70	.957	14.2 *
	26, 183 micron spheres	r_i/r_j = .14	
40	10/90	1.00	5.57
40	20/80	1.00	4.90
40	30/70	.995	4.81
40	30/70	1.03	4.58
40	40/60	1.01	4.86
40	50/50	1.01	5.06
40	60/40	1.01	5.26
40	70/30	1.00	6.42
40	80/20	1.03	6.88
40	90/10	(1.05)	(9.20)
40	90/10	1.00	9.72
20	30/70	1.00	1.77
30	30/70	.998	2.68
50	30/70	.999	10.1
60	30/70	.988	29.2
20	50/50	1.01	1.83
30	50/30	.999	2.80
45	50/30	1.02	7.57
50	50/50	.993	12.4
55	50/50	1.01	21.6
60	50/50	(1.08)	(83.2)

TABLE 13 -- Continued

Experimental Results for Bimodal Suspensions

Concentration Volume %	Composition % Small/% Large	Power Law Index	Relative Viscosity, μ_r, or μ_r^*
	26, 221 micron spheres	$r_i/r_j = 0.12$	
40	20/80	.968	4.55*
40	30/70	.945	4.22*
40	40/60	.908	4.13*
40	50/50	.792	3.91*
20	30/70	1.01	1.75
30	30/70	1.00	2.42
	61, 125 micron spheres	$r_i/r_j = 0.49$	
40	30/70	1.01	7.81
40	40/60	1.01	7.33
40	50/50	1.01	8.51
20	40/60	1.02	2.00
30	40/60	1.01	3.52
30	40/60	1.01	3.84
40	40/60	1.02	8.45
	61, 183 micron spheres	$r_i/r_j = 0.33$	
40	30/70	1.01	5.87
40	40/60	1.01	5.78
40	50/50	1.01	5.81
40	60/40	1.01	6.02
40	60/40	1.01	6.14
40	70/30	1.01	6.17
30	40/60	.995	2.81
50	40/60	(1.04)	(17.8)
60	40/60	(1.32)	(138.)
	61, 221 micron spheres	$r_i/r_j = 0.28$	
40	30/70	.985	5.64
40	40/60	.980	5.34
40	50/50	1.00	5.73

TABLE 13 -- Continued

Experimental Results for Bimodal Suspensions

Concentration Volume %	Composition % Small/% Large	Power Law Index	Relative Viscosity, μ_r, or μ_r^*
	125, 183 micron spheres	$r_i/r_j = 0.68$	
30	30/70	1.00	3.02
30	40/60	.997	3.10
30	50/50	1.00	3.18
20	40/60	1.00	1.86
40	40/60	1.00	6.96
40	40/60	1.01	7.13
50	40/60	(1.10)	(29.5)
	125, 221 micron spheres	$r_i/r_j = 0.57$	
40	30/70	.987	7.16
40	40/60	.984	6.39
40	50/50	.975	6.55

* denotes $\mu_r^* = \frac{K^2}{\mu_r}$.

() denotes results for dilatant suspensions.

Calculation of the Mooney Crowding Factors. The crowding factors, λ_{12} and λ_{21}, which appear in the bimodal form of the Mooney equation,

$$\mu_r = \exp\left(\frac{2.5\,\varphi_1}{1 - \lambda_{11}\varphi_1 - \lambda_{21}\varphi_2}\right) \exp\left(\frac{2.5\,\varphi_2}{1 - \lambda_{22}\varphi_2 - \lambda_{12}\varphi_1}\right)$$

were determined by the simultaneous solution of the following rearranged logarithmic form on λ_{21}, λ_{12} coordinates:

$$\lambda_{12} = \frac{1}{\varphi_1} - \lambda_{22}\frac{\varphi_2}{\varphi_1} - \frac{\varphi_2/\varphi_1}{\frac{\ln \mu_r}{2.5} - \frac{\varphi_1}{1 - \lambda_{11}\varphi_1 - \lambda_{21}\varphi_2}}$$

Each bimodal suspension is represented by a separate curve on the λ_{21}, λ_{12} coordinates. Figure 19 shows the (λ_{21}, λ_{12}) plots for the 61/125 bimodal suspensions. Those suspensions with equal total concentration have composition as a parameter and are represented by closely spaced curves of very similar shape with no definite common (λ_{21}, λ_{12}) point. Those suspensions with repeated compositions have total concentration as a parameter and are represented by a family of curves of continuously varying shape whose common point can be seen to be the point of mutual tangency. The simultaneous solution was found by numerically searching the λ_{21}, λ_{12} coordinate system for that set of (λ_{21}, λ_{12}) for which the squared error sum given by $\Sigma\left[(\mu_r(\text{experimental}) - \mu_r(\text{calculated}))/\mu_r(\text{exper})\right]^2$ was minimized. This is the fitting criterion recommended by Cramer and Marchello (13).

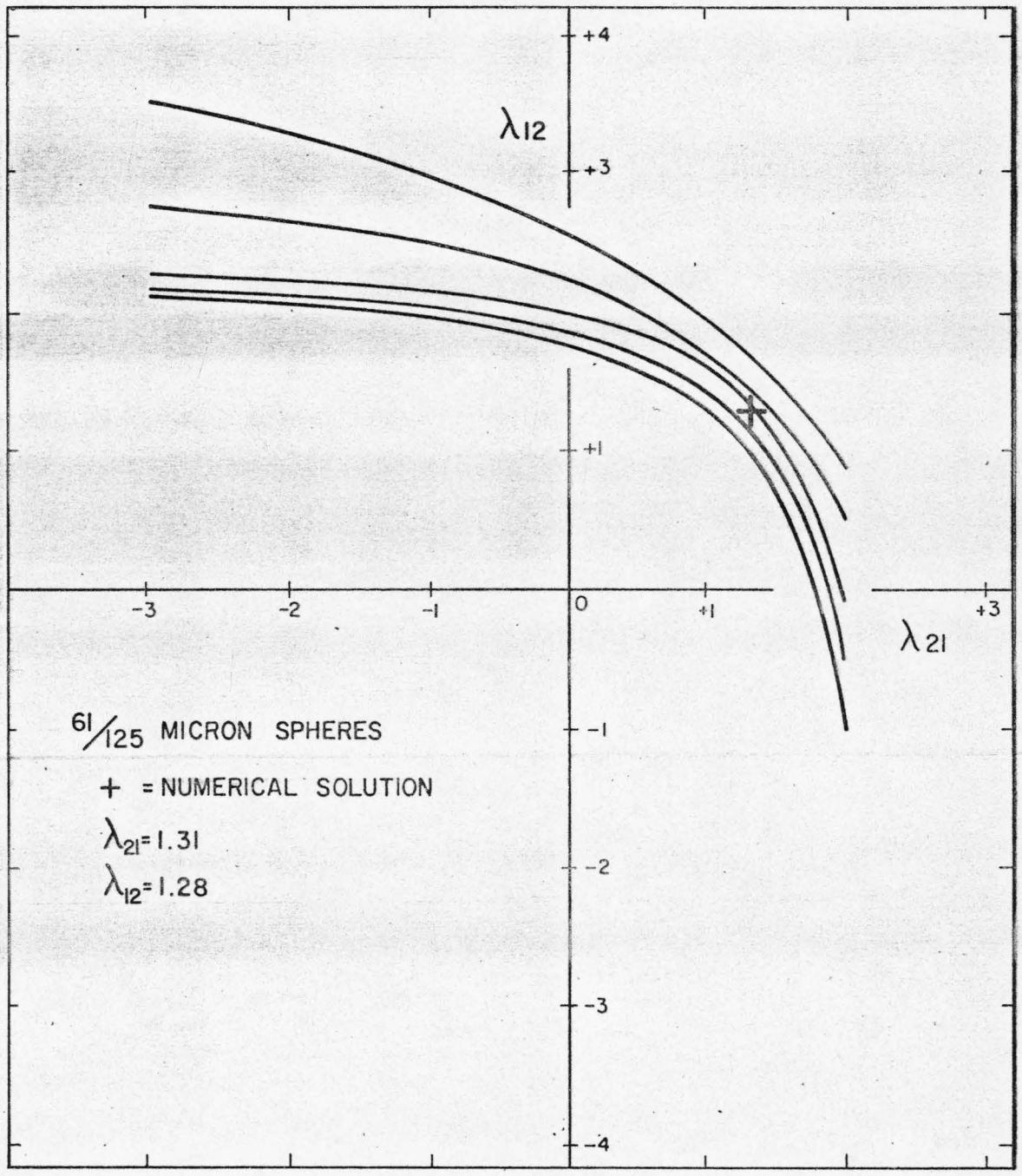

Figure 19. (λ_{21}, λ_{12}) plots for the 61/125 bimodal suspensions.

Figure 20 shows the curves for the 125/221 bimodal suspensions (all at 40 volume percent total concentration) which have no obvious simultaneous solution. In cases like this, the loci of $(\lambda_{21}, \lambda_{12})$ having minimum values of the squared error criterion were determined.

Figure 21 shows the most typical situation in which the various curves are more or less tangled. In cases like this, the curves were forced into the configuration of Figure 19 by adjusting the experimental values of relative viscosity up or down as required. The adjustment of relative viscosity was constrained by the requirement that the adjustment be spread evenly, or nearly so, over all the curves, and of course, that the adjustments be as small as possible. Once the curves were untangled in this way, the numerical search for the least squared error value(s) of $(\lambda_{21}, \lambda_{12})$ was performed as described earlier.

The results of these procedures are collected in Figure 22 where the four numerical solutions obtained and the minimum error loci for all the size combinations are shown on the same coordinates. A smooth curve was fitted by eye to the four numerical solutions, and the coordinates of the intersections of the minimum error loci and the smooth curve read off as the desired values of $(\lambda_{21}, \lambda_{12})$. These values are replotted in Figure 23 as a function of size ratio, and tabulated in Table 14 as the principal result of this research.

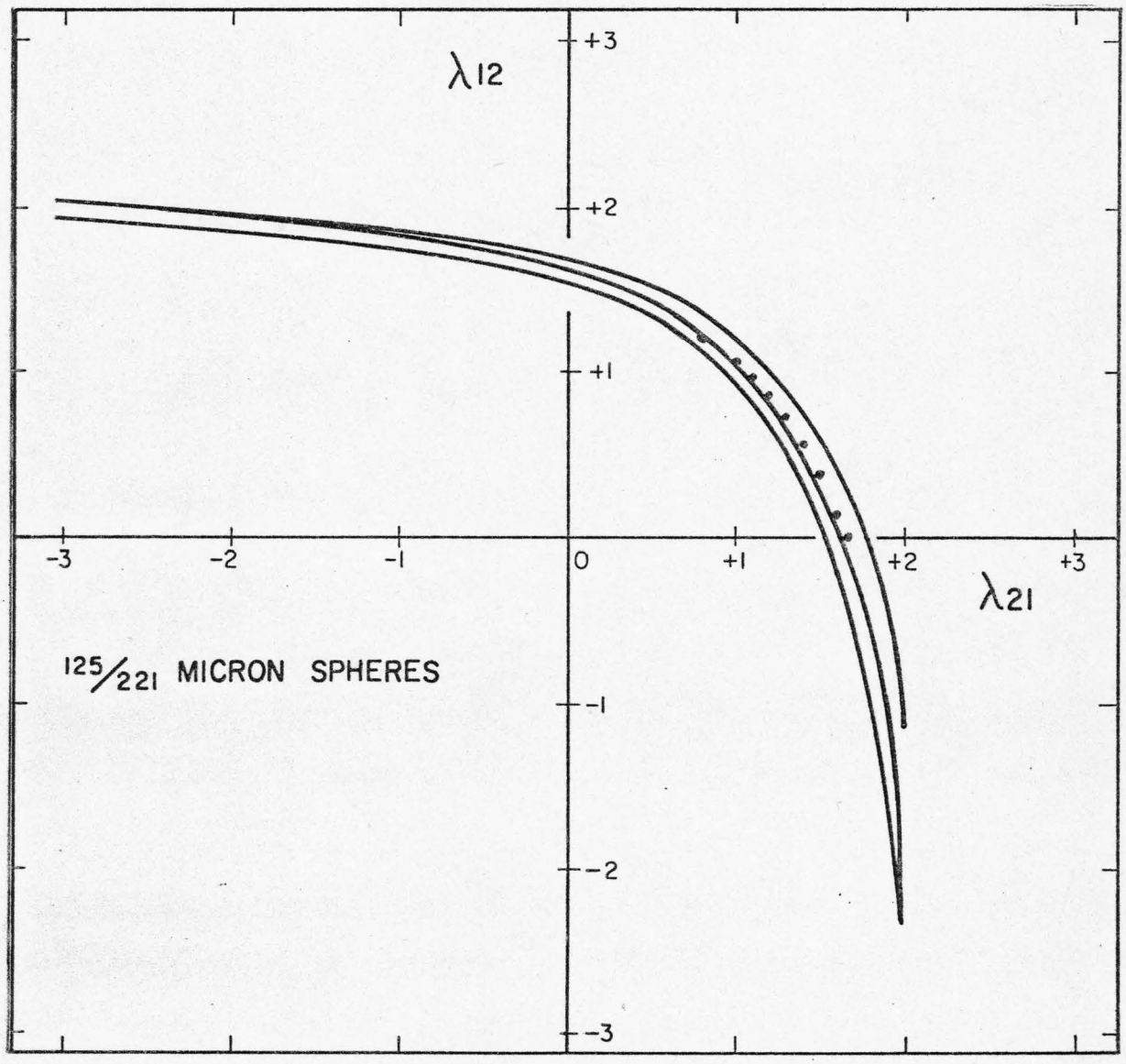

Figure 20. $(\lambda_{21}, \lambda_{12})$ plots for the 125/221 bimodal suspensions.

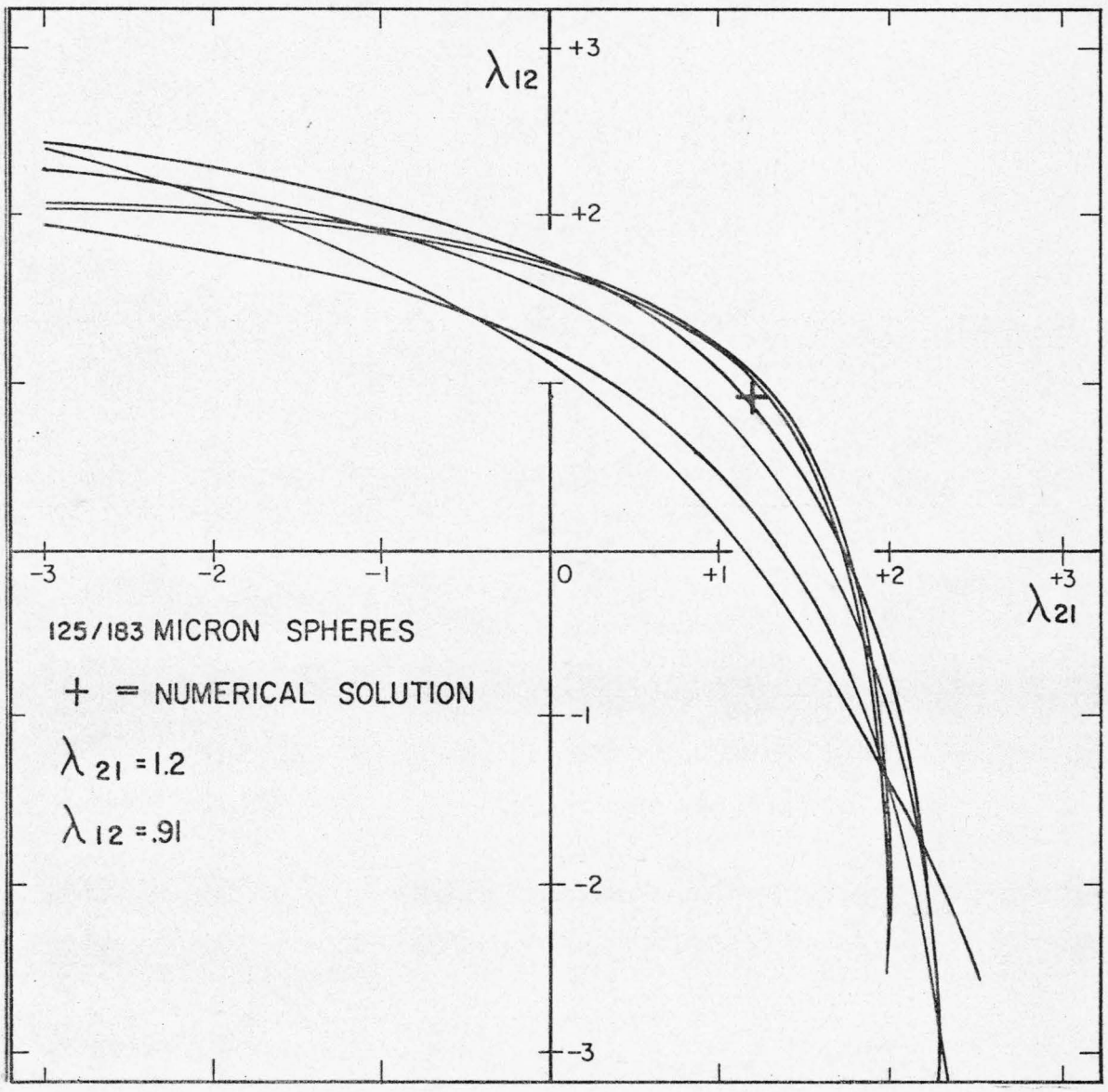

Figure 21. $(\lambda_{21}, \lambda_{12})$ plots for the 125/183 bimodal suspensions.

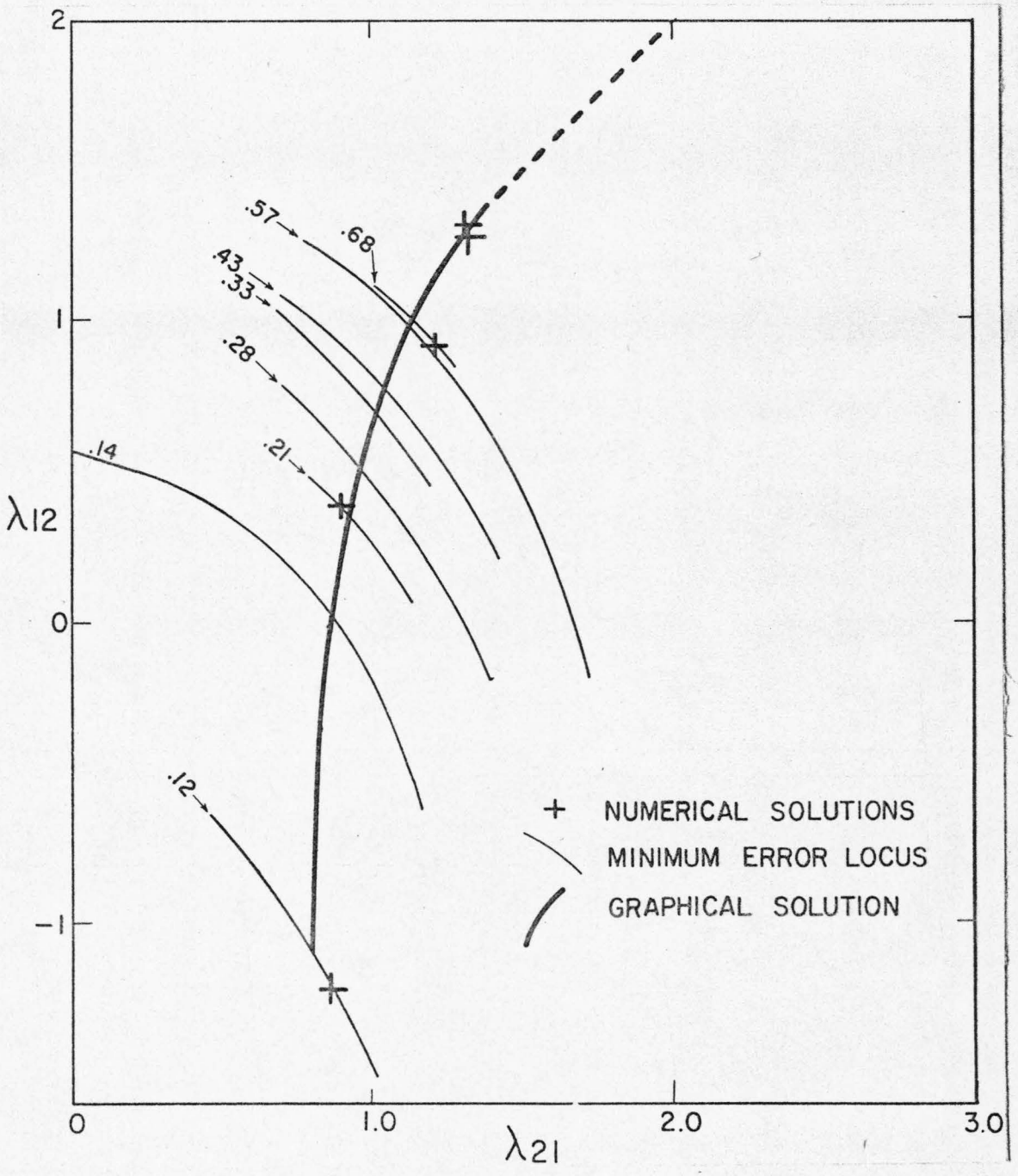

Figure 22. Graphical solution for $(\lambda_{21}, \lambda_{12})$ as a function of size ratio.

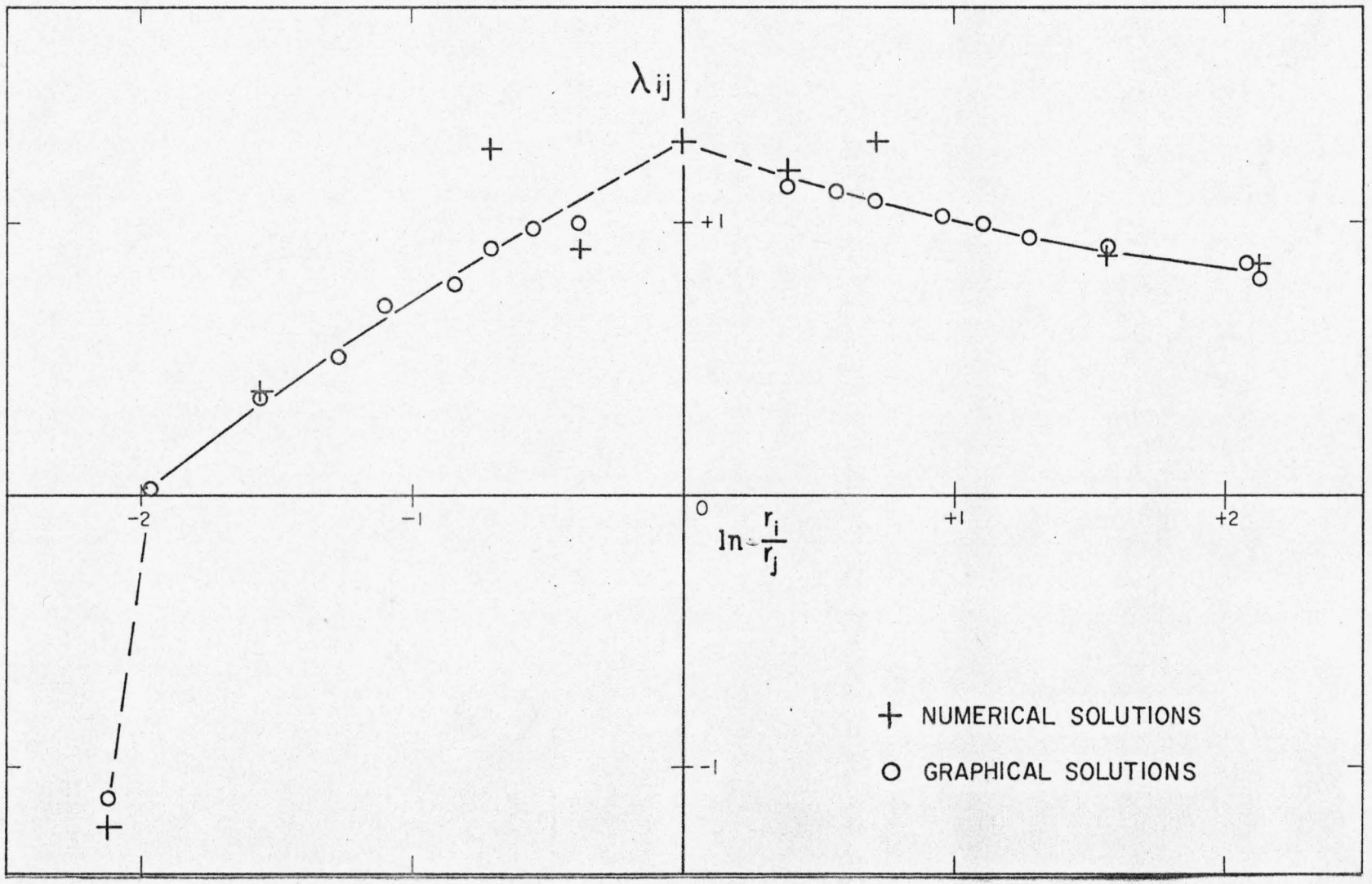

Figure 23. Mooney bimodal crowding factors, λ_{12} and λ_{21}, as a function of size ratio.

TABLE 14

The Mooney Crowding Factors as a Function of Size Ratio

Sphere Sizes	$\frac{r_i}{r_j}$	$\frac{r_j}{r_i}$	Numerical Solution	Graphical Solution
			λ_{21} , λ_{12}	λ_{21} , λ_{12}
26/61	0.43	2.33	locus	1.03, 0.77
26/125	.21	4.76	0.89, 0.38	.92, .35
26/183	.14	7.1	locus	.86, .02
26/221	.12	8.3	.86,-1.22	.80,-1.12
61/125	.49	2.04	1.31, 1.28	1.08, .90
61/183	.33	3.0	locus	1.0 , .69
61/221	.28	3.57	locus	.95, .50
125/183	.68	1.47	1.20, 0.91	1.13, .99
125/221	.57	1.75	locus	1.12, .98

The comparison of the experimental values of relative viscosity with those calculated from Mooney's equation with the graphical solution values of λ_{21} and λ_{12} is shown in Figures 24 through 32. The agreement is generally fair except for the 61/125 system which is everywhere poor for undiscovered reasons, and for the 26/183 system in which the small sphere end of the composition range shows extreme diameter dependency.

Identification of minimum relative viscosity compositions. The minimum relative viscosity compositions for a bimodal suspension can be determined from the experimental λ_{21}, λ_{12} values and the first derivative of the bimodal Mooney equation with respect to composition, with total concentration as a parameter. The messy algebra can be avoided by a trial and error computer calculation which locates the composition at which the first derivative of relative viscosity changes sign. The results are shown in Table 15.

The minimum relative viscosity composition is a function of total concentration and size ratio but not of the Einstein coefficient or the Mooney self-crowding factor. The variation of F_{min}, the fraction small spheres, with total concentration and size ratio is illustrated by Figure 33.

Effect of size distribution. Two questions are of considerable interest in the matter of the effect of size distribution: the first is how much did the remaining diameter variation within each size fraction of spheres used in the bimodal suspensions in-

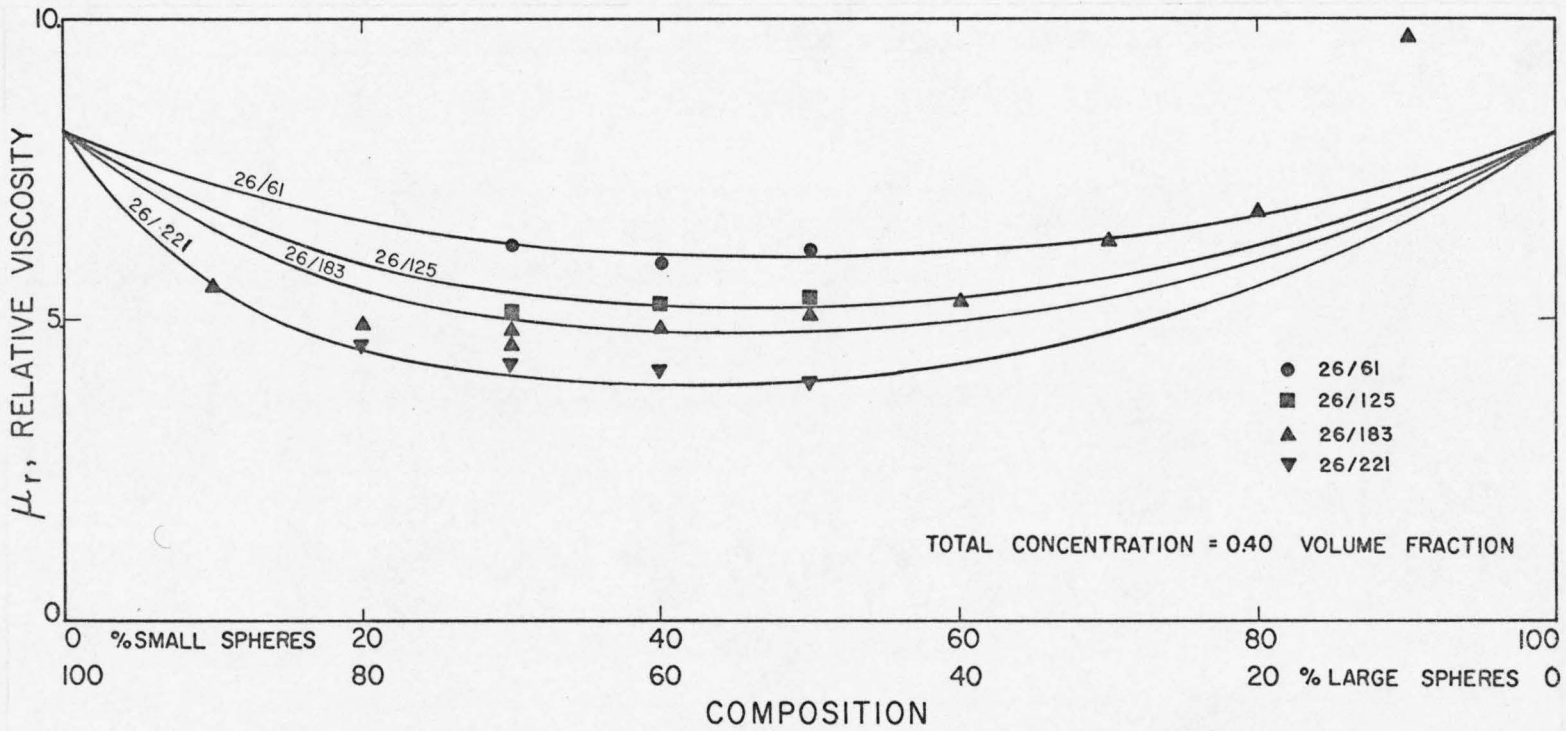

Figure 24. Comparison of experimental and calculated relative viscosities for 26/61, 26/125, 26/183, and 26/221 bimodal suspensions.

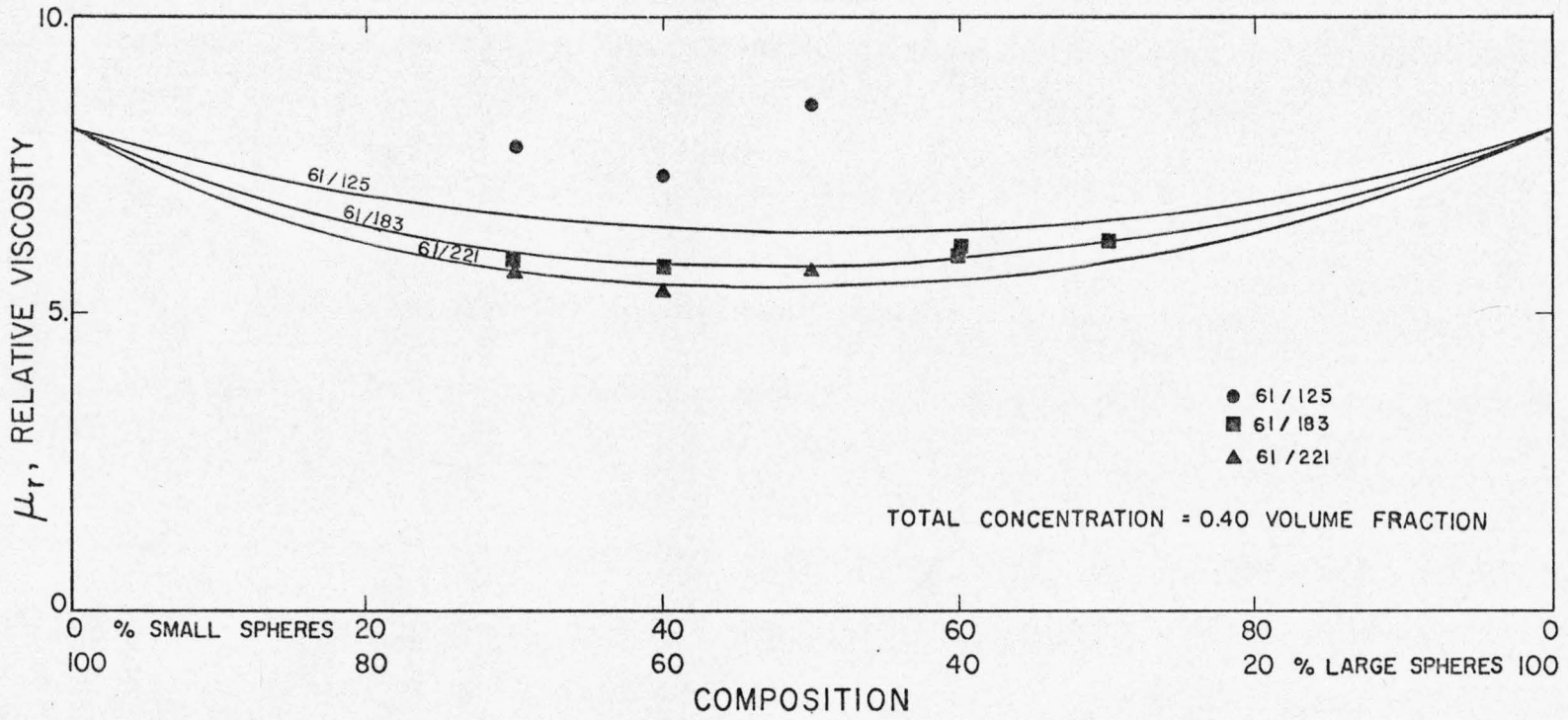

Figure 25. Comparison of experimental and calculated relative viscosities for 61/125, 61/183, and 61/221 bimodal suspensions.

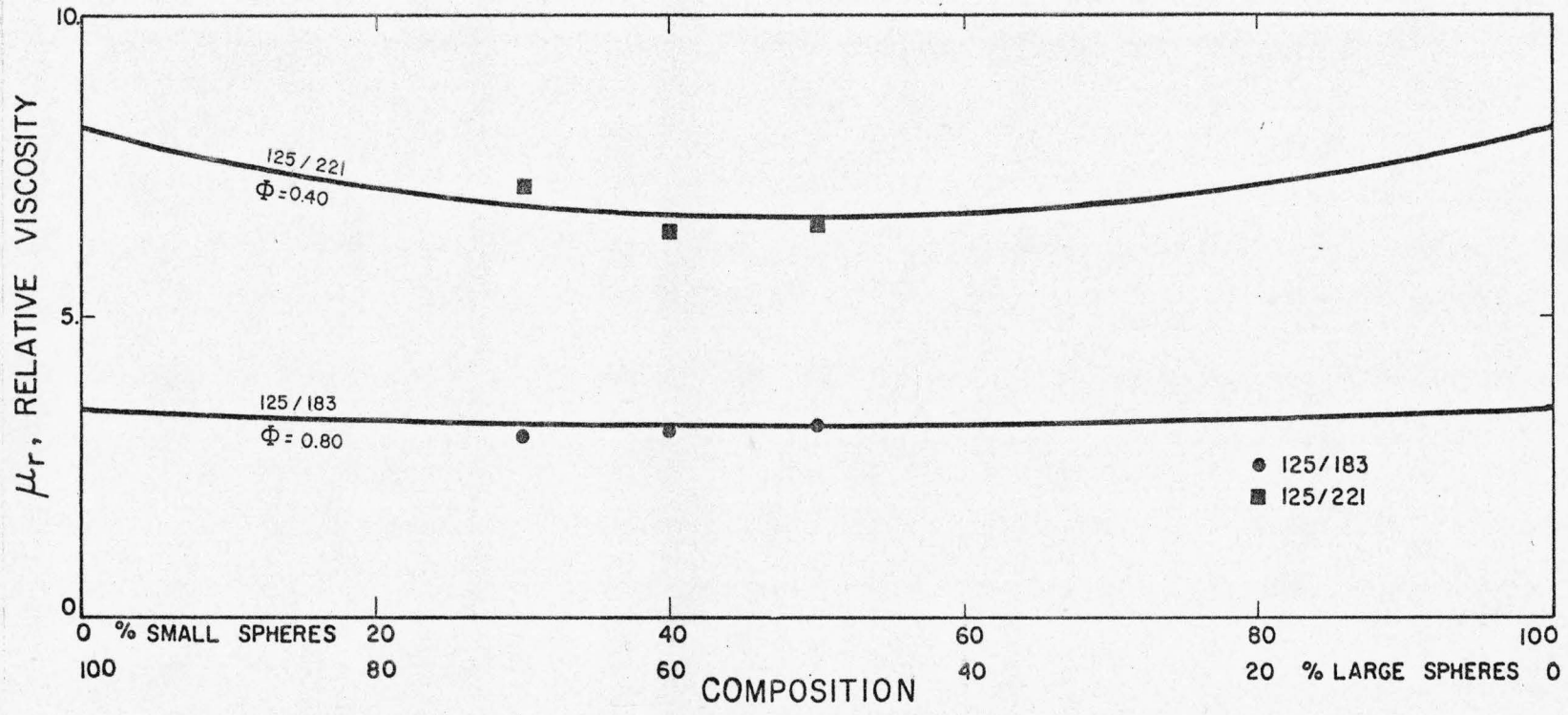

Figure 26. Comparison of experimental and calculated relative viscosities for 125/183 and 125/221 bimodal suspensions.

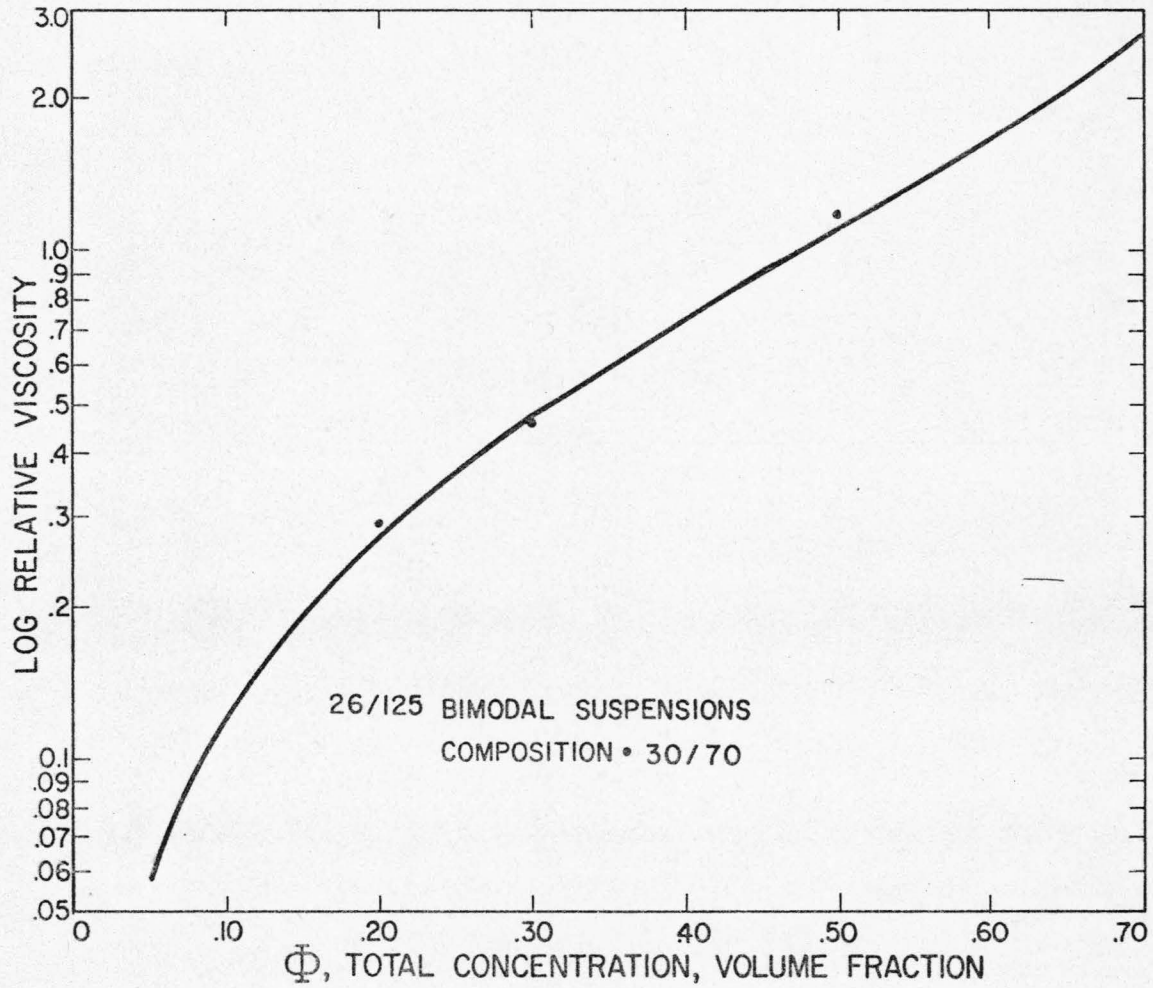

Figure 27. Comparison of experimental and calculated relative viscosities for 26/125 bimodal suspensions of 30/70 composition.

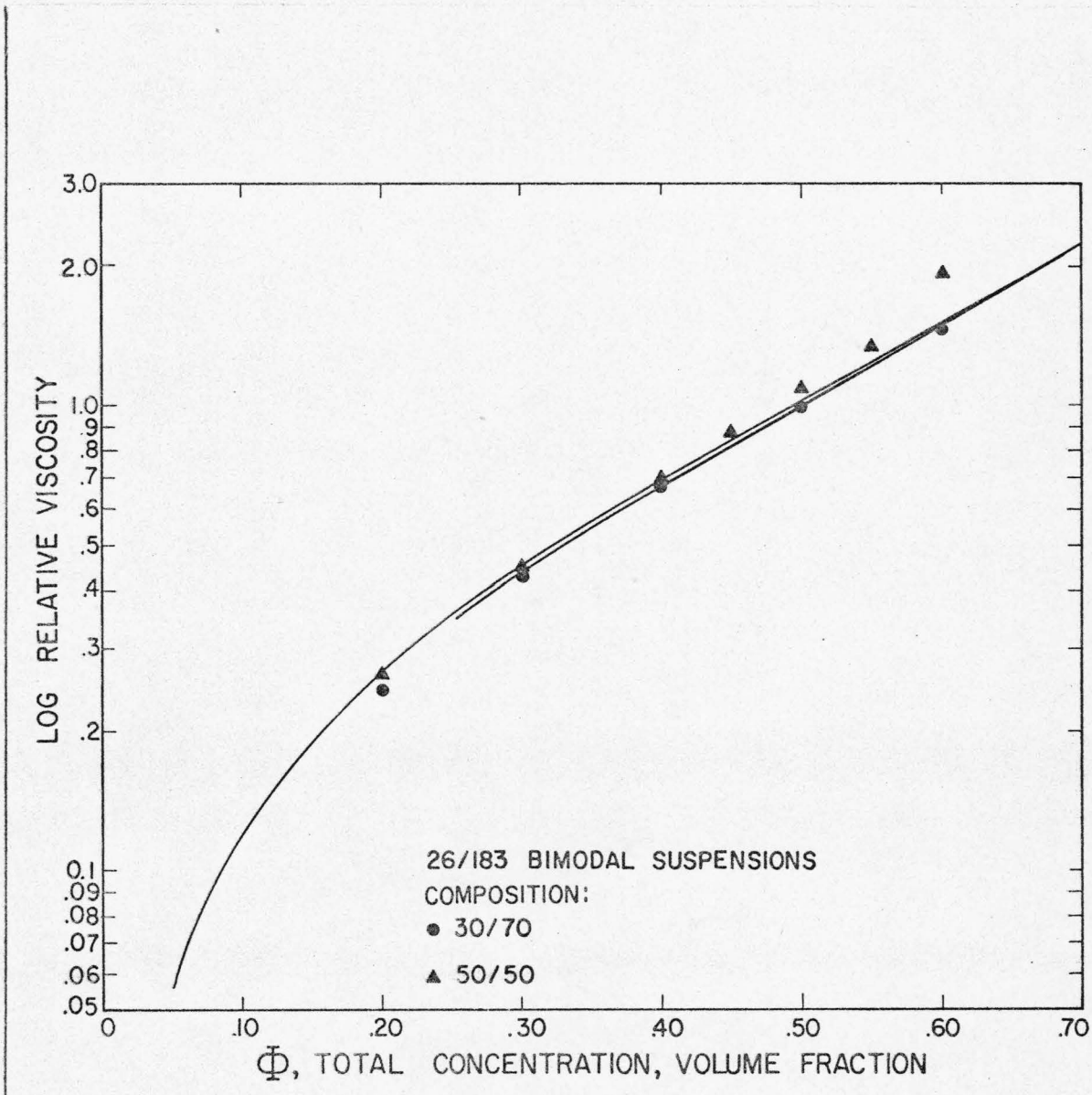

Figure 28. Comparison of experimental and calculated relative viscosities for 26/183 bimodal suspensions of 30/70 and 50/50 compositions.

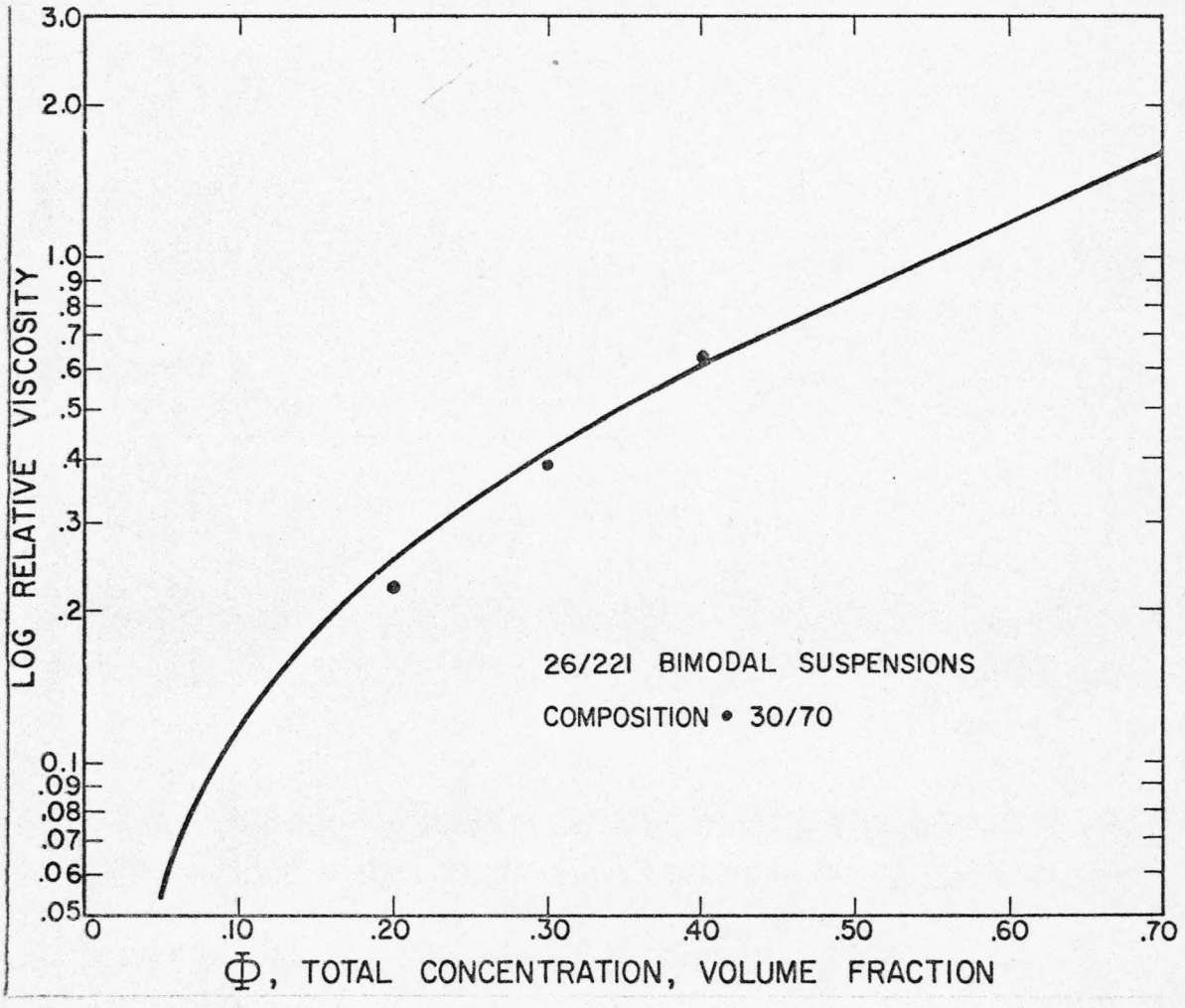

Figure 29. Comparison of experimental and calculated relative viscosities for 26/221 bimodal suspensions of 30/70 composition.

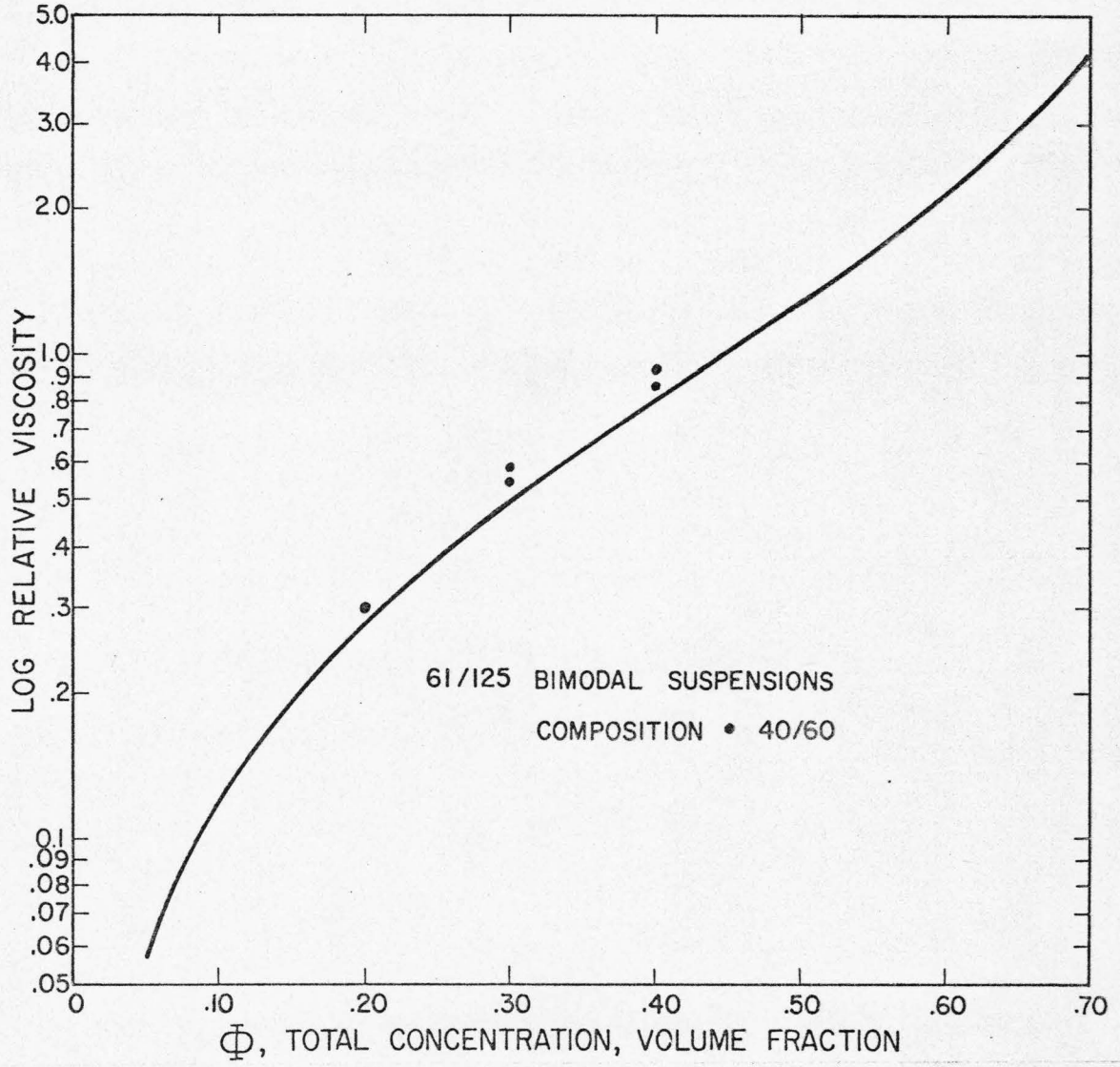

Figure 30. Comparison of experimental and calculated relative viscosities for 61/125 bimodal suspensions of 40/60 composition.

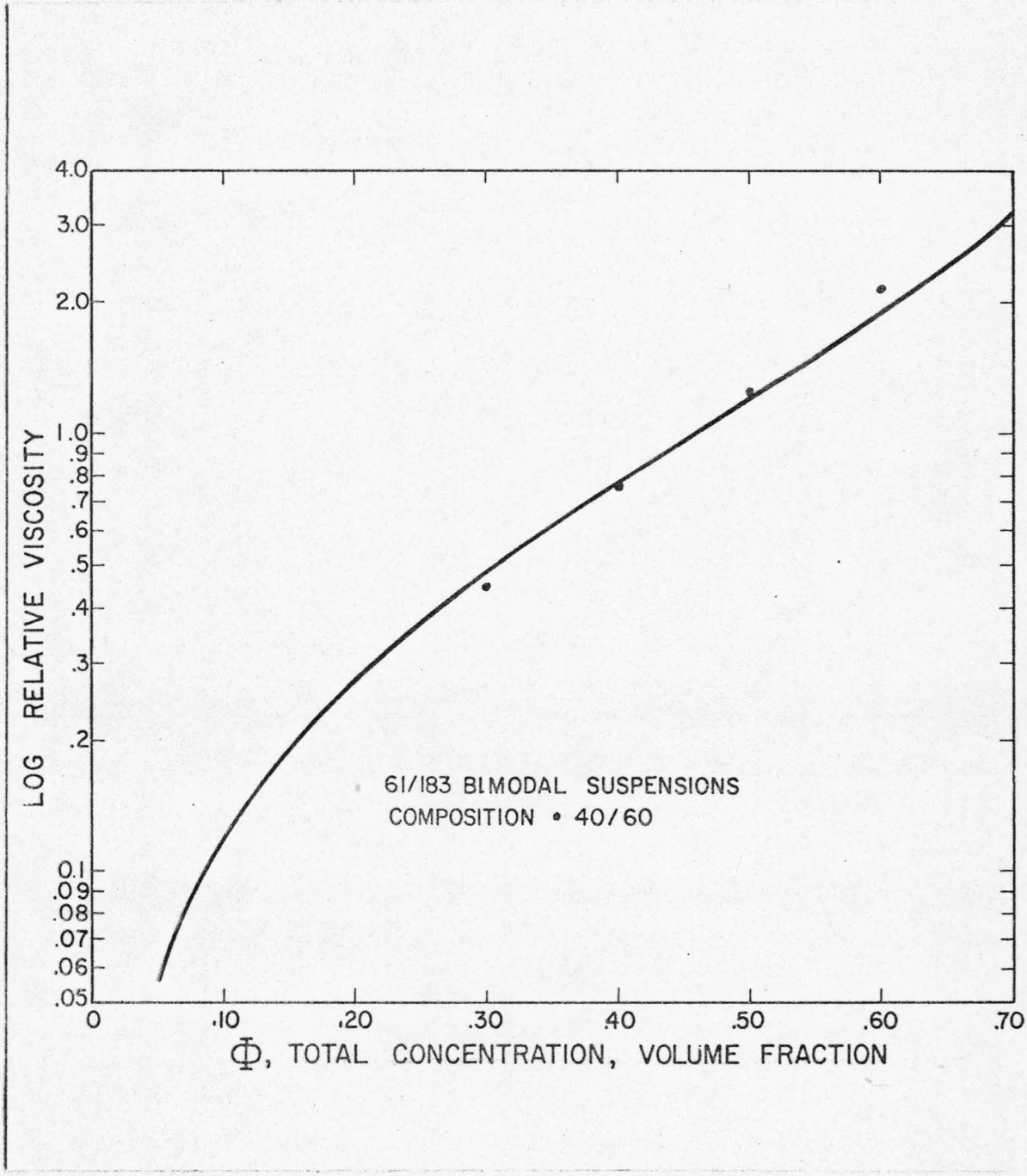

Figure 31. Comparison of experimental and calculated relative viscosities for 61/183 bimodal suspensions of 40/60 composition.

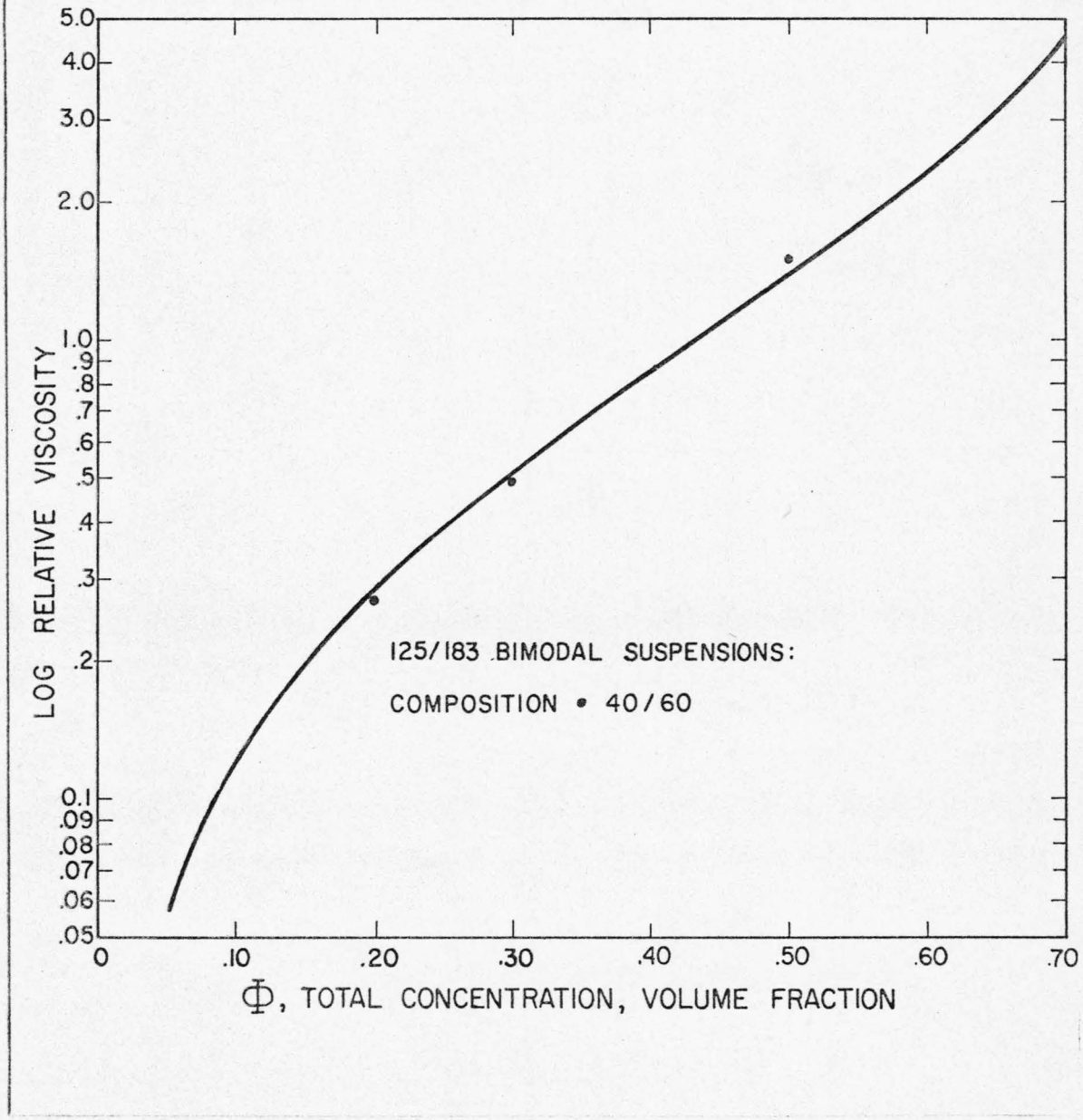

Figure 32. Comparison of experimental and calculated relative viscosities for 125/183 bimodal suspensions of 40/60 composition.

TABLE 15

Bimodal Composition for Minimum Relative Viscosity

Total Concentration: Forty Volume Percent

Size Ratio	Fraction Small Spheres
0.12	0.407
.14	.448
.21	.462
.28	.468
.33	.477
.43	.480
.49	.485
.57	.488
.68	.488

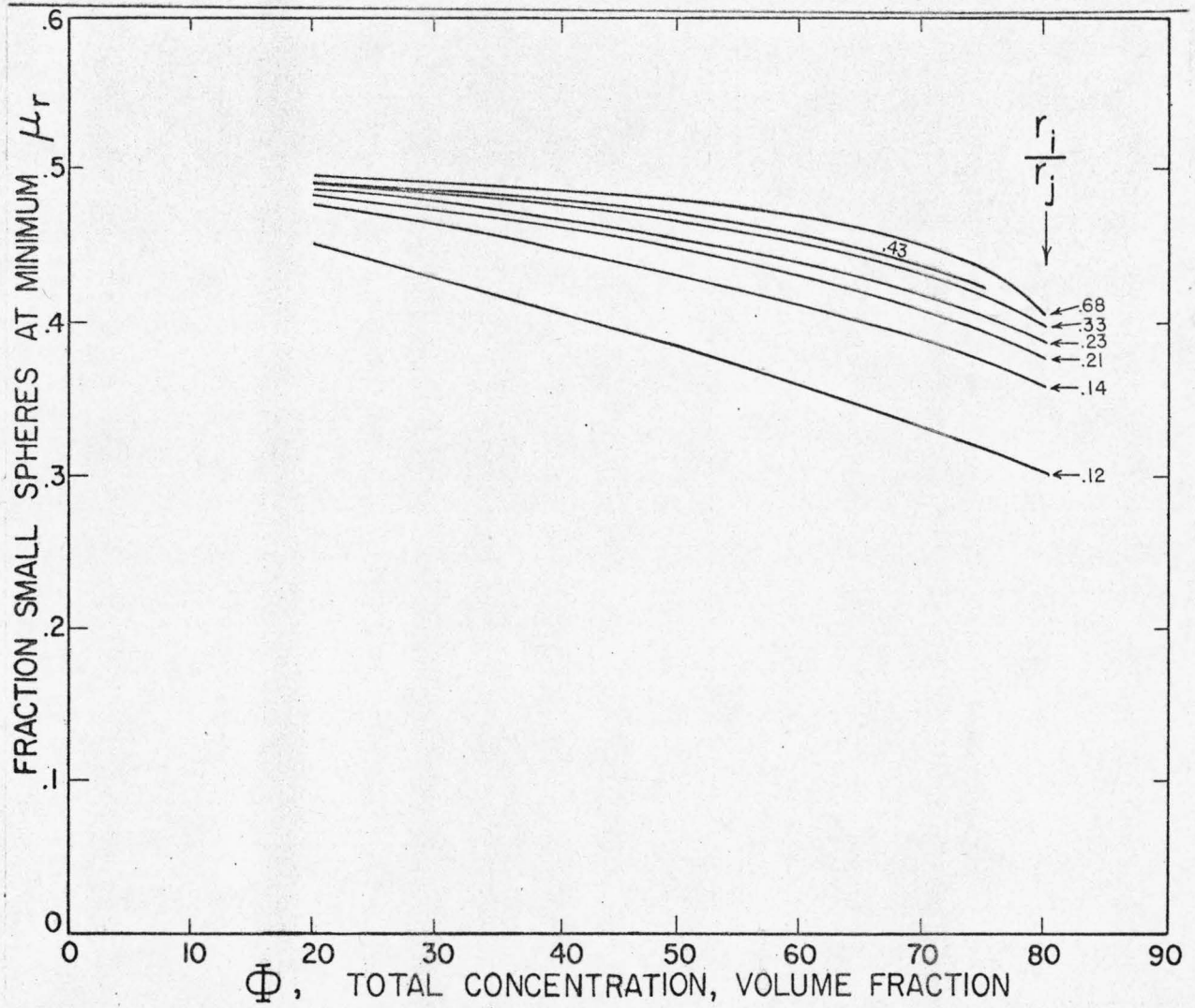

Figure 33. Variation of the fraction of small spheres for minimum bimodal relative viscosity with size ratio and total concentration.

fluence the bimodal relative viscosity, and the second is how closely must the spheres be sized in order to result in monodisperse suspensions?

These questions may be investigated with Figure 34 which shows the ratio of the minimum bimodal relative viscosity to the monomodal viscosity at corresponding total concentrations, as a function of size ratio and total concentration, and with Table 16 which shows the interquartile size ratios obtained if the size fractions are imagined to be sharply defined 50/50 bimodal mixtures of spheres of the 25th and 75th percentile diameters.

The magnitude of the effect of diameter variation in the bimodal case can be estimated by employing the synthetic fluid concept in the following way. Take as an example the worst case: a 40/60 bimodal suspension of 26 and 221 micron spheres. The volume fraction of 26 micron spheres is 0.16, and the volume fraction of the 221 micron spheres is 0.24. Imagine the mixture of 26 micron spheres and the suspending fluid to be a 50/50 bimodal suspension of spheres with a size ratio of 0.557, and a total volume fraction of 0.16/(1-.24), or 0.21. From Figure 33 the ratio of minimum bimodal relative viscosity to the monomodal viscosity is 0.97. The mixture of the 221 micron spheres and the synthetic fluid composed of the small spheres plus liquid is imagined to be a 50/50 bimodal suspension of spheres with a size ratio of 0.879 and a total volume fraction of 0.24: from Figure 33 the corresponding ratio is 0.98. The relative

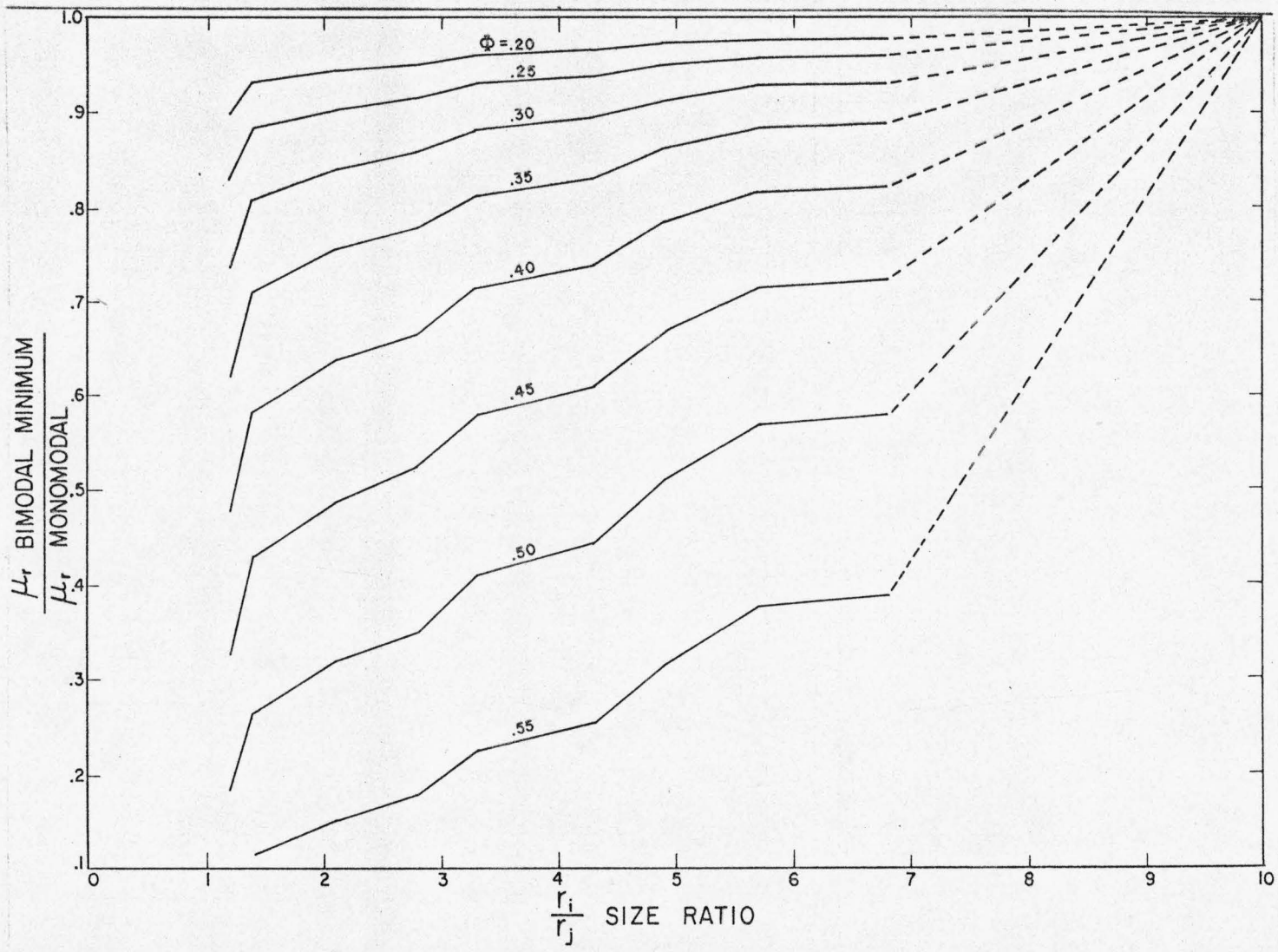

Figure 34. Ratio of minimum bimodal relative viscosity to monomodal relative viscosity at equal total concentrations.

TABLE 16

Interquartile Size Ratios within Size Fractions of Spheres

Size Fraction Median Diameters Microns	Percentile Diameters, Microns		Interquartile Size Ratio
	25th	75th	
26	20	36	0.557
61	58	64.5	.9
125	116.5	129	.91
183	175	190	.922
221	207.5	236.5	.879

viscosity of the bimodal synthetic fluid suspension is seen to have been reduced to (0.97)(0.98) or to 0.95 of the expected value of a bimodal suspension of purely monomodal size fractions. The size spread within the size fractions is seen to be a minor influence upon the relative viscosity of bimodal suspensions.

The same procedure indicates that the 61, 125, 183, and the 221 micron diameter monomodal suspensions at concentrations of 40 volume percent or less may be expected to have less than a six percent reduction in relative viscosity due to diameter variation within the size fractions. The 26 micron spheres could have as much as 19% reduction, but such a large reduction would have been obvious and influential in the extrapolation of relative viscosity to zero sphere diameter. No such reduction exists in the present experimental data for monomodal suspensions. The likely reason for the absence of this large potential reduction in the relative viscosity of the 26 micron suspensions is the continuous nature of the actual size distribution within the size fraction. The estimation procedure employed here makes the conservative assumption of a distinctly separated bimodal size distribution which, in fact, does not occur. The intermediate sizes actually present effectively spoil the viscosity reduction potentially available through the imagined bimodal size distribution.

The results are, then, that the variation of sphere diameter within the size fractions would not be a large influence upon the bimodal results, and are a potentially large influence upon the

monomodal measurements only in the case of the 26 micron spheres. Since there were no clearly discernable effects observed in the experimental results, it is concluded that the size fractions used were sufficiently narrow to assure they behaved as single distinct sizes, and that further fractionation by diameter would not significantly alter the conclusions reached on the basis of the experimental data reported here.

Effect of incremental additions of a second size of sphere. An interesting application of the Mooney bimodal interaction parameters is to the question of whether or not the relative viscosity of a monomodal suspension can be reduced in absolute magnitude by the addition of a second size of sphere. The answer is: yes, it can, as shown in Figure 35 for the case of a suspension initially at 40 volume percent large spheres. The addition of a second size of sphere will always reduce the slope of the relative viscosity versus concentration line, but only for the proper choice of size ratio and concentration will the slope be reduced to less than zero. The approximate boundary of conditions for which the slope of relative viscosity versus concentration is zero is shown in Figure 36. The combinations of size ratio and concentration of larger spheres represented by the area above the line in Figure 36 are those for which the relative viscosity of a suspension will decrease for the initial additions of a second, smaller size of sphere.

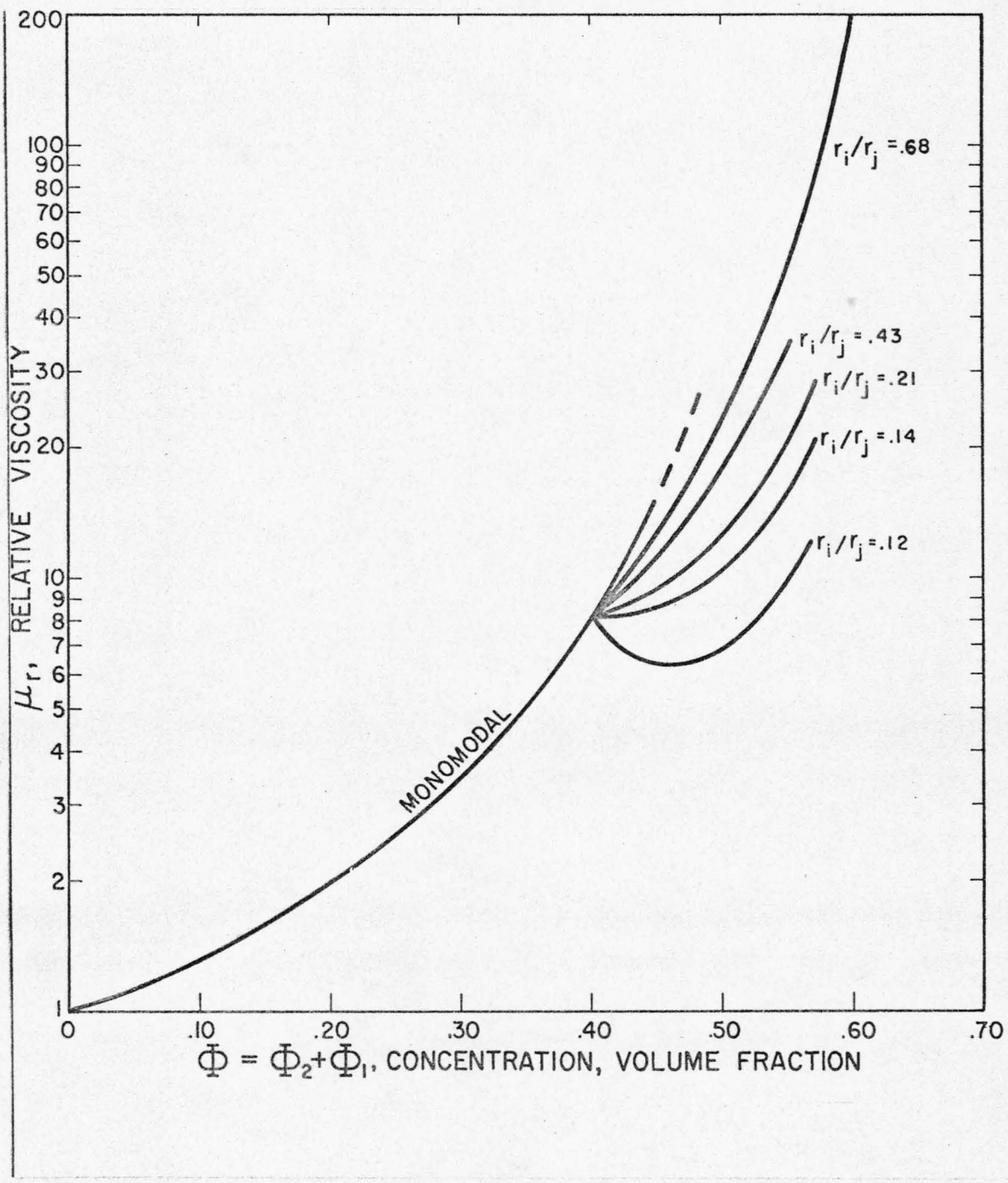

Figure 35. Effect of incremental additions of a second, smaller size of sphere.

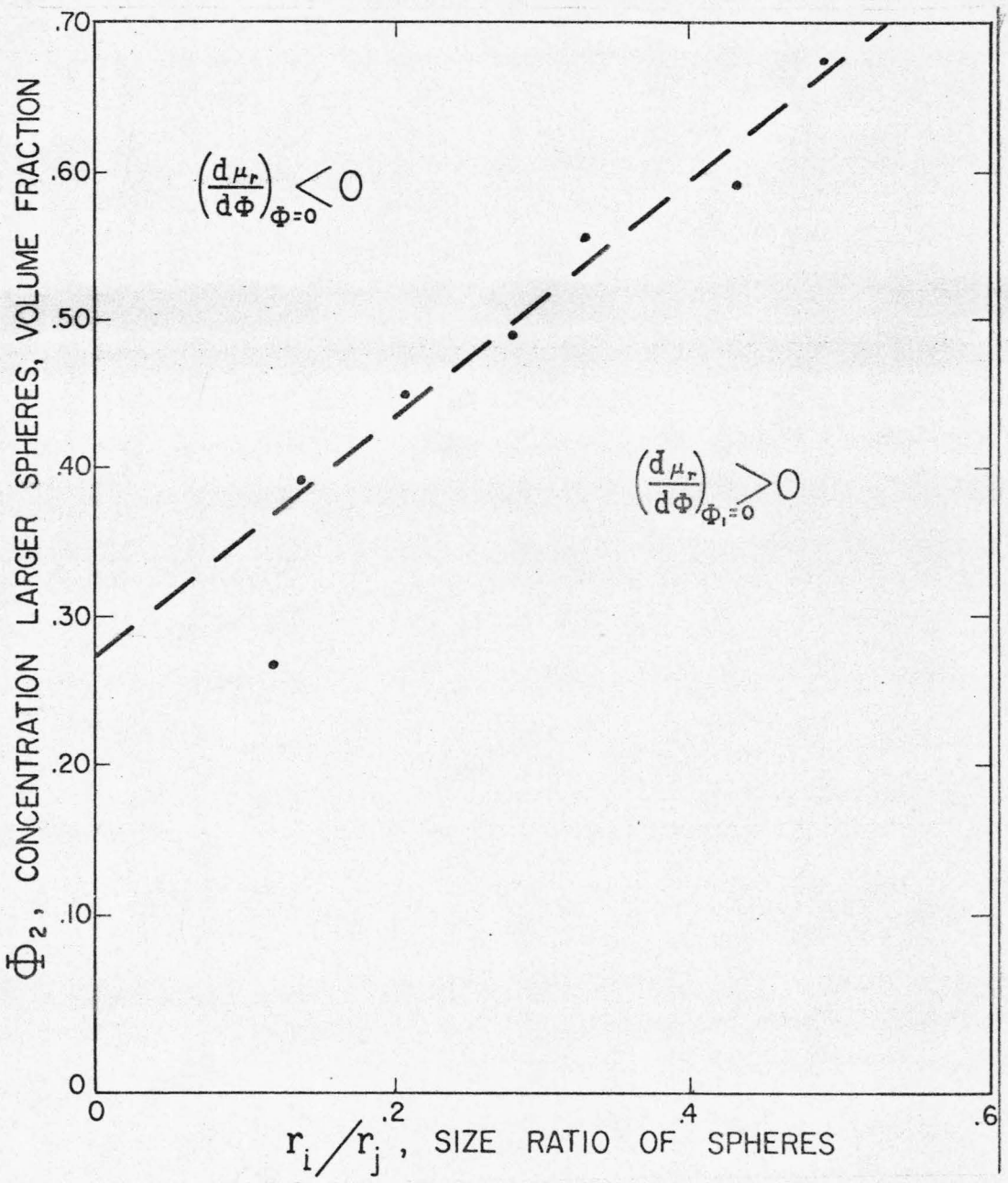

Figure 36. Size ratios and concentrations of large spheres at which relative viscosity will decrease upon addition of smaller spheres.

The addition of a second, larger size of sphere will increase the relative viscosity of a suspension but at a lower slope than for corresponding additions of the original size.

Strictly speaking, Figure 36 is valid below concentrations of 45 percent when considered in terms of relative viscosity. However, addition of a second, smaller size of sphere to a monomodal suspension more concentrated than 45 percent will reduce the suspension's power law index and reduce the suspension's resistance to flow, up to the limit of bimodal concentration for Newtonian flow for the particular size ratio involved.

Comparison of the results to the literature. The conclusions of Ward and Whitmore (55) were confirmed, with a higher value for the concentration limit of Newtonian flow. Their qualitative conclusions concerning the dependence of relative viscosity upon size distribution have been extended to a quantitative relationship. The experimental results of Eveson et al. (18) are confirmed in most part, especially in regard to the location of the minimum in relative viscosity as a function of composition in bimodal suspensions. Their very low concentration limit for Newtonian flow is suggestive of the influence of electroviscous effects upon the 38 micron spheres used as the small size fraction. The present results agree with those of Maron and Madow (34) in that power law flow was observed for concentrations exceeding the limit for Newtonian flow but the power law indices do not agree. The present

results indicate a much higher limit of concentration for Newtonian flow than their result of 25 volume percent. The location of the minimum in relative viscosity as a function of bimodal composition is generally confirmed. Williams' (56) results are generally confirmed and extended by the results reported here. The concentration limit for Newtonian flow in monomodal suspensions was found here to be less than his 50 volume percent. His bimodal results are confirmed and extended to a quantitative relationship between size distribution, concentration, and relative viscosity. His observations on non-Newtonian flow in suspensions of micron-sized spheres were also confirmed. The qualitative results of Sweeny and Geckler (50) for bimodal suspensions are confirmed by the results reported here, bearing in mind the shear rate dependence of their results. The experimental results of Ting and Luebbers (52) are based on measurements at a single rate of shear and are not strictly comparable to the results reported here. The present results are very nearly in quantitative agreement with the results of Eveson (17) at 20 volume percent and extend his work to higher concentrations and quantitative relationships between composition and the relative viscosity of bimodal suspensions. The only other experimental values for the Mooney crowding factors λ_{12} and λ_{21} are those of Sweeny (49). Keeping in mind that Sweeny's experimental data showed time dependency, the present results are compared to Sweeny's in Figure 37 where the agreement is seen to be good. The present results confirm Chong's theoretical prediction of minimum bimodal relative

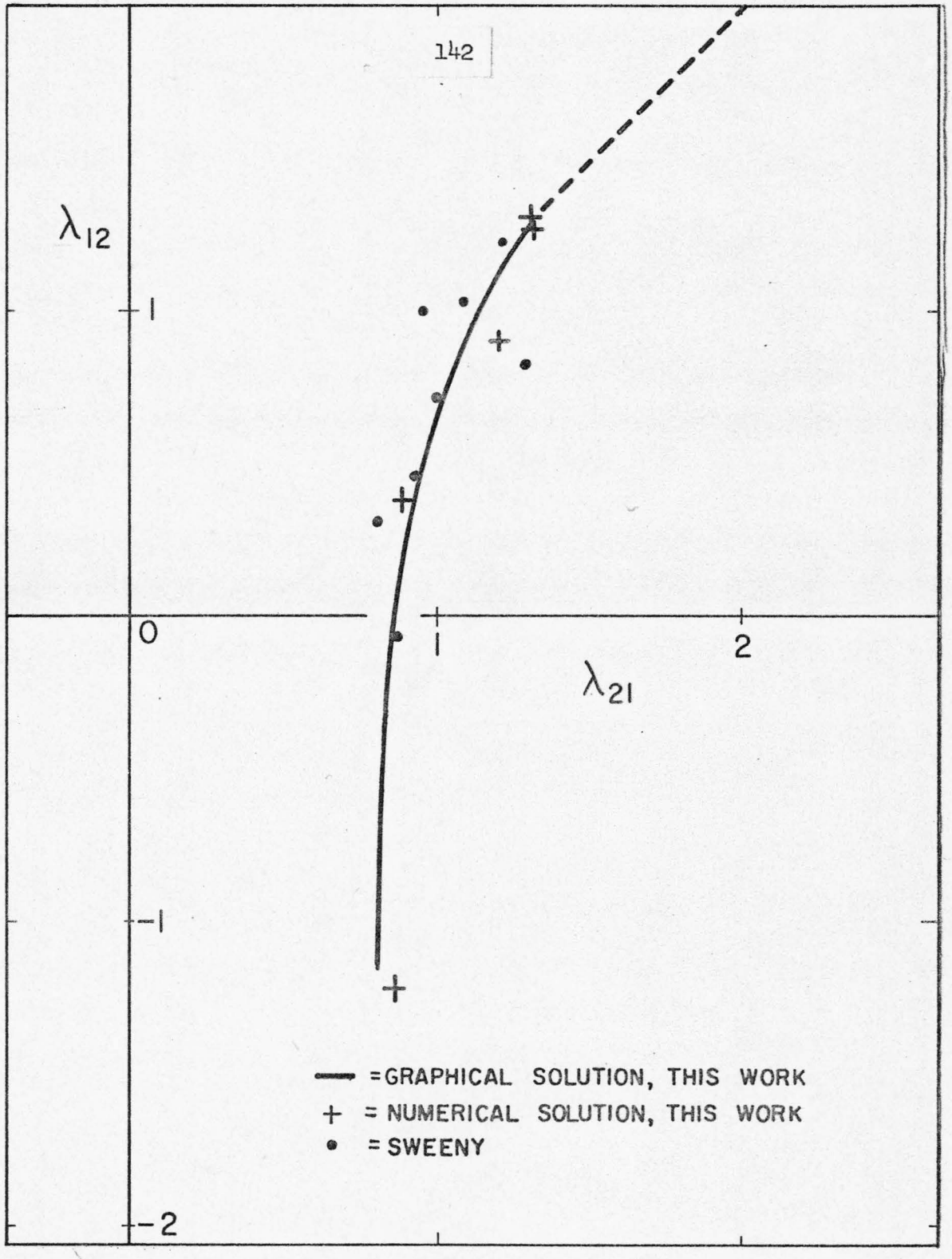

Figure 37. Comparison of experimentally determined Mooney bimodal crowding factors.

viscosity as a function of concentration, as shown in Figure 38, but are quite at odds with his experimental results in the matter of flow behavior of concentrated suspensions at low shear rates. Brodnyan's results (8) for suspensions of submicron polymer latices are corroborated, and extended to higher concentrations and a wider range of size ratios. Brodnyan's results indicate that sphere diameter does not affect the relative viscosity of suspensions of very small spheres provided electroviscous effects can be suppressed.

The experimental results reported here agree very nicely with the predictions of the phenomenological theory by Farris (19). The present experimental results show the bimodal reduction in relative viscosity to be appreciable at lower total concentrations than predicted by Farris, but show the same location for the minimum in relative viscosity as a function of composition. The predicted effect of the addition of a second size of spheres to a monomodal suspension is corroborated by the experimental results, which add the size ratio and concentration bounds for the effect, removing the non-interaction condition required by Farris' development.

The present work differs sharply with Farris' discussion in the matter of the limits of Newtonian flow, beyond which the simple term "relative viscosity" does not apply. The results reported here show monomodal suspensions to be possibly Newtonian up to concentrations between 45 and 50 volume percent, and bimodal suspensions to be possibly Newtonian up to the vicinity of 60 volume percent.

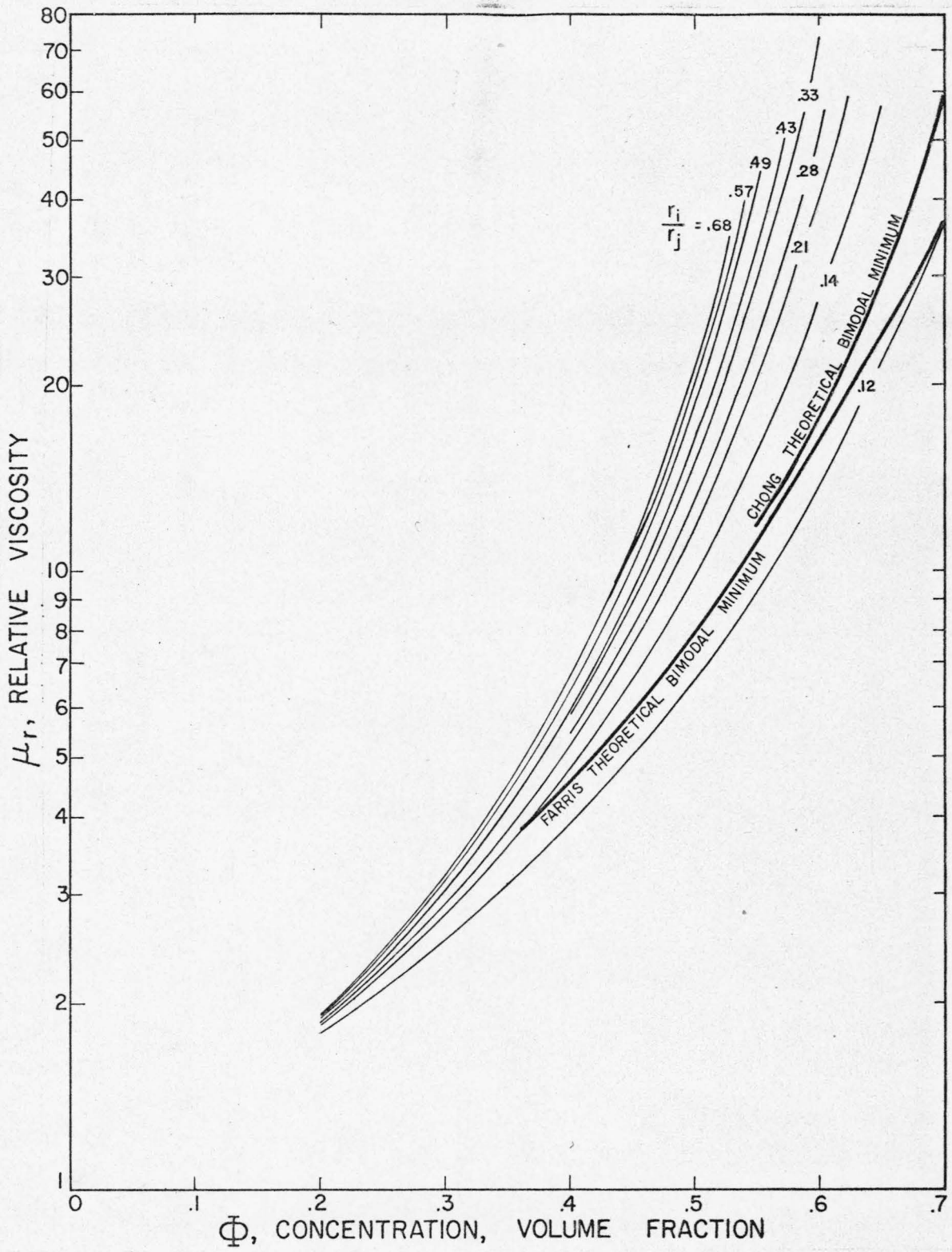

Figure 38. Minimum relative viscosities in bimodal suspensions.

Above such concentrations, some parameter or combination of parameters other than relative viscosity is required to adequately represent the flow behavior of concentrated suspensions of spheres.

Trimodal Suspensions

Results. The results of the experimental measurements upon trimodal suspensions of 26 micron, 61 micron, and 183 micron spheres with a constant total concentration of 45 percent solids by volume are shown in Table 17 where the influence of the 26 micron spheres is again reflected by reduced power law indices. The Casson viscosity, K^2, was employed to calculate the relative viscosity, μ_r^*. Forty-five volume percent total concentration is the limit of total concentration at which the suspensions are still Newtonian at the pure component vertices on the composition diagram. The relationship between trimodal composition and relative viscosity, μ_r^*, for this system, size ratios 0.14, 0.33, 1.0 is displayed in Figure 39 where equal relative viscosity contours are drawn on a three-component composition diagram. The two-component relative viscosities along the boundaries were calculated from Mooney's equation.

A minimum in relative viscosity, μ_r^*, as a function of composition was anticipated at the intersection of the three lines drawn from each of the three bimodal compositions of minimum relative viscosity to the opposing vertex of the triangular composition diagram. For the system investigated here, this was at a composition of 20 percent of 26 micron spheres, 30 percent of 61 micron spheres, and 50 percent of 183 micron spheres. As Figure 39 shows, in this area of the composition diagram the relative viscosity, μ_r^*, declines monotonically in the direction of the 26/183 bimodal mini-

TABLE 17

Experimental Results for Trimodal Suspensions

Sample Nr.	Composition			Power law Index	K^2	μ_r^*
	183μ %	61μ %	26μ %			
1	50	30	20	.966	.428	7.44*
2	60	30	10	.984	.455	7.91*
3	40	30	30	.907	.421	7.32*
4	40	40	20	.953	.461	8.02*
5	60	20	20	.975	.412	7.17*
6	50	20	30	.910	.405	7.04*
7	50	40	10	.972	.441	7.67*
8	70	20	10	.980	.418	7.27*
9	70	10	20			
10	60	10	30			
11	50	10	40			
12	80	10	10	.99	.442	7.69*
13	40	50	10	1.00	.492	8.56*

* denotes $\mu_r^* = \frac{K^2}{\mu_o}$; Size Ratios: 0.14, 0.33, 1.0.

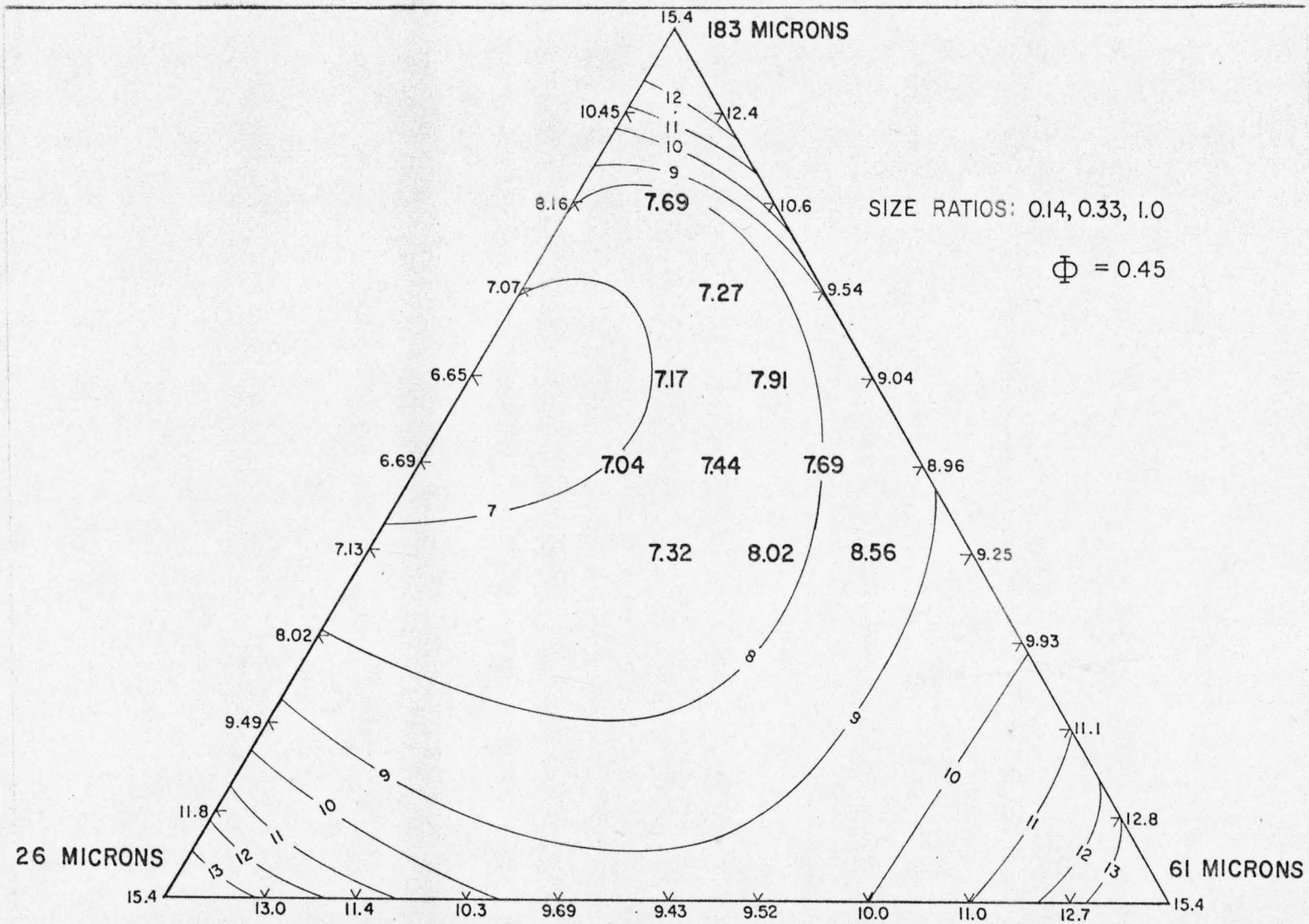

Figure 39. Relative viscosity as a function of composition in trimodal suspensions with total concentrations of 45 volume percent of solids.

mum in relative viscosity at 44 percent 26 micron spheres and 56 percent 183 micron spheres.

The present results indicate that three-component suspensions of the size ratios 0.14, 0.33, 1.0 do not exhibit a minimum in relative viscosity, μ_r^*, at concentrations of 45 volume percent total concentration or less.

Comparison of results with the literature. The present results are not directly comparable to the results of Ting and Leubbers (52). The results of Metzner and Whitlock (35) are corroborated in that rheological dilatancy was not observed in this trimodal system at a total concentration of 45 volume percent. The same agreement is noted with Eveson's (17) low concentration trimodal suspensions. The observations by Parkinson et al. (39) and by Sacks et al. (44) that the addition of a third, intermediate size of sphere to a suspension increases the relative viscosity at a total concentration in the vicinity of 45 volume percent were confirmed.

The theoretical predictions for non-interacting spheres by Farris (19) are generally confirmed for the trimodal system investigated here, with the major reservation that Farris takes no account of the concentration limits for Newtonian flow in his use of the term "relative viscosity". The trimodal composition for minimum relative viscosity at very high total concentrations predicted by Farris is in good agreement with that anticipated here on the basis of the experimentally determined bimodal minimum relative viscosity compositions.

Additional experimental data are required to define the limits of Newtonian flow for trimodal suspensions in which electroviscous effects have been suppressed as a function of size ratios and total concentration. The area of the anticipated minimum in relative viscosity, near 20 percent small, 30 percent intermediate, and 50 percent large, would be the area of greatest interest.

IV

CONCLUSIONS AND RECOMMENDATIONS

Conclusions

Monomodal suspensions. Monomodal suspensions of neutrally buoyant, rigid spheres in Newtonian fluids are Newtonian fluids at concentrations up to 35 volume percent solids. Between 35 and 45 volume percent solids, a power law index of unity is included within the 95 percent confidence limits calculated for the mean experimental power law flow index, but at 47.5 volume percent solids, units is excluded by the 99 percent confidence limits.

The relative viscosity of suspensions of spheres is independent of sphere diameter in the absence of electroviscous effects. The experimental, zero diameter, extrapolated relative viscosity determined as recommended by Thomas (51) as a function of concentration is:

Concentration, Vol.%:	20	30	35	40
Relative viscosity:	2.00	3.40	5.42	7.92

The self-crowding factor, λ_{ii}, in the monomodal form of Mooney's (37) equation is determined to be 1.308.

Within the precision of the experimental results reported here, there was no statistically significant wall effect.

A size fraction of spheres may be considered monomodal with good accuracy if the interquartile size ratio is 0.9 or greater.

For an interquartile size ratio of 0.9, the maximum potential reduction in relative viscosity is estimated to be six percent. The presence of intermediate sizes, as in a continuous size distribution, will limit reductions in relative viscosity to less than six percent.

Bimodal suspensions. Bimodal suspensions of neutrally buoyant, rigid spheres in Newtonian fluids in the composition range of 30 to 50 percent by volume of small spheres appear to be Newtonian fluids for total solids concentrations at least as large as 40 volume percent, but not as large as 60 volume percent. The limits of concentration for Newtonian flow in bimodal suspensions are a function of concentration, composition, and size ratio which remains to be determined.

The values of the crowding factors in the bimodal form of Mooney's (37) equation, as function of size ratio are:

$$\lambda_{11} = \lambda_{22} = 1.308$$

Size ratio	λ_{21}	λ_{12}
0.12	0.80	-1.12
0.14	0.86	0.02
0.21	0.92	0.35
0.28	0.95	0.50
0.33	1.0	0.69
0.43	1.03	0.77
0.49	1.08	0.90
0.57	1.12	0.98
0.68	1.13	0.99

The crowding factors are independent of sphere size, concentration, and shear rate for suspensions within the limits of concentration for Newtonian flow and in which electroviscous forces are absent. Bimodal suspensions have a wide minimum in relative viscosity as a function of composition at constant total concentration. The composition exhibiting minimum relative viscosity is a function of total concentration but not of the self-crowding factor or the Einstein coefficient.

Trimodal suspensions. Trimodal suspensions with size ratios of 0.14, 0.33, 1.0 are expected to be Newtonian fluids at concentrations of 45 volume percent in the absence of electroviscous effects, but do not exhibit a minimum in relative viscosity as a function of composition at total concentrations of 45 volume percent or less.

Recommendations

Further investigations. The variation in power law index of monomodal suspensions as a function of concentration between concentrations of 40 and 60 volume percent solids should be determined with greater accuracy.

The limits of Newtonian flow in bimodal and trimodal suspensions should be determined as a function of size ratios, composition, and total concentration. The variation of power law index with the same parameters should be determined outside the limits of Newtonian flow for suspensions. The values of φ_m for multimodal suspensions of fixed size ratio and composition may be correlatable with the properties of packed beds of spheres of similar characteristics.

Bimodal crowding factors should be determined at small size ratios, less than 0.15, with better suppression of electroviscous effects.

Trimodal suspensions should be investigated for the existence of a realizable minimum in relative viscosity as a function of composition at total concentrations greater than 45 volume percent.

Experimental technique. A more reliable test for the occurrence of wall effects in suspension viscometry is needed.

The separation of spheres by specific gravity as well as by size is necessary, and should probably precede the separations by size. The separation by size can be accomplished satisfactorily using standard testing screens.

REFERENCES

1. American Society for Testing Materials. "Standard Method of Test for Specific Gravity and Absorption of Fine Aggregate, C128-59," in 1967 Book of A.S.T.M. Standards. Part 10. Philadelphia: A.S.T.M., 1967.

2. American Society for Testing and Materials. "Standard Method of Test of Specific Gravity of Hydraulic Cement. C 188-44", p 172 of Vol 9, 1971 Annual Book of A.S.T.M. Standards. Philadelphia: A.S.T.M., 1971.

3. American Society for Testing and Materials. "Standard Specifications for A.S.T.M. Thermometers, E1-66", in 1967 Book of A.S.T.M. Standards. Part 30. Philadelphia: A.S.T.M., 1967.

4. American Society for Testing and Materials. "Standard Method for Inspection, Test, and Standardization of Etched Stem Liquid-in-Glass Thermometers, E77-66", in 1967 Book of A.S.T.M. Standards. Part 30. Philadelphia: A.S.T.M., 1967.

5. American Society for Testing and Materials. "Standard Specifications for Sieves for Testing Purposes, E11-61", in 1967 Book of A.S.T.M. Standards. Part 30. Philadelphia: A.S.T.M., 1967.

6. Allen, S. J. and K. A. Kline. "The Effects of Concentration in Fluid Suspensions." Trans. Soc. Rheol. 12:3, 457-468. 1968.

7. Bagnold, R. A. "Experiments on a Gravity-free Dispersion of Large Solid Spheres in a Newtonian Fluid Under Shear." Proc. Roy. Soc. A 225, 49-63. 1954.

8. Brodnyan, J. G. "The Dependence of Synthetic Latex Viscosity on Particle Size and Size Distribution." Trans. Soc. Rheol. 12:3, 357-362. 1968.

9. Casson, N. "A Flow Equation for Pigment-Oil Suspensions of the Printing Ink Type." P. 84-104 in Rheology of Disperse Systems, C. C. Mills (ed.), New York: Pergamon Press. 1959.

10. Chong, J. S. "The Rheology of Concentrated Suspensions." Unpublished Ph.D. thesis, Department of Chemical Engineering, University of Utah, 1964. University Microfilms 65-1776. See also:

Chong, J. S., E. B. Christiansen and A. D. Baer. "Rheology of Concentrated Suspensions." J. Appl. Polym. Sci. 15:8, 2007-2021. 1971.

11. Clarke, B. "Rheology of Coarse Settling Suspensions." Trans. Instn. Chem. Engrs. 45:6, T251-256. 1967.

12. Cokelet, G. R., F. J. Hollander, and J. H. Smith. "Density and Viscosity of Mixtures of 1,1,2,2-Tetrabromoethane and 1-Bromododecane." J. Chem. Eng. Data 14:4; pp. 470-473. 1969.

13. Cramer, S. D. and J. M. Marchello. "Procedure for Fitting Non-Newtonian Viscosity Data." A.I.Ch.E. Journal 14:5; pp. 814-815. 1968.

14. Davidson, J. F., J. R. A. Pearson and V. A. Vanoni. "Report on the I.U.T.A.M. Symposium on the Flow of Fluid-Solid Mixtures." J. Fluid Mech. 39:2; pp. 375-405. 1969.

15. Eilers, H. "Die Viskositat von Emulsionen hochviskoser Stoffe als Funktion der Konzentration." Kolloid-Z., 97; 313. 1941.

16. Einstein, A. "A New Determination of Molecular Dimensions." Ann. Physik, 19; 289 (1906); 34, 591 (1911). See also Investigations on the Theory of the Brownian Movement. R. Furth, ed. A. D. Cowper, transl. Dover Publications, 1966.

17. Eveson, G. F. "The Viscosity of Stable Suspensions of Spheres at Low Rates of Shear." Rheology of Disperse Systems. C. C. Mill, ed. Pp. 61-83. London: Pergamon Press. 1959.

18. Eveson, G. F., S. G. Ward and R. L. Whitmore. "Anomalous Viscosity in Model Suspensions." Disc. Faraday Soc., 11; 11. 1951.

19. Farris, R. J. "Prediction of the Viscosity of Multimodal Suspensions from Unimodal Viscosity Data." Trans. Soc. Rheol. 12:3. Pp. 281-301. 1968.

20. Ford, T. F. "Viscosity-Concentration and Fluidity-Concentration Relationships for Suspensions of Spherical Particles in Newtonian Fluids." J. Phys. Chem. 64; 1168. 1960.

21. Frankel, N. A. and A. Acrivos. "On the Viscosity of a Concentrated Suspension of Solid Spheres." Chem. Engrg. Sci. 22; 847. 1967.

22. Frazer, H. J. "Experimental Study of the Porosity and Permeability of Clastic Sediments." J. Geol. XLIII; 909. 1935.

23. Furnas, C. C. "Grading Aggregates. I. Mathematical Relations for Beds of Broken Solids of Maximum Density." I&EC. 23; 1052. 1931.

24. Gay, E. C., P. A. Nelson and W. P. Armstrong. "Flow Properties of Suspensions with High Solids Contents." A.I.Ch.E. Journal. 15:6; pp. 815-822. 1969.

25. Gilinson, P. J., C. R. Dauwalter and E. W. Merrill. "A Rotational Viscometer Using an A.C. Torque to Balance Loop and Air Bearing." Trans. Soc. Rheol. VII; 319. 1963.

26. Haughey, D. P. and G. S. G. Beveridge. "Structural Properties of Packed Beds--A Review." Can. J. Chem. Eng. 47:2; pp. 130-140. 1969.

27. Hudson, D. G. "Density and Packing in Aggregates of Mixed Systems." J. Appl. Phys. 20; 154. 1949.

28. Keller, J. B., L. A. Rubenfeld and J. E. Molyneux. "Extremum Principles for Slow Viscous Flows with Applications to Suspensions." J. Fluid Mech. 30:1; pp. 97-125. 1967.

29. Krieger, I. M. "Shear Rate in the Couette Viscometer." Trans. Soc. Rheol. 12:1; pp 5-11. 1969.

30. Lee, D. I. "The Viscosity of Concentrated Suspensions." Trans. Soc. Rheol. 13:2; pp. 273-288. 1969.

31. Lewis, T. B. and L. E. Nielsen. "Viscosity of Dispersed and Aggregated Suspensions of Spheres." Trans. Soc. Rheol. 12:3; pp. 421-443. 1968.

32. Manegold, E., R. Hoffmann und K. Solf. "Uber Kapillarsysteme, XII. I. Die Mathematiche Behandung ideoler Kugelpackungen und das Hohlraum-volumen realer Gerustshukturen." Kolloid-Z., 56; 142. 1931.

33. Manley, R. St. J. and S. G. Mason. "Viscosity of Suspensions of Spheres: A Note on the Particle Interaction Coefficient." Can. J. Chem. 32; 763. 1954.

34. Maron, S. H. and B. P. Madow. "Rheology of Synthetic Latex. IV. Effect of Polydispersity on Flow Behavior." J. Coll. Sci. 8; 300. 1953.

35. Metzner, A. B. and M. Whitlock. "Flow Behavior of Concentrated (Dilatant) Suspensions." Trans. Soc. Rheol. II; 239. 1958.

36. Minnesota Mining and Manufacturing Company. "Technical Data Sheet. 'Superbrite' (R) Brand Glass Beads." 1966.

37. Mooney, M. "The Viscosity of a Concentrated Suspension of Spherical Particles." J. Coll. Sci. 6; 162. 1951.

38. Moulik, S. P. "Proposed Viscosity Concentration Equation Beyond Einstein's Region." J. Phys. Chem. 72:13; pp. 4682-4684. 1968.

39. Parkinson, C. S., S. Matsumoto and P. Sherman. "The Influence of Particle Size Distribution on the Apparent Viscosity of Non-Newtonian Dispersed Systems." J. Coll. Int. Sci. 33:1; pp. 150-160. 1970.

40. Prager, S. "Diffusion and Viscous Flow in Concentrated Suspensions." Physica 29; 129. 1963.

41. Roscoe, R. "The Viscosity of Suspensions of Rigid Spheres." Brit. J. Appl. Phys. 3; 267. 1952.

42. Rutgers, Ir. R. "Relative Viscosity and Concentration." Rheol. Acta 2:4; 305. 1962.

43. Rutgers, Ir. R. "Relative Viscosity of Suspensions of Rigid Spheres in Newtonian Liquids." Rheol. Acta 2:3; 202. (1962); 3:2; 118. (1963).

44. Sacks, M. E., M. J. Romney and J. F. Jones. "Some Pumping Characteristics of Coal Char Slurries." I&EC Chem. Proc. Des. Dev. 9:1; pp. 148-153. 1970.

45. Simha, R. "A Treatment of the Viscosity of Concentrated Suspensions." J. Appl. Phys. 23; 1020. 1952.

46. Simha, R. and T. Somcynsky. "The Viscosity of Concentrated Spherical Suspensions." J. Coll. Sci. 20, 278. (1965).

47. Seshadri, V. and S. P. Sutera. "Apparent Viscosity of Coarse Concentrated Suspensions in Tube Flow." Trans. Soc. Rheol. 14:3; pp. 351-373. 1970.

48. Stone-Masui, J. and A. Watillon. "Electroviscous Effects in Dispersions of Monodisperse Polystyrene Latices." J. Coll. Int. Sci. 28:2; pp. 187-202. 1968.

49. Sweeny, K. H. "The Rheology of Suspensions." Unpublished paper presented before the Symposium on High Energy Fuels, 135th National Meeting of the American Chemical Socity, Boston, Mass., 1959. Contribution 236 of the Chemical Division, Aerojet-General Corp., Azuza, Calif.

50. Sweeny, K. H. and R. D. Geckler. "The Rheology of Suspensions." J. Appl. Phys. 25; 1135. 1954.

51. Thomas, D. G. "Transport Characteristics of Suspension: XII. A Note on the Viscosity of Newtonian Suspension of Uniform Spherical Particles." J. Coll. Sci. 20; 267. 1965.

52. Ting, A. P. and R. H. Luebbers. "Viscosity of Spherical and Other Isodimensional Particles in Liquids." A.I.Ch.E. Journal, 3; 111. 1957.

53. Union Carbide Corporation, Catalog "UCON Fluids and Lubricants". Union Carbide Corporation, 270 Park Avenue, New York, N. Y. 10017.

54. Vand, V. "Viscosity of Solutions and Suspensions. I. Theory." J. Phys. Coll. Chem. 52; 277. 1948.

55. Ward, S. G. and R. L. Whitmore. "Studies of the Viscosity and Sedimentation of Suspensions. Part I. The Viscosity of Suspension of Spherical Particles." Brit. J. Appl. Phys. 1; 286. 1950.

56. Williams, P. S. "Flow of Concentrated Suspensions." J. Appl. Chem. 3; 120. 1953.

57. Yerazunis, S., J. W. Bartlett and A. H. Nisson. "Packing of Binary Mixtures of Spheres and Irregular Particles." Nature 195; 33. 1962.

A P P E N D I C E S

TABLE A 1

Cup Speeds in Radians per Second

Insco Gearbox Settings	Motor Speed 1300 rpm	1800 rpm
1000/1	.00430	.00596
500/1	.00967	.0134
200/1	.0241	.0334
100/1	.0483	.0668
50/1	.0965	.134
20/1	.241	.334
10/1	.483	.669
5/1	.967	1.34
2/1	2.42	3.35
1/1	4.83	6.69

TABLE A 2

Thermometer Comparisons

Temperature °C (9C 8068)	Temperature Error °C PB 1065
25.245	-0.06
27.46	- .09
29.685	- .135
31.91	- .11
34.155	- .055
36.415	- .015
38.56	+ .03
38.53	+ .025
37.16	- .015
34.965	- .06
32.745	- .120
30.575	- .125
28.365	- .13
26.16	- .08
25.295	- .08

Temperature °C (9C 8068)	Temperature Error °C 2C 9285
37.80	-0.15
37.30	- .15
36.80	- .12
37.12	- .14
37.62	- .15
38.07	- .17
38.59	- .17
39.10	- .14
31.41	- .15
32.42	- .16
33.41	- .16
34.15	- .17
34.98	- .18
35.96	- .16
36.90	- .16
37.97	- .17

TABLE A 3

Viscosities of Standard Oils

Oil	Temperature, °C			
	20	25	37.78	98.89
S-3-70101	3.789 cp	3.321 cp	2.459 cp	0.9121 cp
S-6-57-2h	9.490	7.910	5.262	1.484
S-60-65-1a	156.9	114.1	55.75	6.531
S-60-68-1c	163.4	118.9	58.05	6.749
S-60-70105	146.7	105.9	51.07	5.899

TABLE A 4

Raw Data for Standard Oils

Insco Ω_o	1000/1 .0043	500/1 .00967	200/1 .0241	100/1 .0483	50/1 .0965	20/1 .241	10/1 .483	5/1 .967	2/1 2.42	1/1 4.83	Setting Rad/Sec
Bob, Cup				M, Torque, dyne - cm							Cup Temp °C
					S-3-70101						
5S	.124	.278	.690	1.34	2.72	6.84	13.4	27.3	70.0	140.	37.0
3G	.127	.273	.683	1.30	2.66	6.74	13.0	26.7	69.2	137.	37.0
					S-6-57-2h						
4G	.184	.420	1.03	2.10	4.26	10.4	21.1	42.7	105.	219.	37.0
3G	.380	.693	1.58	3.14	6.23	15.0	30.0	60.7	149.	307.	37.0
3G	.311	--	1.60	3.04	5.99	14.3	29.1	58.6	142.	297.	37.0
5S	.284	.607	1.45	2.92	5.86	14.4	29.0	58.6	146.	298.	37.0
3G	.26	.586	1.40	2.88	5.78	14.0	28.8	58.1	141.	296.	37.0
					S-60-65-1a						
4G	2.18	4.86	11.9	23.9	47.8	117.	237.	476.	---	---	37.2
3G	2.99	6.70	16.2	33.0	67.1	161.	328.	671.	---	---	37.2
3S	2.85	6.40	15.5	31.6	63.3	155.	314.	628.	---	---	37.0

TABLE A 4 -- Continued

Raw Data for Standard Oils

Insco Ω_o	1000/1 .0043	500/1 .00967	200/1 .0241	100/1 .0483	50/1 .0965	20/1 .241	10/1 .483	5/1 .967	2/1 2.42	1/1 4.83	Setting Rad/Sec
Bob, Cup				M, Torque, dyne - cm							Temp °C
				S-60-68-1c							
3G	3.00	6.79	16.4	33.2	66.8	126.	329.	665.	---	---	37.1
4G	2.12	4.81	11.7	24.2	48.2	117.	238.	481.	---	---	37.2
5S	3.10	7.01	16.7	34.7	69.4	168.	344.	686.	---	---	37.1
6S	2.23	5.02	12.1	24.9	50.0	121.	246.	496.	---	---	37.1
5S	3.24	7.31	17.7	36.2	72.9	177.	358.	724.	---	---	36.1
6S	2.35	5.29	12.7	26.2	52.5	126.	260.	518.	---	---	36.1
5S	3.28	7.38	18.0	36.6	73.9	179.	363.	731.	---	---	35.1
6S	2.43	5.50	13.2	27.1	54.6	132.	269.	540.	---	---	35.1
5S	3.55	8.02	19.3	39.6	79.8	195.	395.	792.	---	---	34.1
6S	2.51	5.70	13.7	28.1	56.8	136.	278.	562.	---	---	34.1
5S	3.69	8.35	20.4	41.2	82.9	201.	409.	815.	---	---	33.1
6S	2.69	6.10	14.7	30.1	60.6	145.	298.	601.	---	---	33.1
5S	3.02	6.75	16.5	33.5	67.3	-164.	330.	658.	---	---	37.9
6S	2.13	4.79	11.6	23.7	47.5	114.	233.	470.	---	---	37.9
5S	2.75	6.28	15.2	31.0	62.4	151.	306.	616.	---	---	39.1
6S	2.00	4.52	10.9	22.1	44.6	107.	218.	437.	---	---	39.1
5S	2.94	6.66	15.9	33.0	66.2	158.	328.	659.	---	---	37.9
6S	2.08	4.73	11.4	23.3	47.2	114.	233.	470.	---	---	37.9
3G	2.86	6.42	15.4	31.9	64.1	154.	319.	640.	---	---	37.9
4G	2.08	4.73	11.4	23.3	47.2	114.	233.	471.	---	---	37.9
3G	2.86	6.35	15.3	31.5	63.3	154.	314.	635.	---	---	37.7
3G	2.92	6.54	15.8	32.5	65.2	157.	324.	650.	---	---	37.1
4G	2.22	5.02	12.1	24.8	50.1	121.	248.	501.	---	---	37.1

TABLE A 4 -- Continued

Raw Data for Standard Oils

Insco	1000/1	500/1	200/1	100/1	50/1	20/1	10/1	5/1	2/1	1/1	Setting
Ω_o	.0043	.00967	.0241	.0483	.0965	.241	.483	.967	2.42	4.83	Rad/Sec
Bob, Cup				M, Torque, dyne - cm							Temp °C
				S-60-68-1c Continued							
6S	2.16	4.87	11.5	23.9	48.0	115.	239.	479.	--	--	37.7
5S	2.88	6.45	15.8	32.0	64.2	158.	320.	644.	--	--	37.7
5S	2.96	6.68	16.4	33.0	66.7	163.	330.	669.	--	--	37.1
3G	2.91	6.62	15.9	32.8	66.2	159.	327.	660.	--	--	37.1
5S	2.88	6.54	15.9	32.6	65.2	159.	323.	650.	--	--	37.1
				S-60-70105							
5S	2.57	5.83	14.1	28.7	58.3	140.	286.	580.	--	--	37.0
3G	2.58	5.87	14.1	28.9	58.4	140.	288.	582.	--	--	37.0
3S	2.48	5.64	13.7	27.9	56.6	136.	279.	565.	--	--	37.0
3S	2.67	5.96	14.4	29.6	59.9	144.	296.	598.	--	--	37.0
4S	1.88	4.30	10.4	21.1	42.8	103.	211.	423.	--	--	37.0
Ω_o	.00596	.0134	.0334	.0668	.134	.334	.669	1.34	3.35	6.69	Rad/Sec
				S-60-70105 Continued							
3S	3.66	8.29	20.3	41.2	82.7	203.	412.	827.	--	--	37.0
4S	2.62	5.90	14.2	29.2	58.8	141.	290.	586.	--	--	37.0
3S	3.86	8.66	21.1	43.0	86.6	211.	429.	862.	--	--	37.0
4S	2.76	6.32	15.4	31.1	62.8	153.	311.	625.	--	--	37.0

TABLE A 5

Raw Data for Monomodal Suspensions

Insco Ω_o	1000/1 0.0043	500/1 .00967	200/1 .0241	100/1 .0483	50/1 .0965	20/1 .241	10/1 .483	5/1 .967	2/1 2.42	1/1 4.83	Setting Rad/Sec
Conc %	Torque, dyne-cm.										
				26 micron spheres Bob 3 Grooved Cup (G)							
0	0.262	0.572	1.45	3.88	5.85	14.34	39.0	59.5	150.	314.	
20	.526	1.19	3.00	6.04	11.6	29.6	59.7	117.	302.	620.	
30	.864	1.98	5.31	10.4	20.3	51.6	99.2	204.	528.	--	
40	1.95	4.95	12.1	25.	49.6	121.	245.	495.	--	--	
47.5	5.45	10.6	27.5	59.	117.	318.	630.	--	--	--	
50	5.61	12.9	44.3	84.	206.	568.	--	--	--	--	
				26 micron spheres Bob 4 G							
0	0.189	0.418	0.988	2.02	4.08	9.78	20.3	41.3	103.	220.	
20	.470	.884	2.24	4.71	8.46	21.6	46.6	87.6	226.	475.	
30	.832	1.67	4.04	8.28	16.0	39.0	80.8	159.	397.	814.	
40.1	1.60	3.66	8.36	18.8	38.4	95.4	196.	405.	992.	--	
47.5	4.82	13.7	29.2	65.6	124.	30.5	653.	--	--	--	
50	5.80	15.8	36.6	77.	193.	504.	1080.	--	--	--	
				26 micron spheres Bob 5 Smooth Cup (S)							
0	0.258	0.587	1.42	2.84	5.87	14.1	28.6	59.3	147.	308.	
20	.56	1.17	2.96	5.86	11.2	28.9	57.8	112.	294.	601.	
30	.94	2.00	5.01	9.76	19.3	49.7	94.6	192.	501.	997.	
40	2.24	5.15	12.3	25.6	49.8	123.	248.	494.	--	--	
47.5	4.90	9.60	28.4	59.0	123.	340.	692.	--	--	--	
50	6.30	13.4	38.2	81.0	189.	540.	--	--	--	--	

TABLE A 5 -- Continued

Raw Data for Monomodal Suspensions

Insco Ω_0	1000/1 0.0043	500/1 .00967	200/1 .0241	100/1 .0483	50/1 .0965	20/1 .241	10/1 .483	5/1 .967	2/1 2.42	1/1 4.83	Setting Rad/Sec
Conc %				26 micron spheres		Bob 6 S					
0	0.202	0.445	1.05	2.17	4.37	10.5	21.8	44.5	109.	238.	
20	.380	.824	2.14	4.26	8.04	20.6	41.5	80.4	212.	444.	
30	.680	1.38	3.55	7.40	13.9	34.8	70.4	138.	356.	737.	
40	1.44	3.15	8.00	16.2	32.6	82.0	162.	334.	835.	--	
47.5	3.00	6.70	19.9	40.0	82.5	225.	458.	--	--	--	
50	4.40	11.5	30.4	64.0	135.	373.	770.	--	--	--	
				61 micron spheres		Bob 3 G					
0	0.264	0.566	1.33	2.72	5.43	13.2	27.0	55.2	137.	290.	
20	.532	1.06	2.77	5.52	10.4	26.9	53.9	105.	280.	564.	
35	1.48	3.26	7.98	14.8	31.0	79.1	148.	313.	808.	--	
42.5	2.88	6.90	18.0	36.0	77.5	202.	384.	808.	--	--	
50	9.60	22.0	65.8	140.	326.	790.	--	--	--	--	
				61 micron spheres		Bob 4 G					
0	0.206	0.438	1.02	2.04	4.14	9.94	20.4	42.1	105.	226.	
20	.396	.840	2.08	4.32	7.94	20.9	42.6	81.0	214.	447.	
35	.880	2.12	5.51	10.3	21.3	56.8	105.	222.	585.	--	
42.5	1.72	4.51	11.2	21.4	47.4	134.	250.	554.	--	--	
50	4.67	11.7	42.2	95.0	237.	778.	--	--	--	--	
				61 micron spheres		Bob 5 S					
0	0.280	0.606	1.43	2.93	5.86	14.1	29.0	59.5	147.	311.	
20	.556	1.16	2.96	5.44	11.3	29.6	59.0	115.	302.	623.	
35	1.23	2.82	7.31	13.8	28.3	74.8	141.	292.	764.	--	

TABLE A 5 -- Continued

Raw Data for Monomodal Suspensions

Insco Ω_o	1000/1 0.0043	500/1 .00967	200/1 .0241	100/1 .0483	50/1 .0965	20/1 .241	10/1 .483	5/1 .967	2/1 2.42	1/1 4.83	Setting Rad/Sec
Conc %			61 micron spheres Bob 5 S -- Continued								
42.5	2.68	5.69	15.2	30.6	65.0	168.	334.	698	--	--	
50	5.90	14.8	43.3	92.2	208.	563.	--	--	--	--	
Conc %				61 micron spheres		Bob 6 S					
0	0.193	0.412	0.988	2.02	4.05	9.78	20.1	41.3	104.	223.	
20	.374	.796	2.04	3.98	8.09	20.0	40.1	80.9	207.	425.	
35	.960	2.13	5.33	10.0	20.6	53.0	101.	208.	538.	--	
42.5	1.93	4.14	10.6	21.1	43.6	119.	238.	482.	--	--	
50	5.04	11.4	30.7	69.6	150.	432.	824.	--	--	--	
				125 micron spheres		Bob 3 G					
0	0.276	0.598	1.38	2.80	5.66	13.7	27.9	143.	57.3	300.	
20	.504	1.13	2.93	5.74	11.1	29.1	57.0	295.	113.	602.	
30	.792	1.94	5.24	8.97	19.5	52.5	91.6	544.	201.	--	
40	1.66	4.52	12.2	20.3	51.7	127.	228.	--	513.	--	
45	3.37	14.2	28.4	42.2	125.	348.	441.	--	--	--	
45	5.40	9.90	26.2	56.1	113.	368.	632.	--	--	--	
52.36	15.2	58.8	202.	362.	1000.	--	--	--	--	--	
				125 micron spheres		Bob 4 G					
0	0.217	0.460	1.06	2.13	4.30	10.4	21.2	43.6	110.	235.	
20	.412	--	--	4.79	--	--	45.5	--	--	486.	
30	.713	--	--	8.05	--	--	82.5	--	--	835.	
40	1.37	4.10	--	16.9	41.0	--	207.	477.	--	--	
45	2.48	6.89	--	32.9	73.6	--	365.	747.	--	---	
52.36	9.30	25.7	108.	197.	616.	--	--	--	--	--	

TABLE A 5 -- Continued

Raw Data for Monomodal Suspensions

Insco Ω_0	1000/1 0.0043	500/1 .00967	200/1 .0241	100/1 .0483	50/1 .0965	20/1 .241	10/1 .483	5/1 .967	2/1 2.42	1/1 4.83	Setting Rad/Sec
Conc %				125 micron spheres		Bob 4 G					
0	0.190	0.427	1.04	2.10	4.26	10.3	21.0	43.3	109.	231.	
20	.442	.829	1.71	2.34	7.12	15.9	32.1	66.2	192.	445.	
20	.432	.901	1.89	3.56	7.63	16.8	33.4	72.0	198.	446.	
30	.636	1.54	3.17	5.70	12.6	28.2	53.8	117.	360.	748.	
30	.789	1.52	3.03	6.20	12.2	26.5	59.3	112.	346.	731.	
40	1.60	3.19	8.04	16.7	34.9	80.3	166.	312.	925.	--	
40	1.55	3.57	8.88	17.9	38.9	91.3	184.	376.	921.	--	
52.36	10.4	26.5	73.8	145.	382.	920.	--	--	--	--	
				125 micron spheres		Bob 5 S					
0	0.266	0.592	1.39	2.84	5.76	13.9	28.4	58.4	145.	305.	
20	.500	1.12	2.96	5.58	11.1	29.5	56.6	115.	305.	596.	
30	.800	2.01	5.22	9.23	20.5	53.4	95.9	205.	535.	--	
40	1.70	4.43	11.3	22.2	48.4	134.	251.	542.	--	--	
45	2.72	7.90	21.2	40.6	92.5	267.	466.	--	--	--	
52.36	7.45	25.5	74.0	137.	459.	--	--	--	--	--	
				125 micron spheres		Bob 6 S					
0	0.199	0.428	1.03	2.09	4.21	10.2	21.1	42.8	108.	231.	
20	.395	.818	2.11	4.12	8.22	21.6	42.0	84.7	222.	454.	
30	.593	1.35	3.56	7.06	13.9	37.1	72.2	145.	384.	767.	
40	1.16	2.94	7.86	14.3	31.7	89.1	158.	349.	938.	--	
45	1.95	5.09	14.1	26.0	64.0	172.	331.	720.	--	--	
52.36	4.54	11.6	40.3	75.0	215.	651.	--	--	--	--	

TABLE A 5 -- Continued

Raw Data for Monomodal Suspensions

Insco Ω_o	1000/1 0.0043	500/1 .00967	200/1 .0241	100/1 .0483	50/1 .0965	20/1 .241	10/1 .483	5/1 .967	2/1 2.42	1/1 4.83	Setting Rad/Sec
Conc %				183 micron spheres		Bob 5 S					
0	.338	.656	1.438	2.92	5.76	13.7	28.8	57.6	143.	310.	
15	.438	.977	2.33	4.49	8.72	22.3	44.8	83.5	208.	425.	
20	.50	.956	2.49	4.69	9.14	24.9	47.	94.1	249.	514.	
30	.825	1.73	4.39	8.52	18.0	47.8	86.3	159.	407.	920.	
40	1.46	3.70	6.26	14.4	39.6	59.4	140.	372.	920.	--	
50	7.05	11.7	29.5	55.	142.	249.	535.	--	--	--	
55	8.94	20.7	50.3	123.	258.	675.	--	--	--	--	
0	.326	.634	1.41	2.86	5.71	13.6	27.9	56.6	140.	300.	
5	.321	.663	1.53	3.11	5.95	14.8	30.2	59.4	152.	315.	
10	.332	.682	1.64	3.41	6.53	15.8	33.3	66.6	164.	355.	
25	.568	1.09	3.12	6.97	10.4	33.4	67.4	99.3	298.	658.	
0	.27	.562	1.34	2.76	5.52	13.2	27.5	55.8	138.	297.	
35	.905	2.30	6.08	9.87	20.5	56.2	100.	228.	603.	--	
45	2.76	6.67	15.1	24.8	44.6	118.	240.	558.	--	--	
40	1.36	--	7.30	14.1	36.7	74.8	--	290.	918.	--	
Conc %				183 micron spheres		Bob 5 S					
0	.290	.605	1.4	2.67	5.61	13.46	27.75	56.4	139.6	298.	
30	.642	1.83	4.19	9.0	15.3	40.6	90.2	174.	455.	797.	
30	.824	--	4.46	9.28	--	44.7	105.	--	407.	--	
30	.87	1.81	4.76	8.9	15.3	46.6	84.	161.	383.	--	
30	1.01	1.98	5.01	9.2	18.2	48.4	84.	175.	452.	--	
30	.836	1.89	4.62	7.76	16.6	43.9	71.2	164.	425.	--	
30	.935	2.06	4.44	8.84	18.7	46.1	87.2	159.	418.	--	
30	.856	1.85	4.64	7.36	17.7	45.7	80.4	143.	407.	--	
30	.700	1.89	4.51	8.24	17.0	45.1	84.	142.	433.	--	
30	.998	1.87	--	8.48	17.4	--	71.	154.8	--	--	

TABLE A 5 -- Continued

Raw Data for Monomodal Suspensions

Insco	1000/1	500/1	200/1	100/1	50/1	20/1	10/1	5/1	2/1	1/1	Setting
Ω_o	0.0043	.00967	.0241	.0483	.0965	.241	.483	.967	2.42	4.83	Rad/Sec
Conc %				183 micron spheres		Bob 4 G					
0	.212	.441	1.01	2.05	4.08	9.95	20.1	41.2	104.	222.	
35	.857	2.14	4.70	7.99	17.6	42.5	82.6	157.	393.	820.	
45	2.02	4.32	10.5	19.0	38.1	79.8	134.	356.	--	--	
35	.858	2.15	4.79	8.20	18.0	43.3	88.3	170.	437.	866.	
Conc %				183 micron spheres		Bob 3 G					
45	3.50	7.35	18.2	39.9	86.2	244.	481.	757.	--	--	
35	.951	2.40	6.47	9.99	23.0	62.2	109.	238.	790.	--	
0	.269	.601	1.49	2.99	5.96	14.4	29.4	59.6	145.	313.	
5	.323	.707	1.63	3.24	6.61	15.9	32.1	66.2	165.	351.	
10	.368	.778	1.85	3.48	7.29	18.0	34.7	73.2	185.	394.	
15	.405	.911	2.15	3.92	8.09	20.0	38.2	79.7	210.	471.	
20	.470	1.19	2.69	4.83	10.3	24.9	47.0	98.1	267.	577.	
25	.601	1.59	3.56	6.17	14.1	33.2	60.8	133.	346.	744.	
30	.688	2.03	4.96	7.77	17.5	42.5	83.7	180.	471.	--	
35	1.05	2.59	6.70	10.8	25.2	64.3	114.	242.	795.	--	
40	2.29	5.03	12.4	26.5	53.5	126.	248.	498.	--	--	
45	3.64	8.00	23.2	44.2	90.1	242.	460.	746.	--	--	
50	8.56	21.0	54.9	118.	239.	583.	--	--	--	--	
Conc %				183 micron spheres		Bob 4 G					
0	0.179	0.412	1.01	2.09	4.21	10.3	21.0	43.1	109.	231.	
5	.207	.470	1.14	2.31	4.76	11.4	23.6	48.1	121.	240.	
10	.287	.571	1.26	2.57	5.30	12.7	25.6	53.5	135.	292.	

TABLE A 5 -- Continued

Raw Data for Monomodal Suspensions

Insco Ω_o	1000/1 .0043	500/1 .00967	200/1 .0241	100/1 .0483	50/1 .0965	20/1 .241	10/1 .483	5/1 .967	2/1 2.42	1/1 4.83	Setting Rad/Sec
Conc %			183 micron spheres Bob 4 G -- Continued								
15	.315	.656	1.58	3.06	6.41	15.6	31.1	64.8	165.	349.	
20	.396	.827	1.97	3.49	7.70	19.0	36.7	78.7	202.	425.	
25	.437	1.08	2.57	4.46	9.87	25.0	48.3	98.4	261.	557.	
30	.568	1.48	3.68	5.82	14.5	35.1	61.8	138.	362.	776.	
35	.992	2.20	5.33	10.6	21.1	54.4	103.	205.	600.	--	
40	1.42	2.96	7.98	15.5	31.7	81.7	152.	303.	830.	--	
45	2.14	4.96	12.42	27.5	60.9	141.	264.	537.	--	--	
50	4.48	9.80	28.0	76.8	142.	361.	736.	--	--	--	
Conc %				183 micron spheres Bob 5 S							
0	0.267	0.594	1.39	2.87	5.76	13.9	28.6	58.0	143.	303.	
10	.348	.784	1.90	3.75	7.61	18.5	37.6	76.0	187.	391.	
20	.536	1.17	2.87	5.57	11.0	27.9	55.4	107.	281.	586.	
30	.964	2.04	5.21	9.75	20.3	52.0	98.6	200.	511.	--	
40	2.07	4.73	11.1	23.7	52.0	124.	242.	500.	--	--	
50	5.23	11.8	36.7	82.3	177.	453.	872.	--	--	--	
Conc %				183 micron spheres Bob 6 S							
0	0.215	0.451	1.07	2.21	4.41	10.6	21.7	44.4	112.	239.	
10	.272	.586	1.41	2.87	5.74	14.1	29.0	59.1	146.	308.	
20	.390	.831	2.14	4.28	8.31	21.3	43.5	82.9	217.	451.	
30	.700	1.54	3.89	7.85	15.1	38.3	78.7	149.	376.	804.	
40	1.62	3.60	9.64	19.6	40.3	106.	215.	408.	--	--	
50	4.05	8.46	24.6	56.8	128.	375.	704.	--	--	--	

TABLE A 5 -- Continued

Raw Data for Monomodal Suspensions

Insco Ω_o	1000/1 .0043	500/1 .00967	200/1 .0241	100/1 .0483	50/1 .0965	20/1 .241	10/1 .483	5/1 .967	2/1 2.42	1/1 4.83	Setting Rad/Sec
Conc %				221 micron spheres		Bob 3 G					
0	0.268	0.600	1.47	2.92	5.88	14.5	29.2	59.7	150.	314.	
20	.604	1.36	3.15	5.65	11.0	30.1	55.2	116.	201.	587.	
40	2.56	6.52	17.0	31.8	58.0	165.	333.	602.	--	--	
45	5.17	10.8	30.4	65.1	154.	345.	615.	--	--	--	
50	8.65	23.2	65.0	129.	284.	810.	--	--	--	--	
Conc %				221 micron spheres		Bob 4 G					
0	0.202	0.433	1.02	2.04	4.15	10.1	20.5	42.4	107.	226.	
20	.370	.820	2.13	4.05	8.20	21.6	41.1	82.2	215.	438.	
40	1.51	3.81	8.94	17.1	40.0	89.	182.	382.	--	--	
45	2.75	6.52	16.8	30.2	72.0	200.	330.	730.	--	--	
50	5.90	13.8	43.	87.1	177.	515.	1000.	--	--	--	
Conc %				221 micron spheres		Bob 5 S					
0	0.266	0.574	1.38	2.79	5.59	13.6	27.8	56.8	141.	299.	
20	.510	1.07	2.82	5.44	10.6	27.8	56.5	111.	285.	603.	
40	2.03	5.10	12.7	24.6	60.5	145.	252.	512.	--	--	
45	3.36	7.62	21.1	39.5	93.3	223.	380.	836.	--	--	
50	5.54	13.8	48.5	93.5	200.	560.	950.	--	--	--	
Conc %				221 micron spheres		Bob 6 S					
0	0.210	0.438	1.02	2.05	4.15	10.1	20.5	42.2	107.	226.	
20	.360	.802	2.00	3.88	7.76	19.3	39.7	79.6	200.	430.	
40	1.35	3.36	8.60	17.1	36.0	91.0	172.	347.	902.	--	
45	2.80	5.21	14.7	28.1	61.2	164.	322.	620.	--	--	
50	4.17	9.55	28.8	61.8	134.	351.	710.	--	--	--	

TABLE A 6

Raw Data for Bimodal Suspensions

Insco Ω_o	1000/1 .0043	500/1 .00967	200/1 .0241	100/1 .0483	50/1 .0965	20/1 .241	10/1 .483	5/1 .967	2/1 2.42	1/1 4.83	Setting Rad/Sec
Comp.					Torque, dyne-cm.						
		26/183 micron spheres 40% total concentration						Bob 5 S			
100/0	3.44	8.07	20.0	35.0	70.0	171.	328.	608	--	--	
90/10	2.63	6.12	15.9	29.0	67.5	152.	310.	592.	--	--	
90/10	2.00	4.68	10.8	22.8	49.2	137.	280.	553.	--	--	
80/20	1.51	3.64	8.70	18.3	42.0	92.0	201.	420.	--	--	
70/30	1.61	4.02	8.20	16.8	37.2	87.0	178.	394.	--	--	
60/40	1.35	3.15	7.70	15.6	33.2	78.3	159.	342.	797.	--	
50/50	1.33	2.86	7.47	15.6	30.4	79.1	162.	305.	774.	--	
40/60	1.29	2.86	7.40	14.6	30.2	76.0	147.	306.	740.	--	
30/70	--	2.32	--	--	29.0	--	--	289.	702.	--	
20/80	1.35	2.99	7.65	15.0	30.2	77.3	151.	304.	748.	--	
10/90	1.45	3.70	8.20	16.3	34.3	90.0	172.	340.	851.	--	
0/100	--	4.10	--	--	44.9	--	226.	428.	--	--	
		26/183 micron spheres 50/50 composition Bob 5 S									
20%	0.483	1.06	2.72	4.50	10.3	26.6	53.5	104.	276.	555.	
30%	.765	1.63	4.24	8.38	16.2	41.3	83.9	161.	414.	857.	
45%	1.78	4.28	9.80	21.9	46.2	107.	222.	463.	--	--	
50%	3.74	7.21	17.2	38.7	76.5	180.	372.	753.	--	--	
55%	--	12.5	32.0	60.6	125.	314.	658.	--	--	--	
60%	--	44.0	122.	324.	500.	--	--	--	--	--	
0%	0.262	.587	1.43	2.88	5.84	14.3	29.0	59.3	149.	311.	
0%	.261	.577	1.38	2.81	5.70	13.7	28.1	57.5	141.	302.	

TABLE A 6 -- Continued

Raw Data for Bimodal Suspensions

Insco Ω_o	1000/1 .0043	500/1 .00967	200/1 .0241	100/1 .0483	50/1 .0965	20/1 .241	10/1 .483	5/1 .967	2/1 2.42	1/1 4.83	Setting Rad/Sec
			26/183 micron spheres		30/70 composition			Bob 5 S			
20%	0.439	1.04	2.63	5.08	10.1	25.4	51.0	100.	256.	543.	
30%	.744	1.60	4.02	7.92	15.4	40.2	78.0	162.	392.	821.	
40%	1.37	2.90	7.45	14.0	29.8	73.2	140.	293.	734.	--	
50%	2.73	6.35	14.7	31.7	64.5	152.	304.	620.	--	--	
60%	8.82	17.8	40.5	96.2	180.	442.	--	--	--	--	
			61/125 micron spheres		40% total concentration			Bob 3 S			
0/0	0.239	0.536	1.32	2.64	5.34	13.0	26.4	54.2	136.	285.	
0/0	.240	.546	1.33	2.70	5.48	13.3	27.1	55.4	139.	291.	
0/0	.272	.529	1.34	2.68	5.44	13.1	26.7	55.0	137.	290.	
0/0	.218	.553	1.34	2.72	5.51	13.3	27.2	56.0	139.	294.	
0/100	2.15	4.65	11.3	22.5	44.5	117.	229.	456.	--	--	
30/70	1.94	4.26	11.1	22.7	44.5	125.	233.	449.	--	--	
50/50	1.96	4.88	10.5	22.8	50.7	109.	223.	498.	--	--	
100/0	2.07	5.44	13.8	24.2	55.6	144.	265.	556.	--	--	
40/60	1.82	4.04	10.1	21.2	39.7	105.	223.	418.	--	--	
			61/183 micron spheres		40% total concentration			Bob 3 S			
0/0	0.274	0.610	1.46	3.00	6.02	14.5	29.9	60.9	151.	320.	
0/100	2.06	4.56	11.5	22.2	47.0	110.	236.	438.	--	--	
30/70	1.56	3.19	9.04	17.4	36.0	91.4	178.	365.	937.	--	
40/60	1.51	3.61	9.06	17.9	36.9	90.2	176.	364.	923.	--	
50/50	1.50	3.53	8.88	17.7	36.1	90.0	178.	364.	927.	--	
60/40	1.53	3.57	9.18	18.1	37.9	92.6	184.	381.	961.	--	
60/40	1.70	3.69	9.06	19.0	38.9	94.0	191.	386.	978.	--	

TABLE A 6 -- Continued

Raw Data for Bimodal Suspensions

Insco Ω_o	1000/1 .0043	500/1 .00967	200/1 .0241	100/1 .0483	50/1 .0965	20/1 .241	10/1 .483	5/1 .967	2/1 2.42	1/1 4.83	Setting Rad/Sec
			61/183 micron spheres		40% total concentration				Bob 3 S		
70/30	1.63	3.72	9.64	19.6	38.6	98.2	198.	392.	--	--	
100/0	1.78	4.10	10.5	21.2	43.0	110.	215.	447.	--	--	
			61/183 micron spheres		40/60 composition			Bob 3 S			
30%	0.808	1.79	4.59	8.72	17.7	44.4	83.6	172.	438.	897.	
50%	4.24	10.1	28.0	53.9	112.	290.	564.	--	--	--	
60%	17.2	49.4	188.	406.	--	--	--	--	--	--	
			61/221 micron spheres		40% total concentration			Bob 3 S			
0/0	0.274	0.618	1.49	3.04	6.14	15.0	30.6	62.0	156.	328.	
30/70	1.70	3.97	9.50	18.6	38.9	91.7	176.	342.	930.	--	
40/60	1.73	3.79	9.75	18.7	37.2	93.0	170.	349.	876.	--	
50/50	1.55	3.60	9.14	17.9	34.7	89.0	177.	355.	939.	--	

TABLE A 6 -- Continued

Raw Data for Bimodal Suspensions

Insco Ω_o	1000/1 0.00596	500/1 .0134	200/1 .0334	100/1 .0668	50/1 .134	20/1 .334	10/1 .669	5/1 1.34	2/1 3.35	1/1 6.69	Setting Rad/Sec
					Torque, dyne-cm.						
Comp.		26/61 micron spheres			40% total concentration			Bob 3 S			
0/0	0.321	0.770	1.90	3.87	7.73	18.9	38.7	79.0	200.	420.	
0/100	3.02	6.54	16.6	34.0	70.4	170.	336.	626.	--	--	
30/70	3.01	7.54	16.2	31.6	60.5	141.	276.	541.	--	--	
40/60	3.70	6.99	17.0	33.9	59.8	137.	278.	518.	--	--	
50/50	5.45	10.2	22.7	40.2	68.0	143.	288.	575.	--	--	
100/1	76.0	87.5	116.	135.	178.	284.	452.	--	--	--	
		26/125 micron spheres			40% total concentration			Bob 3 S			
0/0	0.344	0.776	1.89	3.84	7.69	18.8	38.5	78.6	198.	420.	
0/100	2.53	5.84	15.3	30.5	62.3	148.	286.	615.	--	--	
30/70	2.60	5.95	13.1	24.8	48.6	112.	213.	448.	--	--	
40/60	2.72	6.56	19.2	25.5	51.9	114.	219.	465.	--	--	
50/50	2.82	7.05	14.0	29.3	55.7	117.	236.	471.	--	--	
		26/125 micron spheres			30/70 composition			Bob 3 S			
20%	0.657	1.43	3.57	7.30	14.4	35.8	73.0	143.	391.	786.	
30%	1.27	2.58	6.43	12.4	24.6	59.3	116.	228.	583.	--	
50%	6.78	13.8	33.9	65.0	131.	308.	602.	--	--	--	
		125/221 micron spheres			40% total concentration			Bob 3 S			
0/0	0.385	0.834	2.02	4.15	8.30	2.03	41.8	84.6	214.	444.	
30/70	3.03	6.78	16.7	33.3	66.6	166.	313.	639.	--	--	
40/60	2.72	6.16	14.8	32.4	60.0	147.	285.	570.	--	--	

TABLE A 6 -- Continued

Raw Data for Bimodal Suspensions

Insco	1000/1	500/1	200/1	100/1	50/1	20/1	10/1	5/1	2/1	1/1	Setting
Ω_o	0.00596	.0134	.0334	.0668	.134	.334	.669	1.34	3.55	6.69	Rad/Sec
			125/221 micron spheres			40% total concentration			Bob 3 S		
50/50	3.05	6.30	15.3	30.6	61.7	152.	284.	585.	--	--	
0/100	3.12	7.06	16.1	35.8	70.0	168.	342.	650.	--	--	
100/0	3.06	7.18	16.7	34.9	68.7	163.	319.	646.	--	--	
			26/221 micron spheres			40% total concentration			Bob 3 S		
0/0	0.361	0.798	1.95	3.98	7.91	19.4	39.6	80.7	204.	430.	
0/0	.378	.832	2.02	4.10	8.22	20.1	41.0	84.0	212.	445.	
0/100	2.98	6.70	17.1	35.0	61.5	166.	311.	600.	--	--	
20/80	2.08	4.74	10.5	21.8	41.8	98.0	199.	407.	--	--	
30/70	2.18	4.94	11.2	20.8	39.1	97.0	186.	382.	--	--	
40/60	2.69	5.88	12.0	23.7	45.6	94.8	193.	383.	--	--	
50/50	5.30	9.26	19.1	34.5	53.0	108.	208.	394.	--	--	
100/0	9.0	17.0	33.3	55.8	99.7	206.	402.	806.	--	--	
			26/221 micron spheres			30/70 composition			Bob 3 S		
20%	0.630	1.39	3.47	7.05	13.6	34.1	68.9	138.	353.	768.	
30%	.900	2.11	5.25	10.3	20.7	51.9	101.	207.	530.	--	

TABLE A 7

Raw Data for Trimodal Suspensions

Insco Ω_o	1000/1 0.00596	500/1 .0134	200/1 .0334	100/1 .0668	50/1 .134	20/1 .334	10/1 .669	5/1 1.34	2/1 3.35	1/1 6.69	Setting Rad/Sec
					Torque, dyne-cm.						
0	0.369	0.822	2.00	4.06	8.13	19.9	40.6	82.7	210.	442.	
0	.369	.823	2.02	4.12	8.14	20.2	41.3	83.2	213.	448.	
1	3.58	7.57	18.6	35.8	70.6	170.	327.	675.	--	--	
2	3.46	7.46	18.8	36.2	74.6	181.	354.	703.	--	--	
3	5.07	9.60	21.6	40.9	73.6	166.	342.	681.	--	--	
4	4.07	9.18	21.1	39.7	77.5	185.	374.	720.	--	--	
5	3.34	6.87	17.8	34.4	69.2	164.	321.	644.	--	--	
6	4.90	9.30	20.7	38.5	73.1	168.	331.	651.	--	--	
7	3.76	7.58	18.2	39.1	74.8	183.	361.	676.	--	--	
8	3.14	7.25	17.7	35.0	70.3	173.	316.	657.	--	--	
12	3.21	7.00	18.0	35.4	73.9	164.	351.	682.	--	--	
13	3.42	7.54	17.3	38.1	75.8	188.	368.	759.	--	--	